DENDRITIC CELL DYNAMICS IN BLOOD AND LYMPHOID TISSUES DURING PATHOGENIC SIMIAN IMMUNODEFICIENCY VIRUS INFECTION

by

Kevin Neal Brown

B.S., Muhlenberg College, 2001

Submitted to the Graduate Faculty of

Graduate School of Public Health in partial fulfillment

of the requirements for the degree of

Doctor of Philosophy

University of Pittsburgh

2008

UNIVERSITY OF PITTSBURGH

Graduate School of Public Health

This dissertation was presented

by

Kevin N. Brown

It was defended on

December 8, 2008

and approved by

Aaron Barchowsky, Ph.D.
Associate Professor
Department of Environmental and Occupational Health
Graduate School of Public Health
University of Pittsburgh

Adriana Larregina, M.D., Ph.D.
Assistant Professor
Department of Dermatology
School of Medicine
University of Pittsburgh

Phalguni Gupta, Ph.D.
Professor
Department of Infectious Diseases and Microbiology
Graduate School of Public Health
University of Pittsburgh

Dissertation Advisor: Simon M. Barratt-Boyes, BVSc., Ph.D.
Associate Professor
Department of Infectious Diseases and Microbiology
Graduate School of Public Health
University of Pittsburgh

DENDRITIC CELL DYNAMICS IN BLOOD AND LYMPHOID TISSUES DURING PATHOGENIC SIMIAN IMMUNODEFICIENCY VIRUS INFECTION

Kevin N. Brown, Ph.D.

University of Pittsburgh, 2008

Dendritic cells (DC) are a heterogenous population of antigen presenting cells important in both innate and adaptive immune responses. The two major subsets of DC, $CD11c^+$ myeloid DC (mDC) and $CD123^+$ plasmacytoid DC (pDC), are depleted in the blood of human-immunodeficiency virus (HIV) – 1 infected individuals. It has been proposed that DC loss may be due to lymph node recruitment, direct viral infection, bone marrow suppression or death, although this has not been directly addressed. Using the highly relevant, rhesus macaque/simian immunodeficiency virus (SIV) model of HIV infection, we investigated DC dynamics during acute pathogenic SIV infection and simian AIDS. **We hypothesized that SIV infection causes a dysregulation of DC trafficking and death not solely dependent upon direct viral infection.** The specific aims of this project are to: 1) determine the phenotypic heterogeneity of DC in blood from healthy macaques and develop a rapid assay for frequent longitudinal quantitation of absolute DC numbers; 2) determine whether mDC and pDC are recruited to lymphoid tissues in simian AIDS; 3) determine the dynamics and possible mechanisms of pDC loss and redistribution to lymphoid tissue during acute SIV infection. We found that rhesus macaque DC were more phenotypically homogeneous than their human counterparts and could be accurately quantified in small volumes of blood. In monkeys with simian AIDS, DC were depleted in both blood and secondary lymphoid tissues associated with increased spontaneous apoptosis. However, the remaining DC were phenotypically normal. During acute SIV infection, pDC responded to infection in a biphasic manner, with rapid mobilization into blood

followed by depletion in both blood and lymphoid tissue. However, pDC production from bone marrow was normal and BrdU-labeling indicated increased pDC mobilization and recruitment to lymphoid tissues despite net loss of pDC. In lymph nodes, pDC were directly infected with virus, activated, and undergoing increased levels of apoptosis but retained functional TLR7 signaling. The findings in this study are significant to public health because defining the mechanisms leading to DC loss will offer new opportunities for therapeutic interventions to augment immune responses in HIV-infected individuals.

TABLE OF CONTENTS

LIST OF FIGURES

ACKNOWLEDGEMENTS

There exists an endless list of individuals to whom I am deeply indebted for aiding in the pursuit of my doctoral studies.

First and foremost, I extend a warm and sincere thank you to my dissertation advisor and friend, Dr. Simon M. Barratt-Boyes, for providing continued guidance, support and encouragement from the time we began our scientific endeavors together in the summer of 2001 and fostering my development for continued success. Secondly, to my dissertation committee, Drs. Barchowsky, Larregina and Gupta, for keeping me focused and providing helpful comments to pursue more successful and informative experimental avenues.

To the past and present members of the Barratt-Boyes lab, Danielle, Nada, Sherrianne, Xiangdong, Viskam and Adam, our candid discussions and shared frustrations contributed to making graduate school an enjoyable journey with many fond memories. To Mike and Larry, both played an instrumental role in providing the fundamental tools to conduct science in a thorough and efficient manner, as well as becoming life-long friends.

Dr. Todd Reinhart who always had the door open for discussions of managing life and career, keeping me on schedule with committee meetings and the final completion of my Ph.D. and most of all, asking provocative questions during seminars.

I would like to thank the patience and assistance of the IDM and Center for Vaccine Research administrative staff, who tolerated frequent and impromptu interruptions.

My classmates and Pittsburgh friends, notably Jeff and Amanda Cheng for providing a welcoming home and delicious food during the last few months of my studies and Douglas Barnes.

To my parents, sister and family, thank you for the unconditional love, support and encouragement you provide as I continue on my journey. Lastly and most of all, I must thank the love of my life and best friend Shauna Clark, who has traveled this road with me unwaveringly, keeping the fire of the soul burning brightly, and inspiring me each and every day.

1.0 INTRODUCTION

1.1 GLOBAL HIV EPIDEMIC

Human immunodeficiency virus type 1 (HIV-1), the causative agent of acquired immune deficiency syndrome (AIDS) in the human population, is a member of the genus *Lentivirus* in the family *Retroviridae*. HIV-1 is primarily transmitted through heterosexual contact, although injection drug use, men who have sex with men (MSM) and mother-to-child transmission also constitute a considerable fraction in some countries. Currently, there are an estimated 37 million people living with HIV-1/AIDS worldwide and in 2007, there were 2.7 million new HIV infections and 2 million HIV-related deaths (1). However, some regions of the world, notably sub-Saharan Africa, are more heavily affected by this devastating disease, accounting for 67% of all people living with HIV and 75% of AIDS deaths in 2007. In addition to regional differences, the burden of HIV is disproportionately distributed among women and ethnic minorities. In 2007, women represented nearly half of all HIV-infected people worldwide (1) and in the United States, while African-Americans accounted for only 13% of the population in 2003, they represented approximately 49% of new HIV/AIDS diagnoses (2).

1.2 DYNAMICS OF HIV/SIV INFECTION

HIV-1 and pathogenic SIV infection are characterized by three major phases: primary infection, an asymptomatic or chronic phase, and a symptomatic phase or AIDS. Primary infection is defined by a massive increase in plasma viral load and loss of $CD4^+$ T cells followed by a decrease to a viral load set-point associated with the initiation of antiviral immune responses. Within 1-2 weeks of SIV infection (3, 4) or 4-6 weeks post-HIV infection (5, 6), direct viral infection leads to the massive and selective loss of $CD4^+$ T cells within the mucosa-associated lymphoid tissues (7) independent of the route of transmission (3, 8, 9). Following this massive loss, acute infection in both humans and macaques is resolved with the onset of antigen-specific immune responses (10-13), encompassing the asymptomatic or chronic phase of infection. Eventual progression to the symptomatic phase or AIDS occurs after $CD4^+$ T cell depletion accompanied by a variety of opportunistic infections, hematological and sometimes neurological disorders (14). Due to the similarities between HIV-1 infection of humans and pathogenic SIV infection of macaques, the rhesus macaque/SIV model is well suited for the study of HIV pathogenesis (15).

1.3 DENDRITIC CELL SUBSETS

Dendritic cells (DC) are a heterogeneous population of bone marrow-derived antigen-presenting cells important in both innate and adaptive immune responses. DC are present in different stages of maturation in blood as well as in lymphoid and non-lymphoid organs (16). DC can be subdivided into two major subsets based on the lack of expression for markers of T cells (CD3), B cells (CD19 or CD20), monocytes (CD14), and natural killer cells (CD56), collectively referred to as Lineage-negative, and positive expression of the class II major histocompatibility complex (MHC II) specifically human leukocyte antigen (HLA)-DR. In humans and rhesus macaques, the two main DC types are defined as $CD11c^{+}CD123^{-}$ myeloid or 'conventional' DC (mDC) or $CD11c^{-}CD123^{+}$ plasmacytoid DC (pDC).

1.3.1 Myeloid DC

1.3.1.1 General characteristics

Myeloid DC (mDC) are central to generating T cell responses to invading pathogens (16). In humans, mDC are defined as Lineage-negative (Lin^{-}, $CD3^{-}$ $CD14^{-}$ $CD20^{-}CD56^{-}$) $HLA\text{-}DR^{+}$ cells expressing the integrin CD11c, and are similarly defined in rhesus macaques (17). mDC are mainly derived from myeloid progenitor cells in bone marrow and treatment of humans and rhesus macaques with fms-like tyrosine kinase 3-ligand (Flt3-L) *in vivo* dramatically increases

the number of circulating mDC (17-19). However, under inflammatory conditions monocytes in blood can give rise to cells with phenotypic and functional features of DC (20-23) but in the steady state, DC do not seem to be derived from monocytes, with circulating immature mDC distinguished from monocytes (21, 23, 24). In humans and rhesus macaques, circulating mDC in blood are phenotypically immature based on low level expression of the costimulatory molecules CD86 and CD40 as well as undetectable CD80 expression (17, 19, 25).

In addition to circulating in blood, mDC populate peripheral tissues such as skin and mucosa as immature cells capable of capturing and processing antigens (16). Following exposure to an invading pathogen, inflammatory mediators induce DC to mature and migrate from peripheral tissues to lymph nodes via afferent lymphatics and stimulate T cells to generate adaptive immunity. The movement of DC into peripheral tissues and localization in lymph nodes is controlled by chemokine receptors and their ligands. Immature mDC express CC chemokine receptors CCR1, CCR2, CCR5, and CCR6 which bind inflammatory chemokines responsible for recruiting DC to inflamed tissues (26, 27). Upon maturation, DC express CCR7 conferring responsiveness to the lymph node-homing chemokines CCL19 (macrophage inflammatory protein 3β) and CCL21 (6Ckine), permitting appropriate localization of DC to the lymph node paracortex for interaction with T cells (27-29). Lymph nodes draining peripheral tissues contain a population of phenotypically mature DC not found in blood, spleen or thymus (30). In the steady state of mice and humans, most lymphoid organ DC display a mature phenotype, expressing the highest levels of HLA-DR, the maturation marker CD83 and costimulatory molecules CD80, CD86 and CD40 (30-32). In humans, migratory DC in lymph nodes originating from Langerhans cells are identified by expression of CD1a and Langerin (33, 34).

Finally, Langerhans cells or skin-migratory DC in humans do not produce IL-12p70 but rather induce T-helper type 1 responses through production of IL-23 (35-37).

1.3.1.2 mDC depletion during HIV and SIV infection

Numerous studies have reported reductions in the number of mDC circulating in the blood of HIV-1 infected individuals (38-44). mDC depletion occurs as early as 4 weeks following HIV infection, although data are conflicting (38, 45) and in anti-retroviral treatment-naïve patients, mDC numbers remain below pre-infection levels. Nevertheless, recovery of mDC numbers can be achieved using anti-retroviral therapy, although results have been conflicting concerning the extent of recovery compared to uninfected controls (38, 42, 44, 46-48). In cynomolgus macaques with chronic SIV infection, absolute numbers of $CD1c^+$ mDC in blood were similar to uninfected controls, suggesting mDC loss may be limited to a specific mDC subset (49).

1.3.1.3 mDC alterations in lymphoid tissue during HIV/SIV infection

A central hypothesis for the loss of circulating mDC during HIV infection has been recruitment of mDC to lymph nodes, based on the bystander maturation of DC by pDC (50). However, the effects of HIV/SIV infection on the frequency and phenotype of mDC in peripheral lymph nodes is limited and often conflicting. During acute HIV infection, in situ analysis of peripheral lymph nodes indicated an accumulation of DC-$SIGN^+$ and $CD40^+$ DC (51). In SIV-infected cynomolgus macaques, migratory $CD1a^+$ persisted in lymph nodes despite disease progression associated with decreases in mature $CD83^+$ DC, suggesting simian AIDS may lead to impaired DC maturation. However, in SIV-infected rhesus macaques with AIDS, decreases in mature

$CD83^+$ DC was associated with loss of these cells from lymphoid tissues and linked to failed migration of Langerhans cells following contact sensitization (52). More recently, mDC with a partial activation phenotype accumulated in lymphoid tissues during asymptomatic chronic HIV-1 infection (53), although this study excluded migratory DC and may reflect recruitment of blood-derived mDC. Therefore, the recruitment of mDC to lymph nodes during HIV or SIV infection remains incompletely defined.

1.3.2 Plasmacytoid DC

1.3.2.1 General characteristics

Plasmacytoid DC (pDC) are relatively rare, innate immune system cells that play a critical role in the host response to viral infection. In humans, pDC are phenotypically defined as lineage-negative ($CD3^-CD14^-CD20^-CD56^-CD16^-$) $HLA\text{-}DR^+$ cells expressing high levels of CD123 (IL-3Rα) and equivalent pDC have been identified in rhesus macaques (17, 49, 54). pDC are derived from hematopoietic progenitor cells in the bone-marrow and enter the bloodstream as end-stage non-dividing cells (55). Administration of hematopoietic growth factors such as Flt3-L *in vivo* leads to dramatic increases in the number of pDC in human blood and rhesus macaque blood and lymphoid tissues (17-19, 56), highlighting the hematopoietic origin of pDC.

Under homeostatic conditions, pDC circulate in the blood and are located in peripheral lymphoid tissues (17, 31, 32). However, pDC may also be found in non-lymphoid sites during inflammatory conditions such as cutaneous lupus erythematosus (57), allergic rhinitis (58), and contact dermatitis (59). In blood, pDC are characterized as immature cells expressing low to undetectable levels of the co-stimulatory molecules CD86 and CD40 (25) and upon arrival in

lymph nodes acquire a mature phenotype with homogeneously high expression of CD40 (31). pDC emigration from blood to lymph nodes is controlled by chemokines. In general, pDC express a multitude of chemokine receptors such as CCR5, CXCR3, CXCR4, and CCR7 (60). In the steady state, pDC migrate to lymph nodes via high endothelial venules (HEV) using the CXCR4 ligand SDF-1/CXCL12 and L-selectin (CD62L - peripheral lymph node addressin) (61). Following inflammation, pDC are rapidly mobilized and recruited to inflamed lymph nodes in a CXCR3-dependent manner corresponding to increased expression of the interferon –γ –inducible chemokines Mig/CXCL9 and IP-10/CXCL10 (62, 63). pDC activation through pathogen sensing or CD40 ligation, leads to the upregulation of functional CCR7 and responsiveness towards the chemokines SLC/CCL19 and ELC/CCL21, thereby localizing pDC in T cell-rich areas of lymph nodes (63).

1.3.2.2 Role of pDC in viral immunity

pDC are the most potent producers of anti-viral type I IFN, mainly IFN-α (62, 64, 65). IFN-α is produced by pDC in response to a wide variety of pathogens, including enveloped viruses such as herpes simplex virus (65), influenza virus (66, 67), HIV-1 and SIV (68, 69), as well as parasites (70) and DNA containing unmethylated CpG sequences typical of microbial DNA (62, 65). The ability of pDC to secrete IFN-α in response to such a vast array of pathogens is mainly through the detection of distinct pathogen-associated molecular patterns by the pattern recognition receptors Toll-like receptor (TLR) 7 and TLR9 (71). TLR7 recognizes single-stranded RNA and synthetic imidazoquinoline compounds, used in the treatment of human papilloma virus infections (71, 72). TLR9 recognizes unmethylated CpG-oligodeoxynucleotide-containing DNA such as the CpG-rich DNA viral genomes of herpes simplex viruses (HSV) 1

and 2 as well as mouse cytomegalovirus (71). In addition to type I IFN, pDC produce TNF-α and a broad range of other proinflammatory cytokines upon activation and are the major DC subset in lymph nodes innately producing cytokines (32, 73).

pDC-derived type I IFN directly controls virus infection in murine coronavirus and HSV models (74, 75). Moreover, pDC-derived IFN-α is capable of limiting HIV replication in $CD4^+$ T cells (76-78), highlighting the role of pDC in controlling HIV infection. Live or replication defective HIV-1 viral binding via CD4 mediates endocytosis of HIV and endosomally delivered viral RNA stimulates type I IFN production by pDC through TLR7 (79), indicating pDC activation occurs independent of direct viral infection.

pDC play a central role in activating host innate and adaptive immune responses. pDC activation results in both direct and/or indirect activation of many other cell types, including mDC, NK cells, and T cells. pDC exposure to HIV-1 induces the phenotypic maturation of pDC and upregulation of functional CCR7, with IFN-α production resulting in bystander maturation of mDC, which are not activated directly by HIV-1 (50). In addition, pDC help lymph node DC to induce robust virus-specific T cell responses (80) and increase NK cell-mediated cytotoxicity, IFN-γ production and early anti-viral resistance (81). pDC-derived IFN-α also provides an important signal for T helper precursor differentiation in favor of a T helper type 1 immune response (82) and directly amplifies $CD8^+$ T cell expansion after viral infection (83).

1.3.2.3 pDC depletion and dysfunction during HIV and SIV infection

pDC are depleted in blood during both HIV and SIV infection (38, 43, 44, 46, 47, 49, 54, 84-87), which is correlated with high viral load and the occurrence of opportunistic infections and Kaposi sarcoma (87). In primary HIV infection, pDC are lost in parallel with $CD4^+$ T cells in blood and is inversely correlated with plasma viral load while in chronic HIV infection, pDC loss from blood is correlated with clinical state and predictive of disease progression (41-43, 46). Even in pediatric patients, pDC counts are lower in viremic children with declining $CD4^+$ T cells compared to children with stable $CD4^+$ T cell counts (88). Administration of highly active anti-retroviral therapy (HAART) leads to at least partial recovery of pDC counts in peripheral blood during primary and chronic HIV infection (41, 42, 44, 46, 47) and often correlated with CD4 count recovery and decreased viral loads. Similarly, pDC are depleted in both blood and lymphoid tissues in rhesus, cynomolgus and pig-tailed macaques with chronic SIV infection and AIDS (49, 54, 85) and this loss is inversely correlated with plasma viremia (54). In contrast, nonpathogenic SIV infection of African green monkeys results in early pDC loss during acute infection followed by a return to normal frequencies during the chronic stage of infection (89). Recent evidence indicates that pDC numbers increase in the blood of SIV-infected macaques within the first week of infection (84), consistent with their early role in limiting viral infection (90). However, pDC numbers were significantly depleted through the remaining period of observation in SIV-infected macaques (54, 84).

In addition to the reduced frequencies of pDC in blood during HIV infection, functional defects have also been observed. In individuals with chronic HIV infection, loss of pDC numbers in

blood are correlated with decreased IFN-alpha production (91) and pDC from HIV-infected individuals are less responsive to TLR9 stimulation *in vitro* (46, 91-94). Recently, it has been suggested that diminished pDC responses in HIV-infected patients is a consequence of prior activation via type I IFN or HIV virions (93). Together, these findings suggest reductions in both pDC frequency and function lead to inadequate control of HIV.

1.4 POTENTIAL MECHANISMS OF DC LOSS DURING HIV AND SIV INFECTION

1.4.1 Direct viral infection of DC

pDC in both humans (41, 68, 87, 95, 96) and macaques (49, 54) express the viral receptor CD4 and co-receptors CCR5 and CXCR4 making them likely targets of HIV infection. *In vitro*, pDC can be infected with both CCR5 and CXCR4-tropic strains of HIV-1 (68, 95-98) and preferentially transmit virus to antigen-specific $CD4^+$ T cells (99). pDC isolated from HIV-infected patients show evidence of direct infection (40) and pDC in tonsils and thymus of HIV-infected patients were found containing the HIV p24 antigen, indicating pDC can be productively infected by HIV *in vivo* (96).

Similar to pDC, both humans and macaque immature blood mDC and Langerhans cells in skin express the main viral receptor, CD4, as well as the co-receptor CCR5 (49, 52), implicating mDC may be directly infected with virus. In support of this observation, *in vitro* exposure of mDC to HIV leads to maturation and infection (96, 98) and recent findings demonstrate evidence of infection *in vivo* (40). Moreover, mDC infected *in vitro* preferentially transmit virus to

antigen-specific $CD4^+$ T cells (99). However, in patients treated with HAART and undetectable plasma viral RNA, neither proviral DNA or viral RNA was found in either mDC or pDC, indicating direct infection may not play a role in DC depletion during aymptomatic infection (100). Together, these findings indicate direct viral infection may play a role in the loss of mDC during HIV/SIV infection.

1.4.2 DC recruitment to lymphoid tissues

One of the major mechanisms proposed for the loss of circulating DC has been redistribution to lymphoid tissues. pDC exposure to HIV *in vitro* leads to activation and up-regulation of the chemokine receptor CCR7 (50, 101, 102) responsible for pDC localization to the T-cell rich lymph node paracortex. In addition, pDC activation via HIV leads to the bystander maturation of mDC(50). Notably, CCR7 binds to the inflammatory chemokine MIP-3β/CCL19 which is increased during acute SIV infection. pDC in blood express CXCR3 which binds to the inflammatory chemokines IP-10/CXCL10 and Mig/CXCL9 (62), and pDC recruitment to inflamed lymph nodes occurs in a CXCR3-dependent manner (63). In pathogenic SIV infection of rhesus macaques, the inflammatory chemokines for CXCR3 are increased in lymphoid tissues during both acute and chronic infection (103, 104). Therefore, there is ample evidence implicating DC recruitment to lymphoid tissues during HIV and SIV infection.

1.4.3 Bone marrow suppression

DC are derived from bone marrow progenitor cells (24) and reductions in hematopoietic progenitor cells have been reported in bone marrow during HIV (105-107) and SIV infection

(108-110). Nevertheless, hematopoietic progenitor cells are relatively resistant to HIV with minor frequencies infected *in vitro* and *in vivo* (111). In addition, $CD34^+$ hematopoietic stem cells are resistant to HIV infection despite expression of the viral receptors CD4, CCR5 and CXCR4 (112). Bone marrow stroma plays a critical role in the development and maintenance of hematopoiesis indicating stromal dysfunction may lead to alterations in hematopoiesis. In rhesus macaques, stromal cells express low levels of CD4 and CCR5 and could be infected with SIV *in vitro*, but infected stromal cells were not found *in vivo* (113). Perhaps most importantly, SIV-infected macaques treated with a chimeric Flt3-L and G-CSF receptor agonist, effectively increased both mDC and pDC in blood (114), suggesting bone marrow suppression is not likely to be a significant factor in DC loss.

1.4.4 Bystander apoptosis of DC

Another potential mechanism for the loss of DC during HIV and SIV infection is through bystander apoptosis, a well-described mechanism of T cell loss in HIV and SIV infection (115-119). In HIV-infected individuals, the majority of apoptotic T cells in peripheral blood and lymph nodes are uninfected (117-121) and in SIV-infected macaques, apoptosis occurs predominately in bystander cells (116). The extrinsic pathway of apoptosis is initiated by binding of TNF family ligands to cognate death receptors, classically involving Fas-ligand (FasL) binding to Fas, and numerous studies indicate a role for Fas/FasL in apoptosis of T cells in HIV infection (122-124) and progressive SIV infection (125). Interestingly, binding of FasL to Fas induces the maturation of healthy DC, not death (126). However, Fas-mediated pathways have been implicated in DC apoptosis during measles virus infection (127), suggesting the DC response to Fas may altered in SIV infection. pDC in human tonsils express Fas, however pDC

from both uninfected and HIV-infected individuals were equally susceptible to FasL-induced apoptosis (78). Nevertheless, spontaneous apoptosis mediates the depletion of mDC and pDC in the blood of patients with breast cancer (128, 129). Collectively, the ultimate role of apoptosis in DC loss during HIV and SIV infection remains to be determined.

2.0 HYPOTHESIS AND SPECIFIC AIMS

Dendritic cells (DC) are professional antigen-presenting cells essential for the induction of both innate and adaptive immune responses to pathogens. The two major DC subsets described in humans, mDC and pDC are found in blood as well as in non-lymphoid and lymphoid tissues at low frequencies. It has been well described that mDC and pDC are lost from the circulation in human immunodeficiency virus type 1 (HIV-1)-infected individuals, associated with progression to disease and related to increased viral loads and reduced numbers of $CD4^+$ T cells. It has been suggested that the loss of DC from blood may be due to an increased recruitment in lymphoid tissues, direct destruction due to viral infection, or bone marrow suppression. **We hypothesized that SIV infection causes a dysregulation of DC trafficking and death not solely dependent upon direct viral infection.** In order to address this multifactorial hypothesis, we proposed three specific aims:

1) **Characterize DC in blood and develop a rapid assay for DC enumeration.** DC subsets in blood were phenotypically characterized with particular focus on lineage markers followed by development of a rapid assay for DC enumeration from small volumes of blood.

2) **Determine whether DC are recruited to or lost from lymphoid tissues in simian AIDS.** DC numbers in blood and lymphoid tissue were quantified and

changes in costimulatory molecule expression was performed. In addition, DC in lymphoid tissues were examined for changes in spontaneous cell death as an additional mechanism of DC loss.

3) **Determine whether pDC redistribution to lymphoid tissues, lack of production and mobilization, or direct viral infection leads to loss from blood during acute SIV infection.** Changes in blood pDC numbers were monitored at frequent intervals during the first 14 days of SIV infection in addition to in vivo BrdU labeling and Ki-67 analysis to measure DC mobilization in SIV-naïve controls and animals with acute SIV infection. pDC frequencies were determined in bone marrow, blood and peripheral lymph nodes using flow cytometry and real-time RT-PCR used to determine the frequency of infected DC in lymph nodes from SIV-infected monkeys. Alterations of pDC function were determined using a TLR7/8 agonist and assessment of intracellular TNF-α and IFN-α by flow cytometry.

3.0 CHAPTER ONE. IDENTIFICATION AND RAPID DUAL-PLATFORM ENUMERATION OF PLASMACYTOID AND CD16^{+} MYELOID DENDRITIC CELLS IN RHESUS MACAQUES

3.1 PREFACE

This chapter is adapted from a submitted manuscript (Kevin N. Brown[1,2] and Simon M. Barratt-Boyes[1,2,3]. Work described in this chapter and is in fulfillment of specific aim 1.

[1]Department of Infectious Diseases and Microbiology, Graduate School of Public Health, and [2]Center for Vaccine Research and [3]Department of Immunology, School of Medicine, University of Pittsburgh, Pittsburgh, PA 15261, USA.

3.2 ABSTRACT

Dendritic cells (DC) are a heterogenous population of antigen presenting cells important in the control of innate and adaptive immune responses. Non-human primates are increasingly used for disease, transplantation, and vaccine trial studies, and contribute to our understanding of the role of DC in immunity. However, DC in rhesus macaques have been variably defined in peripheral blood by exclusion using lineage-specific lymphocyte markers leading to discrepancies in both their identification and enumeration. To better understand the phenotypic complexity of rhesus DC, we undertook a multi-parameter analysis of DC in blood and developed a rapid assay for enumeration. Flow cytometric analysis of DC in blood revealed nearly 100% of myeloid DC (mDC) expressed CD16 but not CD8 and moderate levels of both CD11b and CD56. In contrast, plasmacytoid DC (pDC) were phenotypically homogenous. In whole blood samples, simultaneous discrimination of mDC and pDC was inconsistent and resolved by first lysing red blood cells and washing followed by immunophenotypic analysis. Dual-platform analysis relying on mononuclear cell counts and the frequency of DC determined by flow cytometry from small volumes of RBC-lysed blood, averaged 50.0 mDC/μL and 2.5 pDC/μL of blood in normal rhesus macaques. This study provides evidence that rhesus mDC are more phenotypically homogenous than human mDC. In addition, information regarding the phenotypic complexity of rhesus macaque DC and their rapid enumeration may improve our understanding of the role of these cells in infectious disease.

3.3 INTRODUCTION

Dendritic cells (DC) are a heterogenous population of antigen-presenting cells (APC) important in the control of innate and adaptive immune responses (16). In the blood of humans and rhesus macaques, two major populations of DC have been described; $CD11c^{-}CD123^{high}$ plasmacytoid DC (pDC) and $CD11c^{+}CD123^{low}$ myeloid or 'conventional' DC (mDC). Human DC are traditionally identified based on the expression of HLA-DR and lack of expression of lineage markers CD3 (T cells), CD14 (monocytes), CD19 or CD20 (B cells), and CD16 or CD56 (natural killer cells) (65). More recently however, human $CD11c^{+}$ mDC circulating in blood were phenotypically subdivided into three additional subsets based on expression of CD16, CD1b/c, and BDCA-3 (25).

Despite the well characterized delineation of multiple DC subsets and lineage markers used in humans, studies of rhesus macaque DC have not reached a consensus regarding the use of standardized lineage markers (17, 19, 54, 85, 114, 130). In rhesus macaques, immature monocyte-derived DC have been shown to express moderate levels of CD11b, CD56 and CD16 suggesting mDC in blood may exhibit a similar phenotypic profile (131) and rhesus mDC have been subdivided based on CD11b expression (114). In addition, a minor subset of $CD8^{+}$ cells has been identified within the $Lin^{-}HLA\text{-}DR^{+}$ fraction of rhesus blood suggesting some mDC may express CD8 (19). Furthermore, flow cytometric analysis of rhesus blood for candidate NK cells revealed an undefined population of cells that were $CD3^{-}CD8^{-}CD20^{-/dim}CD16^{bright}$ (132),

leaving open the possibility that mDC express CD16 similar to humans (25). Lastly, a small number of $CD14^{-}CD56^{dim}$ cells accounting for less than 2% of lymphocytes and lacking NK cell associated lytic activity was observed in rhesus macaques (133). Therefore, it is imperative that the phenotypic complexity and overlap between rhesus DC and cellular populations such as monocytes and NK cells be addressed to increase our understanding of circulating cells in the peripheral blood of rhesus macaques.

Enumeration of DC subsets in the blood of both humans and rhesus macaques is gaining increased interest, particularly in studies of human immunodeficiency virus (HIV)(38, 39, 41-43, 46, 47, 87) and simian immunodeficiency virus (SIV) infection(49, 54, 85). Although considerable progress has been made towards developing rapid assays for evaluating $CD4^{+}$ T cell numbers (134), standardization of DC counting has been lacking. Historically, the most widely used method for DC and CD4 enumeration has been dual-platform analysis. Using this strategy, the total or absolute number of cells in blood is obtained from three clinical measurements; a white blood cell count, lymphocyte and monocyte percentage (differential), and a DC or $CD4^{+}$ T cell percentage using flow cytometric immunophenotyping. Alternatively, single-platform technologies determine absolute cell numbers in unmanipulated blood in a single tube containing a known number of fluorescent beads. Although considerable progress has been made towards using single-platform counting methods for evaluating $CD4^{+}$ T cell numbers (134), investigation of rapid assays for the enumeration of DC are limited (49, 135, 136).

In this study, circulating rhesus $CD11c^{+}$ mDC were uniformly $CD16^{+}$ $CD11b^{+}$ $CD56^{lo}$ $CD8^{-}$ $CD1c^{-}$ whereas $CD123^{+}$ pDC lacked expression of all these markers. Accurate DC counts were

obtained using a rapid dual-platform assay combining TruCOUNT enumeration of mononuclear cells in whole blood and multiparameter analysis of DC in peripheral blood leukocytes (PBL).

3.4 MATERIALS AND METHODS

3.4.1 Reagents

Antibodies were purchased from BD Biosciences (San Diego, CA) unless noted otherwise: CD3 (SP34), CD4 (L200), CD45 (DO58-1283), CD14 (M5E2), CD20 (2H7, eBioscience), HLA-DR (L243), CD123 (7G3), CD11c (S-HCL-3), CD16 (3G8 and VEP13, Miltenyi Biotec), CD56 (MY31), CD11b (D12 and ICRF44), CD8α (B9.11, Coulter), CD33 (AC104.3E3, Miltenyi Biotec), and CD1c (AD5-8E7, Miltenyi Biotec).

3.4.2 Animals and blood collection

Peripheral blood samples were collected in EDTA (K_2E) and ACD Vacutainers and processed within 4 h of collection from healthy adult rhesus macaques (*Macca mulatta*) of either sex. Complete blood cell counts were performed by an automated hematology blood analyzer approximately 24 h after blood collection by an outside vendor (Antech Diagnostics, Lake Success, NY). All procedures were approved by the University of Pittsburgh Instituitional Animal Care and Use Committee.

3.4.3 Sample preparation

Peripheral blood mononuclear cells (PBMC) were isolated from ACD-collected blood for rhesus macaques and human buffy coats by density gradient centrifugation over Histopaque-1077 (Sigma). In addition, rhesus PBMC depleted of $CD14^+$ monocytes were also used and designated as CD14-negative ($CD14^-$) PBMC. Alternatively, 50 or 100 µL EDTA-collected whole blood was treated with 1 or 2 mL ACK lysing buffer (0.15 M NH_4Cl, 10 mM $KHCO_3$, 0.1 mM Na_2EDTA in dH_2O, pH: 7.2 – 7.4), respectively, for 10 min at room temperature, centrifuged and washed two times with staining buffer prior to the addition of mAb.

3.4.4 TruCOUNT assay

For single-platform TruCOUNT analysis, 50 µL (T cells) or 100µL (DC) of reverse pipetted EDTA-collected peripheral blood was stained directly with mAb mixtures for 15 min at room temperature followed by the addition of 450µL (T cells) or 900µL (DC) BD FACS Lysing Solution for 15 min at room temperature, placed at 4ºC and analyzed within 4 h.

3.4.5 Flow cytometry

TruCOUNT determination of MNC, $CD4^+$ T cells and DC was performed by setting the cytometer threshold on CD45-PerCP fluorescence and acquiring at least 2,500 $CD45^+CD3^+CD4^+$ T cell events and 10,000 HLA-DR^+ events for DC analysis. For TruCOUNT and dual-platform analysis using PBL, $CD4^+$ T cells were identified using CD45-PerCP, CD3- Pacific Blue and CD4-FITC and DC were stained with the following panel: Pacific Blue-conjugated anti-CD3,

CD14, and CD20 (Lineage), HLA-DR-FITC, CD45-PerCP, CD123-PE, and CD11c-APC. For analysis of mDC and pDC in PBMC or $CD14^{-}$ PBMC, cells were stained with Pacific Blue-conjugated lineage markers, HLA-DR-PerCP, CD11c-APC and PE-conjugated CD11b, CD56, CD33, and CD16 or FITC conjugated CD8α and CD1c or CD11b-Alexa488. Expression of additional markers on pDC was determined as above except pDC were labeled using CD123-biotin followed by 20nM streptavidin QDot525 (Invitrogen) incubated at 4ºC for 25 min. Analysis of markers with possible low expression levels was determined using flow minus one (FMO) controls where all parameters used to define gated populations were included except for the antibody of interest (137). 1 - 4 x 10^6 cells were stained followed by incubation with a blue fluorescent amine-reactive viability dye (Invitrogen) for exclusion of dead cells, per the manufacturer's instructions. PBMC and PBL samples were fixed in 1% paraformaldehyde, kept at 4°C and analyzed within 4 h. For evaluation of lineage markers on DC, stopping gates were set at 1,000 mDC events or a minimum of 500 pDC events. For DC analysis in RBC-lysed blood (PBL) stopping gate was set at a minimum of 50 pDC events. For analysis of human PBMC, $CD11c^{+}$ mDC were defined as Lin^{-} (CD3, CD14, CD20, CD56, CD16) $HLA\text{-}DR^{+}$ $CD11c^{+}$ cells and monocytes as $CD14^{+}HLA\text{-}DR^{+}$. Data was collected on a BD LSRII and analyzed using BD FACSDiva software version 5.0.2. Histogram overlays were generated using FlowJo software version 7.4.2 (Tree Star, Ashland, VA).

3.4.6 Statistical analysis

Statistical analysis was perfomed using GraphPad software (San Diego, CA). Differences between counting methods were determined using the nonparametric paired Wilcoxon rank sum test. Two-tailed *P* values < 0.05 were considered significant.

3.5 RESULTS

3.5.1 Rhesus macaque myeloid dendritic cells express CD16, CD11b and CD56

In order to investigate the phenotypic complexity of rhesus macaque DC, we focused on defining the basic phenotypic profile of both mDC and pDC using comparative analysis to monocytes and NK cells by flow cytometry. DC subsets were simultaneously identified in PBMC as CD3, CD14, and CD20-negative (Lineage$^-$) HLA-DR$^+$ CD11c$^+$CD123$^-$ mDC or CD11c$^-$CD123$^+$ pDC (Fig. 1*A*). Rhesus pDC were phenotypically homogeneous and lacked expression of CD11b, CD56, CD8 and CD16, consistent with human pDC (25). However, approximately 50% of CD11c$^+$ mDC expressed moderate levels of CD11b and CD56 (Fig. 1*C*) compared to monocytes (Fig. 1*D*). Strikingly, nearly 100% of circulating mDC expressed CD16 with an intensity similar to rhesus NK cells (Fig. 1, *C* and *D*) and an alternative anti-CD16 mAb (VEP13) provided comparable results (data not shown). In addition, evaluation of an alternative CD11b clone (ICRF44) showed staining of a higher percentage of mDC (Fig. 1*E*). Overall, CD11c$^+$ mDC were 53-85% CD11b$^+$, depending on the mAb used, followed by 53% CD56$^+$ and 96% CD16$^+$ (Fig. 1*E*). Collectively, inclusion of all DC in rhesus peripheral blood is achieved using the standard lineage markers, CD3, CD14, and CD20.

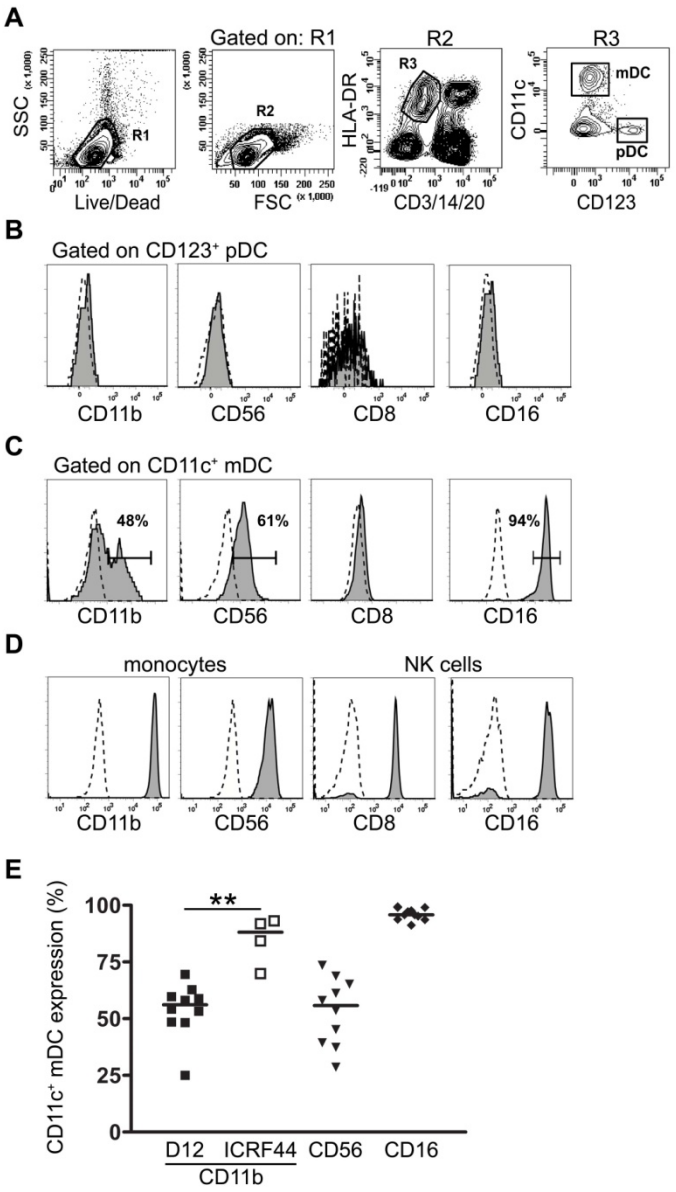

Figure 1. Rhesus macaque CD11c$^+$ mDC express CD11b, CD56 and CD16

A, Representative contour plots demonstrate the gating strategy used to define mDC and pDC in total PBMC or CD14$^-$ PBMC. DC were identified within the CD3/14/20-negative HLA-DR$^+$ fraction of live mononuclear cells (R3) as either CD11c$^+$ mDC or CD123$^+$ pDC. *B*, Phenotypic profile of CD123$^+$ pDC and (*C*) CD11c$^+$ mDC.
D, Expression level of each phenotypic marker by rhesus monocytes (CD14$^+$ HLA-DR$^+$) and natural killer (NK) cells (CD3/14/20-negative HLA-DR-negative). Histograms for each marker (filled histograms) are shown with respective isotype-matched control antibody (dashed lines). Histograms are representative of five (mDC) and two (pDC, monocytes, NK cells) experiments from different animals. *E*, Expression of the indicated markers and mAb clones (CD11b) by CD11c$^+$ mDC. $^{**}P < 0.01$. Symbols represent individual animals and horizontal bars represent the median.

3.5.2 Phenotypic characterization of rhesus CD16^{+} mDC

The finding that 50% of mDC expressed CD11b and CD56 led us to evaluate whether these markers may separate mDC into non-overlapping CD11b^{+}CD56^{-} and CD11b^{-}CD56^{+} subsets. In order to investigate this hypothesis, mDC were simultaneously stained with CD16, CD11b and CD56 (Fig. 2*A*). Based on the limited availability of directly conjugated cross-reactive mAbs, we used the CD11b clone ICRF44, which stains a greater percentage of mDC than clone D12 (Fig. 1*E*). Interestingly, the majority of CD11c^{+} CD16^{+} mDC were CD11b^{+}CD56^{+} and CD11b^{+}CD56^{-} (Fig. 2, *A* and *B*). Therefore, CD11c^{+}CD16^{+} mDC are heterogeneous for CD11b and CD56 with no clear evidence that these markers define non-overlapping mDC subsets.

In a recent study, CD1c was used to identify mDC in cynomolgus macaques and reported to cross react with rhesus PBMC (17, 49). Within the Lineage^{-} HLA-DR^{+} fraction, there was no evidence of CD1c expression by either CD11c^{-} or CD11c^{+} mDC. Parallel analysis revealed CD1c was expressed by approximately 30% of B cells (Fig. 2*C*), similar to humans (138). Evaluation of whether CD33 would further subdivide mDC revealed CD33 reactivity was restricted to rhesus granulocytes with low levels of expression similar to human monocytes (Fig. 2*D*). However, in contrast to humans, rhesus mDC and monocytes completely lacked CD33 expression (Fig 2*D*). Therefore, rhesus mDC lack expression of CD33 and CD1c but nearly all are CD16^{+} and phenotypically heterogenous with respect to CD11b and CD56 expression.

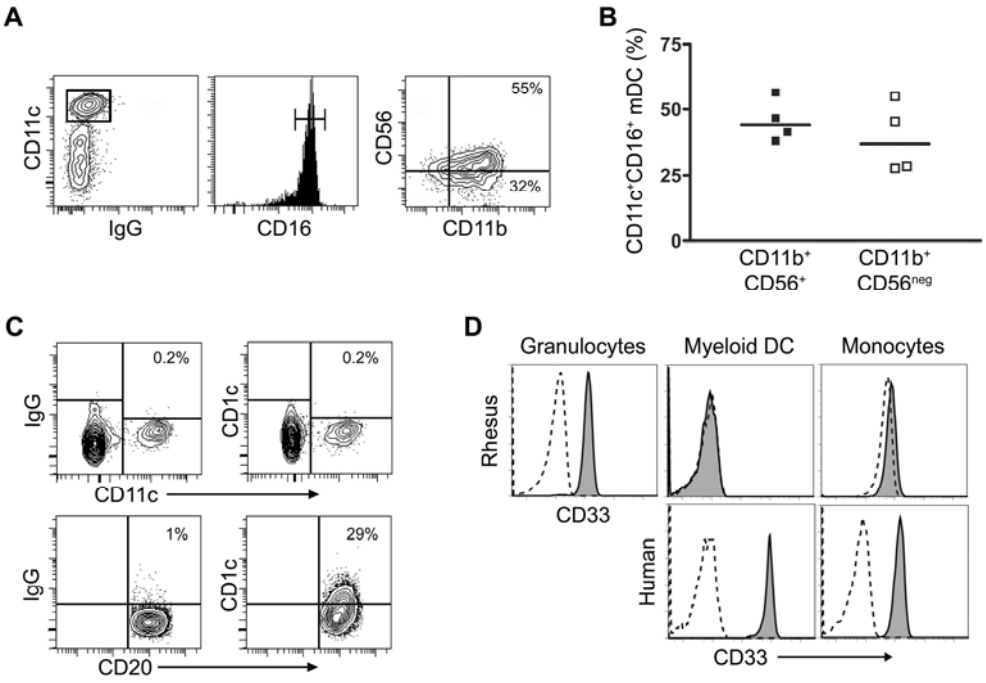

Figure 2. Overlapping subsets of CD11b$^+$ and CD56$^+$ mDC.

A, Plots demonstrate the gating strategy used to define subsets of CD16$^+$ mDC. *B*, Symbols represent individual animals and horizontal bars represent the median. *C*, Representative contour plots of CD1c expression by CD20$^+$ B cells and the Lin$^-$HLA-DR$^+$ fraction of rhesus PBMC (n=4). mDC are CD11c$^+$. *D*, Expression profile of CD33 on rhesus macaque granulocytes (CD45$^+$SSC^{high}), and rhesus or human mDC and monocytes (CD14$^+$HLA-DR$^+$). Histogram overlays are representative of two rhesus and two human samples. Dashed lines represent the level of background staining using the appropriate isotype control.

3.5.3 RBC-lysis yields increased mDC and pDC discrimination in whole blood

Having evaluated the expression of additional lineage markers by mDC in PBMC we sought to determine whether a single-platform cell counting technology could be used to simultaneously quantify both mDC and pDC subsets in undiluted blood from rhesus macaques. Using BD TruCOUNT® tubes, the presumptive DC fraction was identified by sequential gating similar to the analysis of PBMC (Fig. 3*A*). Specifically, mononuclear cells (MNC) containing both lymphocytes and monocytes were defined as CD45$^+$side-scatter (SSC)^{low} and DC identified within the CD3, CD14, CD20 (Lineage)-negative HLA-DR$^+$ fraction of blood (Fig. 3*A*). In

general, the delineation of Lin^{-} from Lin^{+} cells was less pronounced in undiluted blood compared to PBMC (Fig. 3*A*). In addition, the identification of $CD11c^{+}$ cells within the Lineage-negative HLA-DR^{+} fraction compared to isotype control staining was not well defined. However, $CD123^{+}$ pDC were easily identified within the Lineage-negative HLA-DR^{+} fraction of undiluted blood, consistent with the findings of others (49). As an alternative to the isolation of PBMC, we sought to determine whether the same small volume of blood used for TruCOUNT, first cleared of red blood cells (RBC) prior to mAb staining would permit clear discrimination of both mDC and pDC. Strikingly, mDC and pDC were readily identified in samples cleared of RBC and washed prior to the addition of antibodies (Fig. 3*B*). Comparatively, the distinct mDC and pDC populations were identified using either logarithmic or biexponential axis scaling, the latter permitting increased visualization of pDC (Fig. 3*B*, bottom panel). The Lin^{-}HLA-DR^{+} fraction of RBC-lysed whole blood represented approximately 3.6% of mononuclear cells with the majority of cells being mDC (59%) followed by pDC (2.8%) (Fig. 3*C*), similar to previous findings in PBMC (17, 54, 85). Therefore, RBC-lysis of small blood volumes prior to mAb staining permitted increased discrimination of both DC subsets in rhesus macaques.

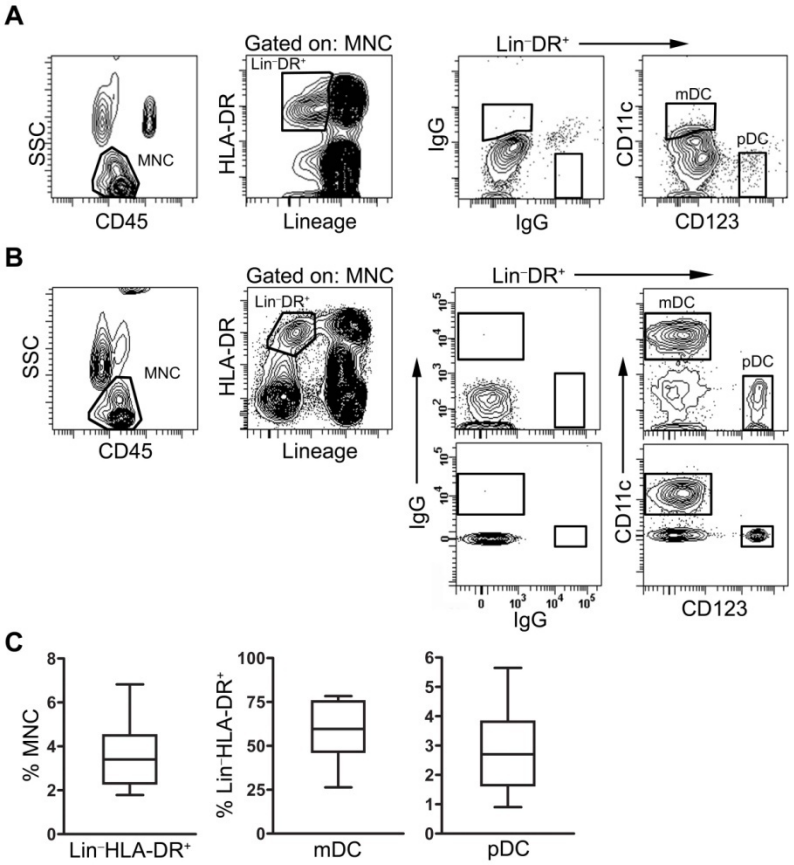

Figure 3. Increased DC subset discrimination in RBC-lysed whole blood.

A, Representative contour plots demonstrate the gating strategy used to define DC in whole blood or (*B*) RBC-lysed/washed blood samples. Mononuclear cells (MNC) were gated based on CD45 and SSC followed by gating on the Lineage-negative HLA-DR$^+$ fraction (Lin$^-$DR$^+$). mDC and pDC gates were determined using appropriate isotype controls. The bottom panels in (*B*) illustrate biexponential scaling to delineate DC subsets. *C*, Percentage of cells within the indicated cellular fractions of RBC-lysed/washed blood samples from rhesus macaques (n = 9). Box plots represent the 25th, 50th, and 75th percentiles and vertical lines represent the minimum and maximum values obtained.

3.5.4 Quantifying rhesus peripheral blood mononuclear cells using TruCOUNT

Given the ease with which DC subsets were identified in RBC-lysed blood, we explored combining single-platform TruCOUNT technology with the percentage of cells within the MNC fraction of blood determined by flow cytometry. First, we compared the absolute number of MNC in blood was compared using traditional complete blood cell counts (CBC) plus differential and gating of $CD45^{+}SSC^{low}$ MNC in TruCOUNT (Fig. 4*A*). Expectedly, there was no significant difference in the absolute number of MNC/μL of blood calculated using CBC results or BD TruCOUNT technology (Fig. 4*B*, $P = 0.5418$). In order to validate an approach using MNC counts determined by TruCOUNT and the percentage of cells within RBC-lysed whole blood (PBL), we turned to $CD4^{+}$ T cell enumeration. Qualitatively, the separation of $CD4^{+}$ T cells in PBL from other lymphocytes was increased compared to staining of undiluted whole blood (Fig. 4, *A* and *C*). Notably, there was no significant difference in either the frequency or absolute number of $CD4^{+}$ T cells in TruCOUNT or PBL samples (Fig. 4*D*). Thus, PBL samples offered the advantage of increasing phenotypic discrimination of $CD4^{+}$ T cells and more importantly, accurate enumeration of cells comparable to single-platform TruCOUNT technology.

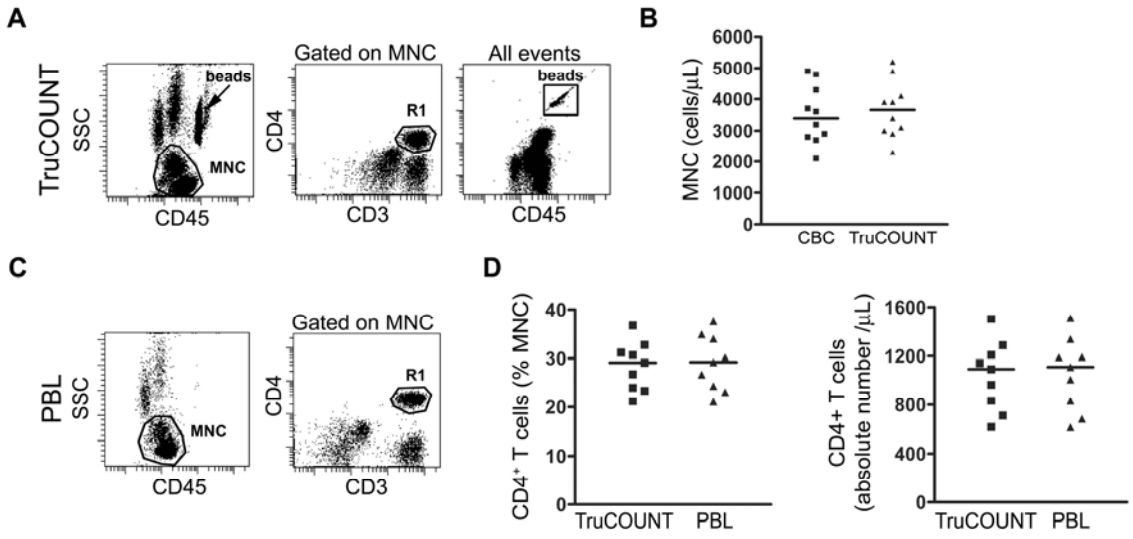

Figure 4. RBC-lysed whole blood permits accurate enumeration of $CD4^+$ T cells.

A, Dot plots demonstrate the gating strategy used to define mononuclear cells (MNC) and $CD4^+$ T cells for TruCOUNT determination of absolute numbers in blood. *B*, Absolute numbers of MNC were obtained using an automated hematology analyzer (CBC) and TruCOUNT technology. Absolute number of cells was determined by including a gate for the number of counting beads. Symbols represent individual animals and horizontal bars represent the median (n=10). *C*, Dot plots demonstrate the gating strategy used to define MNC and $CD4^+$ T cells in RBC-lysed PBL. *D*, Percentage and absolute number of $CD4^+$ T cells was determined for the same sample using TruCOUNT and dual-platform analysis using PBL. Symbols represent individual animals and horizontal bars represent the median. No significant differences were found were *B* and *D*.

3.5.5 Dual-platform quantitation of pDC and mDC in blood

The success of accurately enumerating $CD4^+$ T cells using RBC-lysed PBL combined with MNC counts determined by TruCOUNT led us to evaluate the utility of calculating absolute numbers of DC in the same manner. Similar to our earlier analysis (Fig. 3*B*), the frequency of DC in PBL was determined by gating on $CD45^+SSC^{low}$ MNC, $Lin^-HLA\text{-}DR^+$ cells and finally $CD11c^+CD123^-$ mDC or $CD11c^-CD123^+$ pDC (Fig. 5*A*). Using this dual-platform strategy, there were approximately 50 mDC/μL of blood in normal rhesus macaques (Fig. 5*B*). For pDC, dual-platform enumeration yielded numbers similar to single-platform TruCOUNT, with approximately 2.3 pDC/μL of blood (Fig. 5*C*). In order to quantify fluctuations in DC numbers,

four to six blood samples were obtained from each rhesus macaque over a 2 – 3 month period and enumerated using dual-platform analysis. Both mDC and pDC showed inter-individual variability with more pronounced intra-individual variability in mDC (Fig. 5*D*). Overall, the median absolute number of mDC was 50.1 cells/μL and 2.5 pDC/μL of blood (Fig. 5*E*), consistent with previous findings (17, 49, 54).

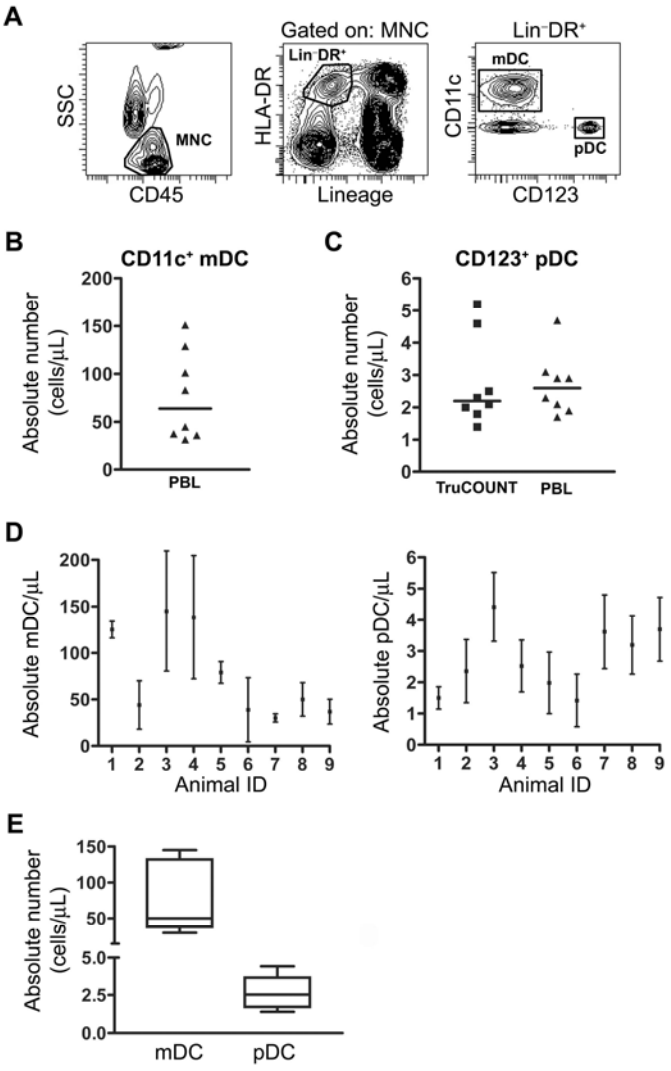

Figure 5. Dual-platform quantitation of rhesus DC subsets in blood.

A, Representative contour plots demonstrate the gating strategy used to define DC subsets in RBC-lysed blood samples. Mononuclear cells (MNC) were gated based on CD45 and SSC followed by gating on the Lineage-negative HLA-DR$^+$ fraction (Lin$^-$DR$^+$) and CD11c$^+$ mDC and CD123$^+$ pDC. *B*, Absolute numbers of mDC and pDC (*C*) were determined using freshly isolated whole blood (TruCOUNT) or RBC-lysed blood (PBL). Absolute numbers of DC in PBL were determined by multiplying the percentage of DC within the MNC fraction by the absolute number of MNC. Symbols represent individual animals and horizontal bars represent the median. *D*, Four to six consecutive counts of mDC (left panel) and pDC (right panel) in individual rhesus macaques over a 2-3 month period. The mean $\pm$ SD is shown. *E*, Absolute numbers of mDC and pDC were determined by combining the median number from the multiple measurements of each animal as shown in (*D*). Box plots represent the 25th, 50th, and 75th percentiles and vertical lines represent the minimum and maximum values (n=9).

3.6 DISCUSSION

The phenotypic complexity of DC subsets in both humans and rhesus macaques has led to considerable differences in DC identification and quantitation. The main contributing factors to these differences are mainly the mAb mixtures used to define Lin^- cells, isolation procedures, gating criteria for flow cytometric analysis and method of counting. Although progress has been made in providing more definitive strategies for DC analysis in humans (25, 136), non-human primate research is lacking in this regard. Therefore, we undertook an analysis of the composition of rhesus macaque Lin^- cells in an effort to define the phenotypic heterogeneity of rhesus macaque DC. In addition, we report that a dual-platform approach requiring simple RBC-lysis prior to mAb incubation provides a rapid assay for accurate assessment of absolute DC numbers comparable to previously used methods of DC enumeration.

Our results demonstrate that all $CD11c^+$ mDC in rhesus macaques are defined as $CD3^-$ $CD14^-CD20^-$ HLA-DR^+ $CD16^+$ and display heterogeneous expression of CD11b and CD56. The small number of $CD14^-CD56^{dim}$ rhesus lymphocytes lacking NK lytic function in previous studies (132, 139) may correspond to the $CD56^+$ mDC reported here. However, CD56 has been shown to be expressed by other cells within the Lin^-HLA-DR^+ fraction of PBMC not accounted for by either mDC or pDC (17). Interestingly, the cross-reactivity of the CD1c mAb used by us and others was restricted to rhesus B cells, consistent with humans. In humans, CD1c is expressed by B cells and a subset of mDC (25, 138) and more recent evidence indicates CD1c is expressed by a subset of Lin^- HLA-DR^+ cells in cynomolgus macaque with a phenotype and frequency consistent with $CD11c^+$ mDC (49). Nevertheless, $CD123^+$ pDC were phenotypically homogenous consistent with previous findings in both humans and macaques (17, 25, 49, 85).

The finding that nearly all rhesus $CD11c^+$ mDC express CD16 also provides considerable insight to immunophenotypic studies. In a previous study delineating NK cell populations in rhesus macaques, a population of $CD3^-CD8^-CD20^-CD16^+$ cells of unknown origin was found lacking expression of a panel of NK or B-cell markers and is likely the $CD11c^+CD16^+$ mDC reported here (132). Furthermore, rhesus macaque NK cells in peripheral blood defined as $CD3^-CD16^+$ would also include $CD16^+$ mDC (140). In contrast to $CD8^+$ rhesus NK cells, $CD16^+$ mDC do not express CD8, indicating NK cells are accurately defined as $CD3^-CD8^+CD16^+$ cells (132) and future studies of macaque DC may incorporate CD8 as an additional lineage marker to exclude NK cells within the Lin^-HLA-DR^+ fraction of blood (49).

Evaluation of performing single-platform counting of DC in rhesus macaques demonstrated poor immunophenotypic delineation and simultaneous identification of mDC and pDC. The reason for the reduced resolution of phenotypically defined cellular subsets in undiluted blood is unclear, although less than optimal binding of anti-human specific mAb on cynomolgus macaque cells has been observed (49). However, RBC-lysis and washing of cells prior to the addition of mAb increased the separation of discrete phenotypically-defined cellular subsets not only for DC but also $CD4^+$ T cells. This assay offers a rapid approach to study the phenotype of peripheral blood cells and should reduce the loss of cells associated with PBMC isolation requiring several washing steps prior to staining. The dual-platform approach resulted in absolute numbers of mDC similar to previous findings in humans (136) and macaques (17, 49). Interestingly, the absolute number of pDC determined using either single or dual-platform analysis was consistent with previous findings in rhesus macaques (17), but lower than pDC in either humans or

cynomolgus macaques (49, 136). The reason for such a difference in pDC frequencies between subspecies is unclear and may reflect true differences as pigtailed macaques contain pDC numbers closer to those reported for cynomolgus macaques (54).

In conclusion, this study further defined the phenotypic profile of rhesus macaque DC in blood and development of a rapid assay for their enumeration. Rhesus mDC were phenotypically heterogenous but all expressed CD16, a marker traditionally associated with rhesus NK cells and a minor proportion of monocytes. The ability to more accurately identify DC and other cells in blood coupled with a rapid assay for their enumeration will greatly enhance the elucidation of their role in both health and disease.

Our results have significant implications for the study of DC in the rhesus macaque and highlight some key similarities and differences between human and rhesus DC subsets. Rhesus blood $CD123^+$ pDC lacked expression of CD11b, CD56 and CD16, as in the human (25). In contrast, rhesus blood $CD11c^+$ mDC were uniformly $CD11b^+$ $CD16^+$ $CD56^{lo}$ $CD33^-$ $CD1c^-$, a phenotype that is quite distinct from human mDC (25). These findings clearly show that inclusion of antibodies to CD11b, CD16 and/or CD56 in the lineage cocktail will result in inadvertent exclusion of mDC from the $lineage^-$ MHC class II^+ gate when analyzing rhesus blood. Moreover, given that rhesus mDC expressed CD16 at intensities equivalent to NK cells when stained with the 3G8 clone, *in vivo* delivery of this antibody designed to deplete NK cells would likely also deplete mDC (141). The lack of CD1c staining on mDC defines an apparent phenotypic difference between rhesus and cynomolgus macaques, where CD1c has been used as an alternative marker to identify blood mDC (49). We found no evidence for the existence of

subsets of mDC in rhesus macaque blood, in contrast to mDC in humans (25). Our antibody panel was limited by the fact that antibodies to BDCA-2 and BDCA-3, which have been used to define discrete mDC subsets in human blood (25, 138), are not cross-reactive in the rhesus macaque (17). It is therefore possible that subsets of mDC do exist in rhesus macaque blood but cannot be identified based on available reagents.

4.0 CHAPTER TWO. PARALLEL LOSS OF MYELOID AND PLASMACYTOID DENDRITIC CELLS FROM BLOOD AND LYMPHOID TISSUES IN SIMIAN AIDS

4.1 PREFACE

This chapter is adapted from a published study (Kevin N. Brown[1,2], Anita Trichel[3], and Simon M. Barratt-Boyes[1,2,4]. 2007. Journal of Immunology 178: 6958-6967).

Work described in this chapter is in fulfillment of specific aim 2.

[1]Department of Infectious Diseases and Microbiology, Graduate School of Public Health, University of Pittsburgh, Pittsburgh, PA 15261

[2]Center for Vaccine Research, University of Pittsburgh, Pittsburgh, PA 15261

[3]Division of Laboratory Animal Resources, University of Pittsburgh, Pittsburgh, PA 15261

[4]Department of Immunology, School of Medicine, University of Pittsburgh, Pittsburgh, PA 15261

4.2 ABSTRACT

Myeloid (mDC) and plasmacytoid dendritic cells (pDC) are lost from the blood of HIV-infected individuals, associated with progressive disease. It has been proposed that DC loss is due to increased recruitment to lymph nodes, although this has not been directly tested. Similar to HIV-infected humans, we found that lineage-negative (Lin^-) HLA-$DR^+CD11c^+CD123^-$ mDC and Lin^- HLA-$DR^+CD11c^-CD123^+$ pDC were lost from the blood of SIV-infected rhesus macaques with AIDS. In peripheral lymph nodes of SIV-naïve monkeys, the majority of mDC were mature cells derived from skin, expressing high levels of HLA-DR, CD83, costimulatory molecules, and the Langerhans cell marker CD1a, whereas pDC expressed low levels of HLA-DR and CD40 and lacked costimulatory molecules, similar to pDC in blood. Surprisingly, both DC subsets were depleted from peripheral and mesenteric lymph nodes and spleen in monkeys with AIDS, although the activation status of the remaining DC subsets was similar to DC in health. In peripheral and mesenteric lymph nodes from animals with AIDS, there was an accumulation of Lin^-HLA-$DR^{mod}CD11c^-CD123^-$ cells that resembled monocytoid cells, but failed to acquire a DC phenotype upon culture, suggesting they were not DC precursors. mDC and pDC from lymphoid tissues of monkeys with AIDS were prone to spontaneous death in culture, indicating that apoptosis may be a mechanism for their loss in disease. These findings demonstrate that DC are lost from, rather than recruited to lymphoid tissue in advanced SIV infection, suggesting systemic DC depletion plays a direct role in the pathophysiology of AIDS.

4.3 INTRODUCTION

Dendritic cells (DC) are a heterogeneous population of APC essential in bridging the innate and adaptive immune responses (16). The two major DC subsets in humans are $CD11c^+$ conventional or myeloid DC (mDC) and $CD123^+$ plasmacytoid DC (pDC) (24, 64). Although mDC and pDC circulate as immature cells in blood, a major stage of their lifecycle takes place in lymphoid organs. mDC populate peripheral tissues as immature cells and migrate to lymph nodes through afferent lymphatics where they constitute the only mature DC population and stimulate antigen-specific T cells (16, 142, 143). In contrast, pDC migrate directly from blood to lymph nodes across high endothelial venules, residing in significant numbers and exhibiting increased recruitment to inflamed lymph nodes where they produce type I IFN and contribute to virus-specific T cell responses (62, 63, 80, 144).

Numerous studies have demonstrated that both mDC and pDC are decreased in blood during HIV infection (38, 39, 41, 43, 46, 87) with decline being inversely correlated with viral load and associated with reduced $CD4^+$ T cell numbers (41, 43). Recently, pDC were shown to undergo phenotypic and functional activation following exposure to HIV-1 in vitro, inducing the bystander maturation of mDC (50). It has been hypothesized that HIV-induced maturation of both DC subsets may lead to increased DC migration to lymph nodes, partly explaining their disappearance from blood as infection progresses (38, 50). There are a lack of data regarding changes in pDC number or phenotype within lymphoid tissue during HIV infection, and few studies defining alteration to mDC. In situ analysis of peripheral lymph node sections indicated that an accumulation of DC-$SIGN^+$ and $CD40^+$ DC occurred during acute HIV infection (51). However, in patients with chronic HIV infection, the proportion of DC in the spleen was the

same as uninfected controls, suggesting DC may not be recruited to lymphoid tissues in this later phase of infection (145). The current lack of a comparative analysis of mDC and pDC subsets in blood and lymphoid tissues leaves the question regarding the ultimate fate of DC during HIV infection unanswered.

Experimental infection of rhesus macaques with pathogenic SIV provides a valuable model to study the relationship between circulating and lymphoid-resident DC, with typical mDC and pDC identified in healthy monkeys (114, 146, 147). Although reports on the effects of SIV infection on circulating DC subsets have been conflicting (114, 146), there is evidence to suggest that SIV infection of macaques alters the status of DC in lymph nodes (52, 148). In the present study we defined mDC and pDC in lymphoid tissues and asked whether DC recruitment to lymphoid tissues during advanced SIV infection explains the loss of circulating DC in blood.

4.4 MATERIALS AND METHODS

4.4.1 Animals and viral infection

Adult, Indian rhesus macaques (*Macaca mulatta*) of both sexes were used. Seven animals were infected intrarectally with a characterized stock of the SIV/DeltaB670 primary isolate (149) and allowed to progress to AIDS as defined by $CD4^+$ T cell loss, increasing virus loads, lymphadenopathy, >20% weight loss, and/or opportunistic infections. Average time post-SIV infection was 50 weeks and the average time to AIDS following SIV/DeltaB670 infection is 11

months (150). Eight animals were used as SIV-naïve controls. All experiments were performed using protocols approved by institutional regulatory committees.

4.4.2 Cell isolation and flow cytometry

PBMC were isolated from heparinized blood by Ficoll gradient centrifugation. Single-cell suspensions of axillary and mesenteric lymph nodes and spleen were generated as described (151). For flow cytometric analysis mAb were purchased from BD Pharmingen or BD Immunocytometry Systems unless otherwise noted. Fresh or frozen PBMC, spleen and lymph node cell suspensions were blocked with FcR-Blocking Reagent (Miltenyi Biotec) for 15 min at 4°C before staining, except when analyzing CD16 expression. Simultaneous identification of mDC and pDC in PBMC and spleen was performed using a lineage (Lin) cocktail of FITC-conjugated mAb against CD3 (SP-34), CD14 (M5E2) and CD20 (2H7), with HLA-DR-CyChrome (G46-6), CD123-PE (7G3), and CD11c-APC (S-HCL-3). Expression of costimulatory molecules and other receptors on $CD11c^+$ mDC in PBMC and spleen was performed by staining with Lin-FITC, HLA-DR-CyChrome, CD11c-APC, and PE-conjugated CD80 (L307.4), CD86 (FUN-1), CD83 (HB15a; Coulter-Immunotech), CD40 (EA-5; Ancell) and CD1a (SK9). The immunophenotype of $CD123^+$ pDC in PBMC and spleen was determined using Lin-APC, HLA-DR-CyChrome, CD123-PE and FITC-conjugated CD80, CD83, CD86, and CD40. Three-color analysis of axillary and mesenteric lymph node single-cell suspensions was performed using Lin-FITC and HLA-DR-CyChrome in addition to PE-conjugated CD11c, CD123, CD14 (MΦP9), CD20 (L27), CD80, CD83, CD86, CD40, or CD1a. Analysis of purified cells was performed using previously mentioned mAb in addition to CD11b (D12), p55 (55K-2; DakoCytomation), CD16 (3G8), and CD45 (D058-1283). Multicolor flow cytometric

analysis of DC activation was performed using Lin-PE-Cy7, HLA-DR-PerCP, CD123-PE, CD11c-APC, FITC-conjugated costimulatory markers and CD20-Pacific Blue (2H7; eBioscience) plus a violet fluorescent LIVE/DEAD fixable dead cell stain (Invitrogen). Viability of cultured lymph node cell suspensions was performed in a similar manner using Lin-PE-Cy7, HLA-DR-PerCP, CD123-PE, CD11c-APC and the LIVE/DEAD stain. Isotype-matched control mAb were included in all experiments. After staining, cells were fixed with 2% paraformaldehyde and 500,000 to one million events acquired using a FACSCalibur or BD LSRII flow cytometer and analyzed with CellQuest Pro (BD Immunocytometry Systems) or BD FACSDiva software (BD Bioscience), respectively. Absolute DC numbers in blood were calculated by multiplying the percentage of $Lin^{-}HLA\text{-}DR^{+}CD11c^{+}$ or $Lin^{-}HLA\text{-}DR^{+}CD123^{+}$ cells in PBMC by the number of mononuclear cells/µl blood as determined by complete blood cell counts. Determination of absolute DC numbers in lymph node was calculated by multiplying the percentage of specific cell populations by the total lymph node cell count per gram of tissue.

4.4.3 Immunofluorescence and light microscopy

For immunofluorescence, lymph nodes were prepared as described (152) and sections incubated with 5 µg/ml purified mouse anti-human CD83, CD123, CD1a, or isotype-matched control Ab for 2 h followed by goat anti-mouse IgG conjugated to Alexa 488 (Molecular Probes) for 2 h. Nuclei were labeled with Hoescht 33342 (Sigma) and slides imaged using an Olympus Provis epifluorescence microscope (Melville, NY). For light microscopy, purified $Lin^{-}HLA\text{-}DR^{+}CD123^{-}$ cells were spun onto glass slides using a Shandon cytocentrifuge (Shandon) and stained with the Hema 3 stain set (Fisher Scientific).

4.4.4 Cell purification and culture

Purification of $Lin^{-}HLA\text{-}DR^{+}CD123^{-}$ lymph node cells was performed by depletion of CD3-, CD14-, and CD20-positive cells using magnetic microbeads (Miltenyi Biotec) according to the manufacturer's instructions. The depleted fraction was then labeled with anti-CD123-PE followed by anti-PE microbeads to remove $CD123^{+}$ pDC. The purity of the remaining cell population assessed by flow cytometry was >90%. Purified cells were cultured at 1 x 10^6/mL in medium alone or with 1000 U/mL recombinant human (rh) GM-CSF and 1000 U/mL rhIL-4 (both from Schering-Plough), 20 ng/mL rhIL-3 (R&D Systems), or 1.0 μg/mL soluble human trimeric CD40L (Immunex) for 24 h. For cell viability experiments, single-cell suspensions of peripheral lymph node or spleen were depleted of CD20-positive cells using magnetic microbeads (Miltenyi Biotec) according to the manufacturer's instructions and cultured at 1 x 10^6/mL for 24 h in medium alone or with 20 ng/mL rhIL-3.

4.4.5 Statistical analysis

Differences between SIV-naïve monkeys and animals with AIDS were determined by comparison of means using the nonparametric Mann-Whitney *U* test. Two-tailed *P* values less than 0.05 were considered significant at an alpha level of 0.05. Differences between DC viability before and after culture were determined by comparison of means using the paired *t* test. One-tailed *P* values less than 0.05 were considered significant. All data are presented as the mean ± SEM.

4.5 RESULTS

4.5.1 Blood mDC and pDC are lost in monkeys with AIDS

To clarify whether DC are reduced in the blood of monkeys with AIDS, the two major DC subsets were identified in PBMC as $Lin^{-}HLA\text{-}DR^{+}CD11c^{+}CD123^{-}$ mDC or Lin^{-} $HLA\text{-}DR^{+}CD11c^{-}CD123^{+}$ pDC (Fig. 6*A*). Previous studies of macaque DC included CD11b and CD16 as lineage markers to stain NK cells (19, 146). However NK cells are found within the Lin^{-} $HLA\text{-}DR^{-}$ fraction of PBMC from rhesus macaques (153) thus eliminating the need to include NK cell markers for exclusion from the $Lin^{-}HLA\text{-}DR^{+}$ fraction of PBMC. In addition, preliminary experiments demonstrated that mDC expressed CD16 as well as low levels of CD11b (data not shown), consistent with the findings of others (114). Hence we did not include mAb to CD16 and CD11b in our analyses. In healthy monkeys and animals with AIDS, mDC predominated in the $Lin^{-}HLA\text{-}DR^{+}$ fraction, while pDC comprised only a minor proportion of cells (Fig. 6*A*), consistent with previous findings (146, 147). In addition, mDC and pDC expressed similar and relatively low levels of HLA-DR in SIV-naïve monkeys (Fig. 6*A*) and animals with AIDS (data not shown). When the absolute number of cells was calculated, mDC and pDC were significantly reduced in the blood of animals with AIDS while the number of Lin^{-} $HLA\text{-}DR^{+}CD11c^{-}CD123^{-}$ cells was relatively unchanged compared to SIV-naïve monkeys (Fig. 6*B*). The phenotype of mDC from SIV-naïve monkeys and animals with AIDS was similar, expressing low levels of CD86 and lacking CD80, CD83, and CD40 (Fig. 6*C*). pDC from both groups were also phenotypically similar, except for a slight increase of CD40 expression in monkeys with AIDS (Fig. 6*D*). These data indicate that circulating mDC and pDC in rhesus

macaques are immature cells that are significantly decreased during simian AIDS, consistent with the findings in HIV-infected individuals (38, 39, 41, 43, 87).

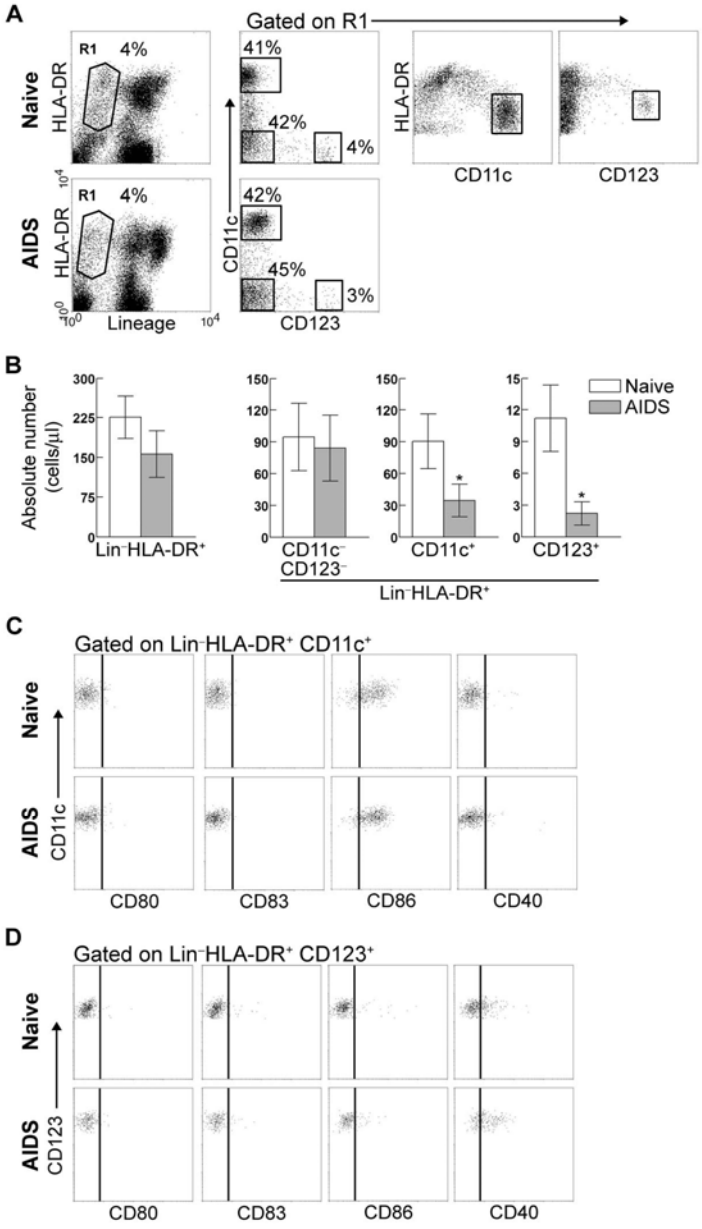

Figure 6. mDC and pDC are decreased in blood during simian AIDS

A, PBMC were gated based on forward/side scatter characteristics and DC identified within the lineage (CD3, CD14, CD20)-negative (Lin^-) HLA-DR^+ fraction (R1) from SIV-naïve animals and monkeys with AIDS. One representative experiment of eight is shown to demonstrate the gating strategy used to identify DC subsets. Numbers represent the percentage of cells within R1. *B*, Absolute number of cells/µl of blood for cell populations within the Lin^-HLA-DR^+ fraction (R1) are shown. Data represent the mean ± SEM for naïve monkeys (n=6) and animals with AIDS (n=4). **P*<0.02. Immunophenotype of (*C*) $CD11c^+$ mDC and (*D*) $CD123^+$ pDC in SIV-naïve animals and macaques with AIDS. One representative experiment of four is shown for both groups. Vertical bars denote the level of isotype control Ab staining.

4.5.2 High proportion of pDC and mature, epidermis-derived mDC in superficial lymph node of healthy macaques

In order to determine the effects of SIV infection on mDC and pDC in lymph nodes we first characterized DC subsets from normal, SIV-naïve macaques in a manner comparative to blood. Initially, a population of cells not observed in blood and expressing high levels of HLA-DR was identified which appeared to express lineage markers, similar to recent studies using human lymph nodes (32). However, staining with different mAb clones than those used in the lineage cocktail revealed a lack of CD14 and CD20 expression, indicating a high level of autofluorescence rather than lineage marker expression (Fig. 7*A*). Therefore, in all future analyses, this unique population was included in the gate defining the $Lin^{-}HLA\text{-}DR^{+}$ fraction of the lymph node. In normal monkeys, the $Lin^{-}HLA\text{-}DR^{+}$ fraction represented only 2% of total lymph node cells and could be subdivided into three populations based on HLA-DR expression; $HLA\text{-}DR^{hi}$, $HLA\text{-}DR^{mod}$, and $HLA\text{-}DR^{lo}$ (Fig. 7*B*). The majority of $CD11c^{+}$ mDC were $HLA\text{-}DR^{hi}$ with a minor proportion being $HLA\text{-}DR^{mod}$, whereas $CD123^{+}$ pDC were exclusively $HLA\text{-}DR^{lo}$ (Fig. 7*B*), demonstrating that mDC and pDC in lymph nodes could be differentiated based on HLA-DR expression, similar to recent findings in humans (32). $Lin^{-}HLA\text{-}DR^{hi}$ mDC uniformly expressed moderate to high levels of CD80, CD83, CD86, and CD40, a phenotype characteristic of mature DC (Fig. 7*C*). In contrast, $Lin^{-}HLA\text{-}DR^{lo}$ pDC lacked CD80, CD83, and CD86, and expressed low levels of CD40, consistent with immature cells (Fig. 7*C*). Lastly, the $Lin^{-}HLA\text{-}DR^{mod}$ population displayed an intermediate phenotype, with the majority of cells expressing CD80, CD86, and CD40 but low to undetectable levels of CD83 (Fig. 7*C*).

In the steady state, the majority of lymphoid organ DC with a mature phenotype are those that migrate from epithelial surfaces (143). Mature DC in peripheral lymph nodes originate from either dermal DC or epidermal LC, the latter identified by strong expression of CD1a (154). Notably, $Lin^{-}HLA\text{-}DR^{hi}$ mDC, but not other DC subsets in the superficial lymph node, expressed CD1a (Fig. 7*C*). In contrast, CD1a was not expressed by cells within the $Lin^{-}HLA\text{-}DR^{+}$ fraction of blood (Fig. 7*D*), consistent with findings in humans (25). Collectively, these findings demonstrate that in superficial lymph nodes from SIV-naïve monkeys, pDC are phenotypically immature and likely derive from blood, whereas the majority of mDC are mature, epidermis-derived cells, consistent with studies of lymph node DC in mice and humans (31, 62-64).

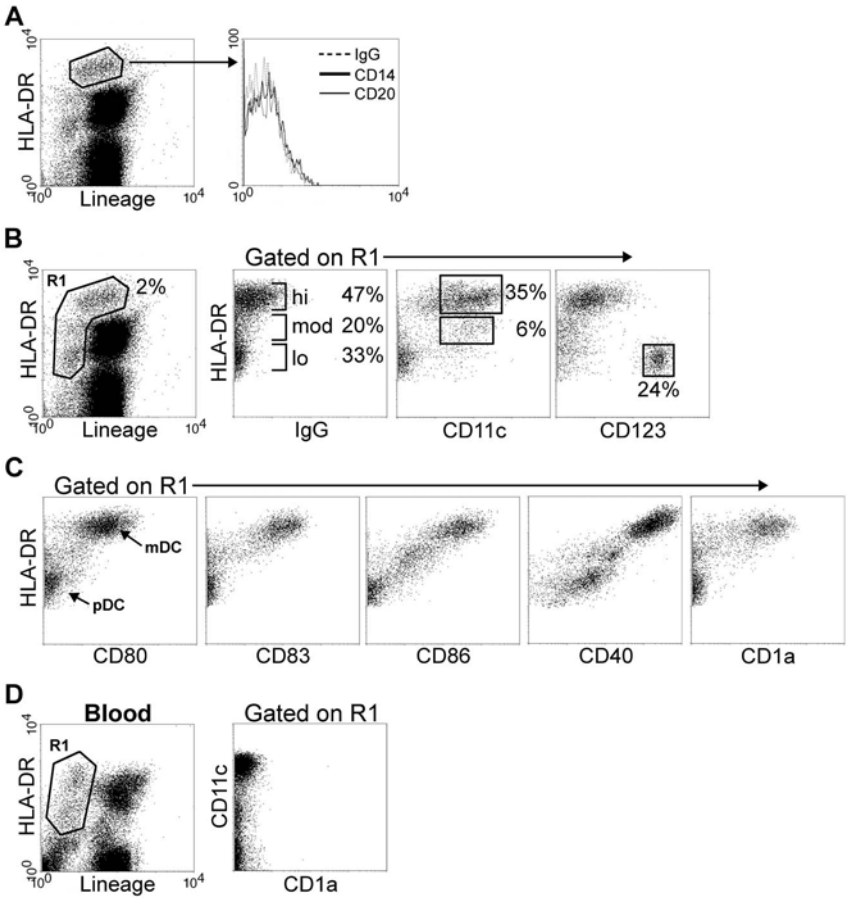

Figure 7. pDC and epidermal-derived mature mDC differentially express HLA-DR in superficial lymph node from normal monkeys

A-C, Axillary lymph node cell suspensions from SIV-naïve monkeys were analyzed by flow cytometry. Total lymph node cells were gated based on forward/side scatter characteristics and DC identified within the $Lin^{-}HLA\text{-}DR^{+}$ fraction (R1). ***A*,** Staining of cells expressing high levels of HLA-DR with isotype control Ab or Ab to CD14 and CD20. *B*, Representative dot plot demonstrating the gating strategy used to define the $Lin^{-}HLA\text{-}DR^{+}$ fraction (R1) of lymph node and the three populations of HLA-DR-expressing cells within R1. Numbers represent the percentage of cells within R1 indicated by gates or brackets. *C*, Expression of maturation and costimulatory molecules and CD1a by $Lin^{-}HLA\text{-}DR^{+}$ cells. *D*, Lack of CD1a expression by the $Lin^{-}HLA\text{-}DR^{+}$ fraction of PBMC. Data shown are representative of four (*A*,*C*,*D*) and 16 (*B*) experiments.

4.5.3 Major loss of pDC and epidermis-derived mature mDC from superficial lymph nodes in monkeys with AIDS

To determine the impact of SIV on DC populations in lymphoid tissue, we analyzed superficial lymph nodes from animals with AIDS. A major loss in the proportion of the $Lin^{-}HLA\text{-}DR^{hi}$ cells was noted, corresponding to a reduction of $CD11c^{+}$ mDC. In addition, there was a dramatic decrease in the proportion of $CD123^{+}$ pDC in monkeys with AIDS compared to SIV-naïve animals (Fig. 8, *A* and *C*). Although reduced, the remaining mDC exhibited a mature phenotype expressing CD80, CD83, CD86, CD40, and CD1a, while pDC only expressed CD40 (Fig. 8*B*), similar to SIV-naive monkeys. Despite the reduction of pDC and mature mDC, the proportion of lymph node cells within the $Lin^{-}HLA\text{-}DR^{+}$ fraction increased in animals with AIDS, related to an increase of $HLA\text{-}DR^{mod}$-expressing cells (Fig. 8, *A* and *C*). This population was not accounted for by either mDC or pDC and displayed a less defined phenotype, expressing CD40, low CD80, heterogeneous CD86, but not CD83 or CD1a (Fig. 8, *A* and *B*). To determine whether decreases in the proportion of mDC and pDC translated to an absolute loss of cells, cell numbers were standardized against tissue mass. The total number/gram of $Lin^{-}HLA\text{-}DR^{+}$ cells did not change between naïve animals and monkeys with AIDS, but the absolute number of $Lin^{-}HLA\text{-}DR^{hi}$ cells was significantly decreased while $Lin^{-}HLA\text{-}DR^{mod}$ cell numbers increased (Fig. 8*D*). When the $Lin^{-}HLA\text{-}DR^{+}$ fraction was analyzed for expression of CD11c and CD123, the absolute numbers of both pDC and mature mDC were significantly decreased compared to SIV-naïve animals (Fig. 8*D*), consistent with the observed changes in cell proportions.

In general, lymph nodes from animals with AIDS contained approximately 50% fewer cells per gram of tissue than SIV-naïve monkeys likely due to tissue fibrosis and lymphadenopathy (data

not shown). Hence, assessment of DC subsets as absolute number of cells/gm of tissue may be influenced by the stage of disease. Therefore, in order to confirm the reduction in both percentage and absolute number of DC in lymph nodes during AIDS, immunofluorescent analysis was performed on lymph node sections. CD83 and CD1a mAb were used to identify mature mDC, as staining was superior to that of the CD11c mAb (data not shown). In naïve animals, both $CD83^{bright}$ and $CD1a^{+}$ cells resided in lymph node paracortical regions outside of follicles (Fig. 8, *E* and *G*). Consistent with our observations by flow cytometry, very few $CD83^{bright}$ or $CD1a^{+}$ cells were found in lymph nodes from animals with AIDS (Fig. 8, *F* and *H*). Staining for CD123 demonstrated that pDC also resided in paracortical areas of lymph node from naïve animals and confirmed their depletion in animals with AIDS (Fig. 8, *I* and *J*).

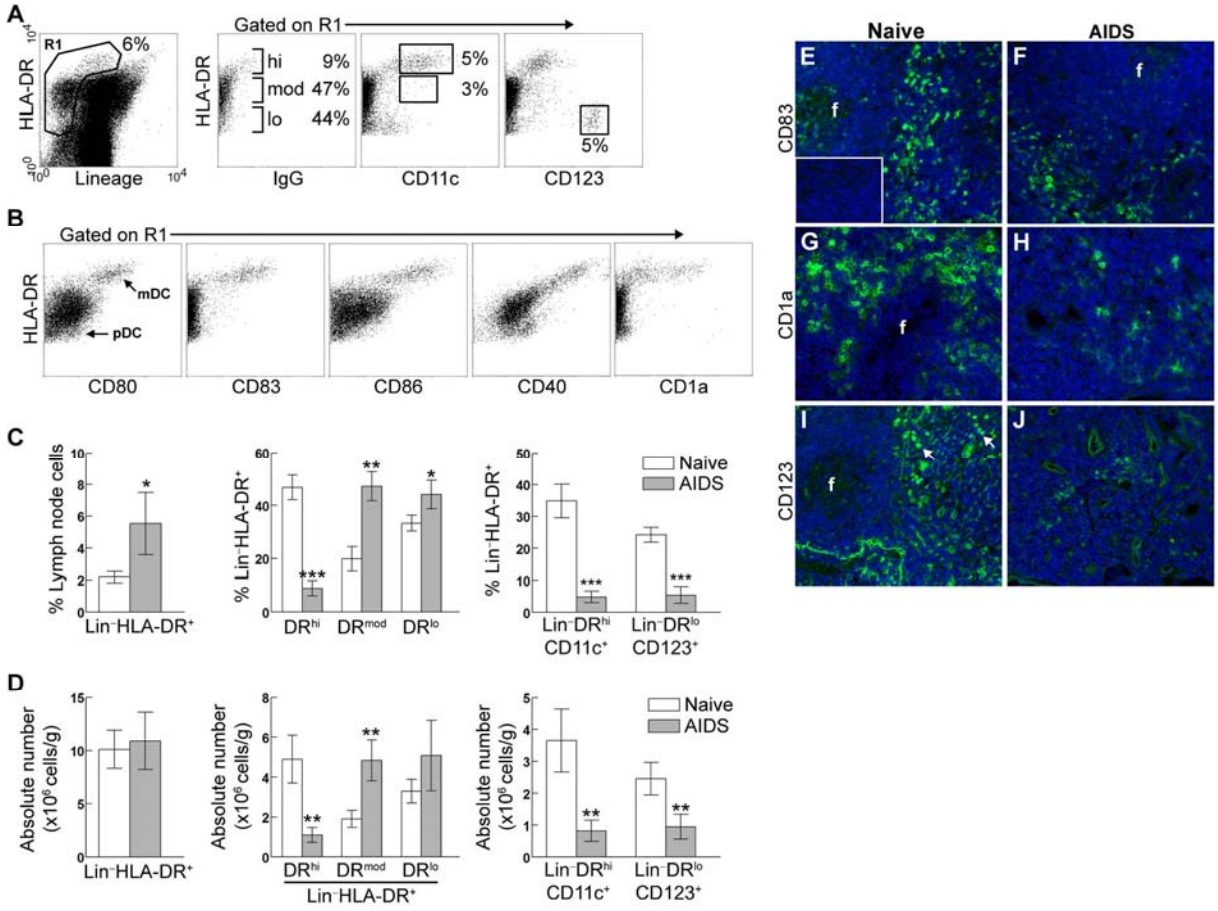

Figure 8. pDC and mature mDC are depleted in superficial lymph node from monkeys with AIDS

A-B, Axillary lymph node cells from monkeys with AIDS were analyzed by flow cytometry and DC identified within the $Lin^{-}HLA\text{-}DR^{+}$ fraction (R1). *A*, Representative plot illustrating the gating strategy used to define R1 and the three HLA-DR-expressing populations within R1. Numbers represent the percentage of cells within R1 denoted by gates or brackets. *B*, Flow cytometric analysis of maturation and costimulatory molecule expression by cells within R1. *C*, Percentage and (*D*) absolute number of cells/gram of tissue within the $Lin^{-}HLA\text{-}DR^{+}$ fraction of lymph node from SIV-naïve monkeys (n=8) and animals with AIDS (n=7). Data represent the mean ± SEM. $*P<0.05$, $**P<0.01$, $***P<0.001$. (*E-J*) Immunofluorescent analysis of axillary lymph node sections from both groups of monkeys for expression of CD83 (*E*,*F*), CD1a (*G*,*H*), and CD123 (*I*,*J*). Isotype control Ab is inset in (*E*). Positive staining for the indicated markers is in green and cell nuclei stained with Hoescht dye in blue. F = follicle. Arrows in (*I*) indicate individual cells expressing CD123. Images are representative of three animals per group. Original magnification 200X.

To further analyze the phenotype of DC subsets in peripheral lymph nodes we used a 6-color flow cytometry panel. We gated out non-viable and $CD20^+$ cells and analyzed pDC and mDC simultaneously (Fig. 9*A*). In SIV-naïve animals, the majority of $Lin^-HLA\text{-}DR^+CD11c^+$ mDC expressed CD80, CD83, CD86, and CD40 (Fig. 9*B*) consistent with our previous results. However in monkeys with AIDS, the remaining mDC lacked CD83, but retained expression of CD40 and low levels of CD80 and CD86 (Fig. 9*B*). This likely reflects the preferential loss of mature, skin-derived mDC from lymph nodes with the remaining mDC being primarily the relatively immature $HLA\text{-}DR^{mod}$ cells (Fig. 8*A*). pDC from SIV-naïve animals and monkeys with AIDS were phenotypically similar and expressed similar levels of CD40 (Fig. 9*B*), suggesting that the remaining pDC did not have an altered state of activation in peripheral lymph nodes.

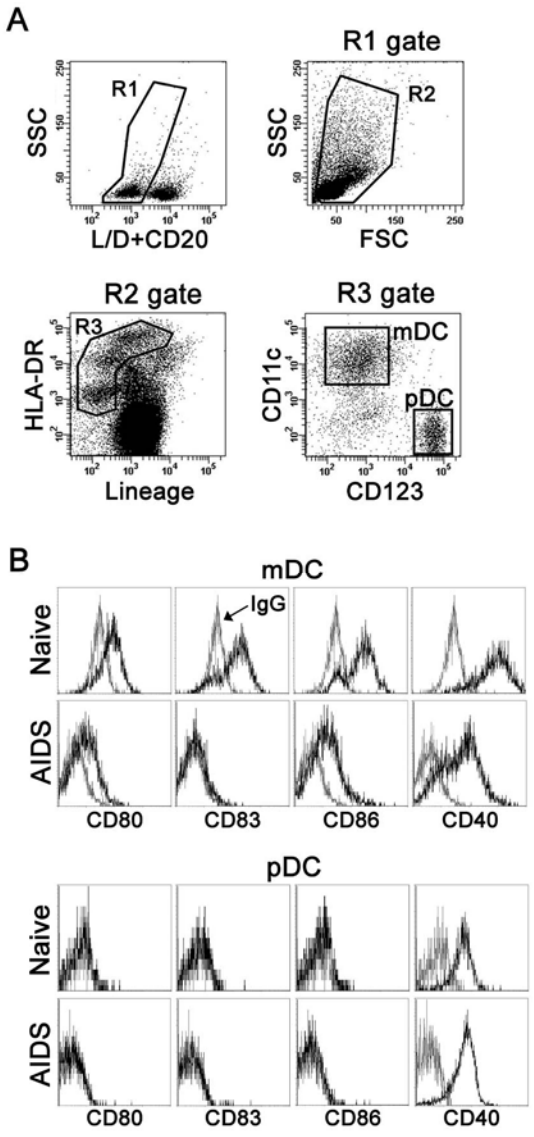

Figure 9. Multicolor analysis of DC subsets in peripheral lymph nodes.

A-B, Lymph node single-cell suspensions were labeled with the indicated mAb followed by staining with the LIVE/DEAD cell viability dye (L/D). *A*, Representative plots from an SIV-naïve animal demonstrating the gating strategy used to define DC subsets. Viable, CD20-negative cells were gated against side scatter (SSC) (R1) followed by an additional forward scatter (FSC)/SSC gate (R2). DC subsets were simultaneously identified within the $Lin^{-}HLA\text{-}DR^{+}$ fraction (R3) and analyzed for maturation and costimulatory molecule expression in (*B).* *B*, Costimulatory molecule expression (heavy line) versus isotype control staining (thin line) in mDC (top panels) and pDC (bottom panels) from SIV-naïve monkeys and animals with AIDS. All data are representative of four SIV-naïve animals and four monkeys with AIDS.

4.5.4 mDC and pDC are decreased in mesenteric lymph node and spleen during AIDS

To determine if the decreases in pDC and mature mDC in superficial lymph nodes during AIDS reflected alterations in other lymphoid compartments, we extended our analysis to the mesenteric lymph nodes. As in superficial lymph nodes, three populations of HLA-DR-expressing cells could be distinguished within the $Lin^{-}HLA\text{-}DR^{+}$ fraction of mesenteric lymph node from SIV-naïve animals, with the majority of mDC being $HLA\text{-}DR^{hi}$ and pDC being $HLA\text{-}DR^{lo}$ (Fig. 10*A*). Furthermore, the pattern of maturation and costimulatory molecule expression of DC closely resembled that of superficial lymph nodes from both groups, with $HLA\text{-}DR^{hi}$ mDC having a mature phenotype and $HLA\text{-}DR^{lo}$ pDC having an immature phenotype (Fig. 10*B*). Notably, Lin^{-} $HLA\text{-}DR^{hi}$ $CD11c^{+}$ mature mDC from both groups lacked expression of CD1a (Fig. 10*B*), consistent with findings in human lymphoid tissues draining mucosal epithelium (31, 155). Overall, the proportion of pDC and mature mDC decreased whereas the proportion of $Lin^{-}HLA\text{-}DR^{mod}$ cells increased in monkeys with AIDS (Fig. 10, *A* and *C*), similar to superficial lymph nodes.

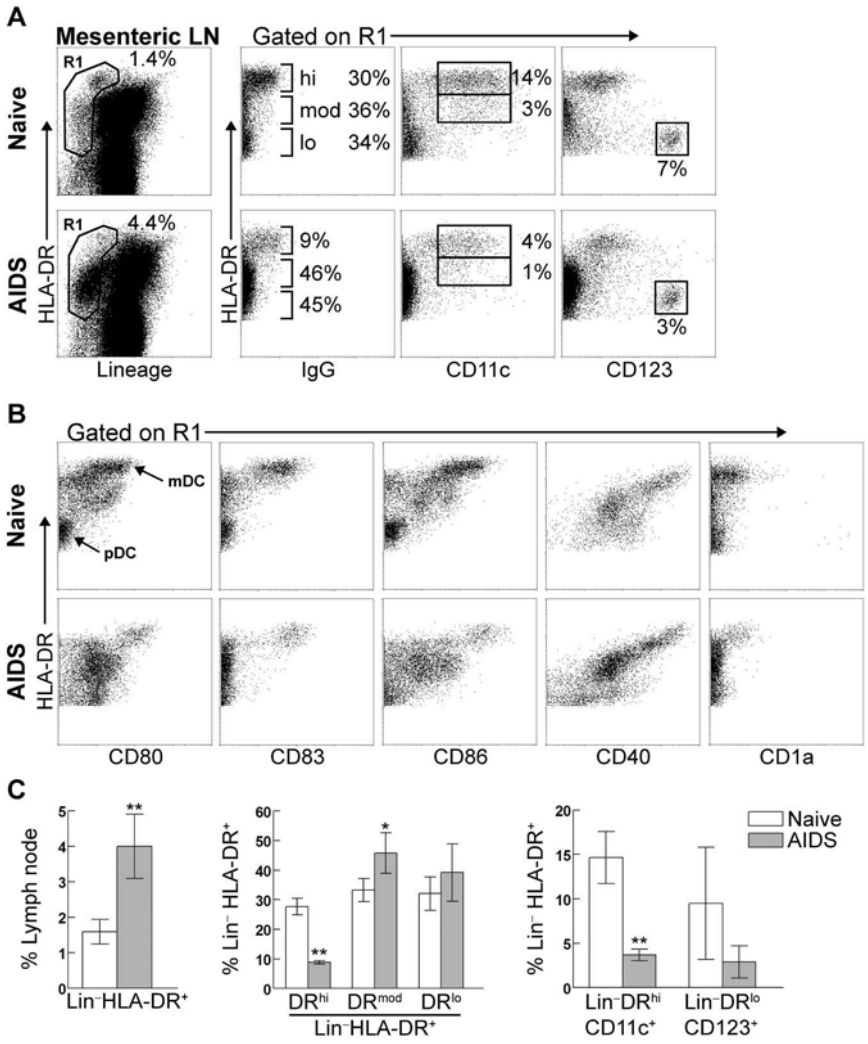

Figure 10. mDC and pDC are decreased in mesenteric lymph nodes from animals with AIDS

A, Mesenteric lymph node cells from SIV-naïve monkeys and animals with AIDS were analyzed by flow cytometry and DC identified within the $Lin^{-}HLA\text{-}DR^{+}$ fraction (R1). A representative dot plot demonstrating the gating strategy used to define R1 and the three HLA-DR-expressing populations is shown. Numbers represent the percentage of cells within R1 indicated by gates or brackets from one representative experiment of 4 (naïve) and 5 (AIDS) animals. *B*, Dot plots demonstrating the expression pattern of maturation and costimulatory molecules and CD1a in an SIV-naïve monkey and an animal with AIDS. mDC and pDC denote the location of these cells within the $Lin^{-}HLA\text{-}DR^{+}$ fraction. Representative of four animals per group. *C*, Percentage of cells within R1. Data represent the mean ± SEM for naïve animals (n=4) and monkeys with AIDS (n=4). **P*<0.04, ***P*<0.02

Finally, we assessed whether DC may have accumulated in the spleen, which anatomically is accessible only via the blood. The spleen lacked the HLA-DRhi population of cells corresponding to epithelium-derived mature mDC in lymph nodes (Fig. 11*A*), consistent with previous finding in mice (143, 156). Both mDC and pDC in spleen were significantly reduced in monkeys with AIDS compared to normal animals (Fig. 11*B*). The phenotype of splenic DC in both groups was similar, except for a marginal increase of CD40 expression in animals with AIDS (Fig. 11, *C* and *D*).

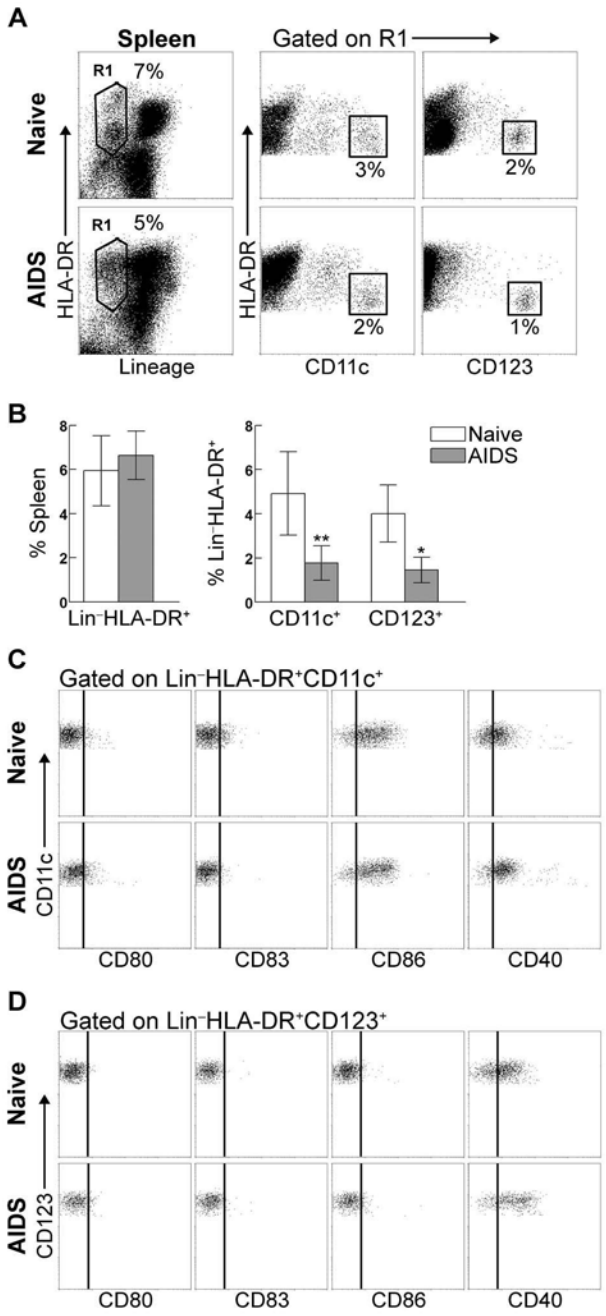

Figure 11. mDC and pDC are depleted in spleen from monkeys with AIDS.

A, Single-cell suspensions of spleen from SIV-naïve monkeys and animals with AIDS were labeled with the indicated mAb and DC identified within the $Lin^{-}HLA\text{-}DR^{+}$ fraction (R1). *B*, Percentages of cells within R1 from SIV-naïve animals (n=5) and animals with AIDS (n=4). Data represent the mean ± SEM. **P*<0.04, ***P*<0.02. *C-D* Dot plots showing the expression of maturation and costimulatory molecules by (*C*) mDC ($Lin^{-}HLA\text{-}DR^{+}CD11c^{+}$) and (*D*) pDC ($Lin^{-}HLA\text{-}DR^{+}CD123^{+}$) in an SIV-naïve animal and an animal with AIDS. Vertical bars denote the level of isotype control Ab staining. All data are representative of five SIV-naïve animals and four monkeys with AIDS.

4.5.5 Lin$^-$HLA-DR^{mod} cells that accumulate in lymph nodes from animals with AIDS do not acquire a DC phenotype following culture

In a previous study, we showed that culture of Lin$^-$HLA-DR$^+$CD11c$^-$CD123$^-$ cells from blood resulted in CD11c expression by a major fraction of cells indicative of DC precursors (147), and it is possible that the population of Lin$^-$HLA-DR^{mod}CD11c$^-$CD123$^-$ cells in lymph nodes during AIDS similarly represent DC precursors. Light microscopic analysis of purified Lin$^-$HLA-DR^{mod}CD123$^-$ cells revealed a dull gray-blue cytoplasm and convoluted nuclei, resembling monocytoid cells (Fig. 12*A*). Flow cytometric analysis of purified Lin$^-$HLA-DR^{mod}CD123$^-$ cells prior to culture demonstrated CD45 and CD40 expression by all cells while approximately 50% expressed the costimulatory molecule CD86 (Fig. 12*A* and *B*). The Lin$^-$HLA-DR^{mod} population lacked expression of the DC markers, CD11c and CD123, consistent with the analysis of total lymph node cells, as well as the pan DC marker p55 (Fig. 12*B*). In addition, freshly isolated cells did not express CD11b or CD16, suggesting they are not NK cells (Fig. 12*B*). To test the hypothesis that Lin$^-$HLA-DR^{mod} CD11c$^-$ CD123$^-$ cells may represent DC precursors, purified cells were cultured in growth factors known to result in DC differentiation. Culture with GM-CSF and IL-4, IL-3, or CD40L did not result in CD11c or CD123 expression (Fig. 12*C*), indicating the Lin$^-$HLA-DR^{mod} cells were unlikely to be DC precursors. In addition, approximately 50% of the cells were non-viable after 24 h by trypan blue exclusion (data not shown), indicating growth factors had no impact on cell survival. Culture also did not result in CD14 or CD20 expression (Fig. 12*C*), ruling out the possibility that this unique population differentiated to a monocyte/macrophage or B cell. Nevertheless, under all conditions the majority of cells upregulated CD86 expression demonstrating an effect of culture (Fig. 12*C*).

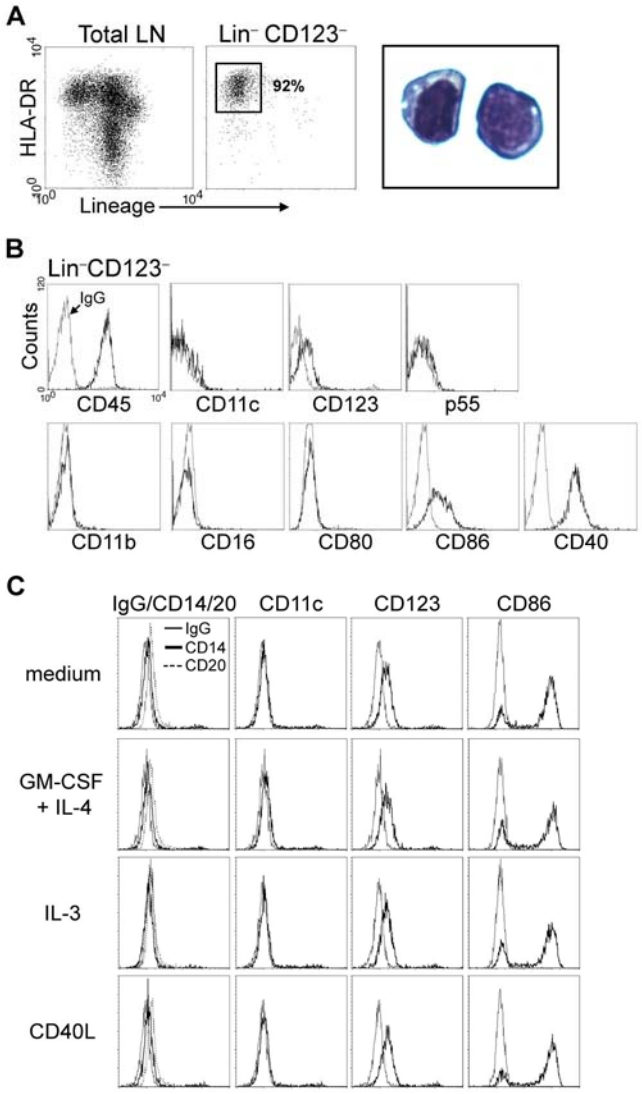

Figure 12. Lin⁻HLA-DR^{mod} cells from monkeys with AIDS are not DC precursors.

A, Lymph node single-cell suspensions were depleted of Lin$^+$ and CD123$^+$ cells and the depleted fraction analyzed by flow cytometry or stained with Hema 3 and examined by light microscopy. Original magnification 1000X. *B*, Purified cells from (*A*) were analyzed with a panel of mAb by flow cytometry. *C*, Purified cells were analyzed by flow cytometry following 24 h culture in the indicated conditions. Data are representative of three animals analyzed.

4.5.6 Spontaneous death of mDC and pDC from lymphoid tissues of monkeys with AIDS

To begin to address the mechanism of DC depletion, we sought to determine whether DC in animals with AIDS may be susceptible to spontaneous cell death in culture. To increase the frequency of DC, we depleted lymph node or spleen cell suspensions of $CD20^+$ B cells, and to provide a survival factor for pDC we included IL-3 (64). Before and 24 h after culture, we used the LIVE/DEAD viability dye to identify post apoptotic or necrotic cells within the mDC or pDC fraction (Fig. 13*A*). We first studied mDC and pDC from spleen, which are phenotypically similar to their respective DC subsets in blood. At the onset of culture, mDC and pDC from both groups contained a similar high percentage of viable cells (Fig. 13*B*). However, there was a significant decrease in the viability of pDC from animals with AIDS, but not from SIV-naïve monkeys (Fig. 13*B*). In addition, mDC viability significantly decreased in animals with AIDS following culture, whereas mDC from naïve monkeys showed a minimal loss of viability (Fig. 13*B*). Similarly, mDC from the peripheral lymph node of animals with AIDS demonstrated a significant loss of viability following culture as compared to mDC from SIV-naïve animals (Fig. 13*B*). Together, these data indicate that both mDC and pDC from animals with AIDS are more prone to spontaneous cell death.

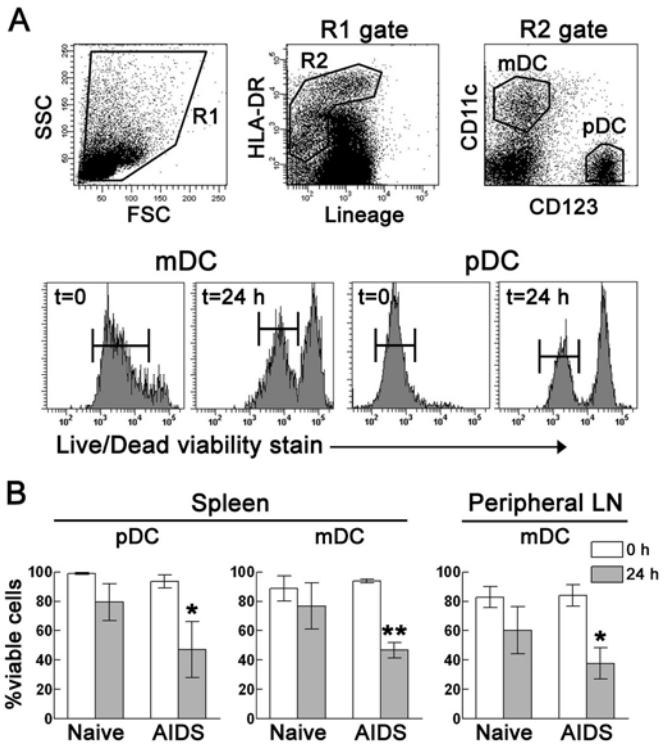

Figure 13. DC from animals with AIDS undergo increased cell death in culture.

A, CD20-depleted single-cell suspensions of peripheral lymph nodes or spleen were analyzed before and 24 h after culture by flow cytometry. Representative dot plots from an SIV-naïve peripheral lymph node sample illustrate the gating strategy used to identify mDC and pDC. The R2 gate used for spleen was similar to Fig. 6. Histograms represent the LIVE/DEAD staining pattern of peripheral lymph node mDC and splenic pDC from an animal with AIDS. Brackets denote the gate used to quantitate viable cells before and after culture. *B*, Percentage of viable cells for pDC and mDC from SIV-naïve monkeys (n=4) and animals with AIDS (n=4) before and after culture. Data represent the mean ± SEM. **P*<0.02, ***P*<0.01.

4.6 DISCUSSION

Our findings contribute considerable insight to the current understanding of DC dynamics during HIV infection and point to a more direct role of systemic DC loss in the pathophysiology of immunodeficiency. We demonstrate that the loss of circulating DC in progressive SIV infection is not due to recruitment to lymph nodes but rather is a component of the generalized loss of both DC subsets from blood and lymphoid tissues. The notion that DC recruitment to lymph nodes may in part explain their disappearance from blood arises from the observed phenotypic activation of DC subsets following in vitro or in vivo exposure to HIV (41, 50, 157). However, clear differences in the phenotypic activation of mDC and pDC was not observed by us or others in SIV-infected macaques (146). Increasing evidence suggests that the interaction between mDC and pDC is important in the induction of virus-specific immune responses in lymph node (80, 144) and stimulation of HIV-specific $CD4^+$ T cell responses (50). Therefore, the loss of both DC subsets from lymphoid tissues in advanced infection would clearly reduce the capacity to respond to HIV or opportunistic infections and could therefore contribute to the onset of immunodeficiency. In contrast, early in HIV infection, DC recruitment to lymph nodes could facilitate viral spread and infection of susceptible T cells (158). Indeed, DC accumulate in the lymph node paracortex during acute infection with either SIV or HIV (51, 52), coincident with massive depletion of memory T cells (7).

The mechanism of DC depletion from blood and lymphoid tissue during AIDS is likely to be complex. Our findings indicate that mDC and pDC undergo spontaneous cell death during culture, supporting the hypothesis that loss of DC may be due to cell death (159, 160). Notably, the amine reactive viability dye used in this study identifies not only necrotic but also late or post

apoptotic cells (161), and preliminary experiments have identified viable DC in lymph nodes of monkeys with AIDS which are annexin V-positive (data not shown) suggesting DC may be undergoing apoptosis. pDC and mDC in blood do harbor virus, suggesting direct infection may contribute to loss of cells from the circulation (40), however exposure of pDC to HIV in vitro promotes pDC survival, not death (50, 97). In addition, the frequency of infected pDC and mDC in tissues appears too low to support a major role of infection in depletion of tissue-resident DC (52, 96, 162, 163). It is possible that apoptosis of DC in HIV and SIV infection is mediated by binding of TNF family ligands to cognate death receptors involving FasL binding to Fas or TNF-related apoptosis-inducing ligand (TRAIL)/DR5 interactions. Fas/FasL and TRAIL/DR5 have been shown to play a role in the apoptosis of T cells in HIV infection (122-124, 164) and both TRAIL- and Fas-mediated pathways have been implicated in DC apoptosis during measles virus infection (127, 165). In addition, we have previously shown that a significant factor in the loss of DC from lymph node may be failed trafficking of DC from epithelial surfaces (52). Consistent with this finding, the predominant mDC population lost from lymph nodes of monkeys with AIDS was the mature, skin-derived DC, while the relatively immature HLA-DR^{mod} mDC subset was decreased to a lesser degree. Although HIV and SIV can infect Langerhans cells (166, 167), evidence for significant infection of Langerhans cells during progressive infection is lacking. Moreover, Langerhans cells migrate with normal efficiency from the skin in SIV-infected monkeys at the time of peak virus load indicating that failed Langerhans cell migration is not simply a function of high virus burden (52). Ultimately, calculating the precise viral burden in mDC and pDC as well as investigating apoptotic pathways will be required to determine mechanisms of DC loss during SIV and HIV infection.

Despite the reduction of pDC and mature mDC in lymph nodes, we observed an increase in a population of Lin^{-}HLA-$DR^{mod}CD11c^{-}$ $CD123^{-}$ cells within the Lin^{-}HLA-DR^{+} fraction of lymph nodes from animals with AIDS resembling monocytoid cells and expressing CD40 and CD86 suggesting a role as an APC. Recently, an increased frequency of circulating blood DC lacking CD11c and CD123 expression that elicited poor T-cell proliferation and IFN-γ secretion was identified in cancer patients (128). Moreover, lymph nodes of HIV-infected subjects were found to contain an abundance of semimature DC defined as being $Lin^{-}CD83^{+}$ $IL\text{-}12^{-}$, which induced allogeneic T cells to adopt a regulatory T cell phenotype (168). While there is no evidence that the Lin^{-}HLA-DR^{mod} cells in our study represent DC, the phenotype of low CD86 and lack of CD80 expression are consistent with these cells being regulatory rather than immunostimulatory DC.

5.0 CHAPTER THREE. PLASMACYTOID DENDRITIC CELL DEATH AND DEPLETION FOLLOWING MASSIVE RECRUITMENT TO LYMPH NODES IN ACUTE IMMUNODEFICIENCY VIRUS INFECTION

5.1 PREFACE

This chapter is adapted from a submitted manuscript (Kevin N. Brown[1,2], Viskam Wijewardana[1,2], Xiangdong Liu[1,2] and Simon M. Barratt- Boyes[1,2,3]). Work described in this chapter is in fulfillment of specific aim 3.

[1]Department of Infectious Diseases and Microbiology, Graduate School of Public Health, and [2]Center for Vaccine Research and [3]Department of Immunology, School of Medicine, University of Pittsburgh, Pittsburgh, PA 15261, USA.

5.2 ABSTRACT

Plasmacytoid dendritic cells (pDC) are lost from the circulation in HIV infection associated with disease progression but the mechanism for this loss is not known. Using precise enumeration and approaches to track recently divided cells, we show that the pDC response to intravenous SIV inoculation in rhesus macaques is highly dynamic with rapid mobilization into blood followed by a 10 to 20-fold increase in pDC recruitment to lymph nodes. However, pDC were depleted from lymph nodes faster than they were replenished. Lymph node pDC had increased levels of apoptosis and necrosis, were uniformly activated and were infected at frequencies similar to $CD4^+$ T cells. Nevertheless, lymph node pDC had essentially normal responses to Toll-like receptor 7 stimulation. We propose that the rapid recruitment of pDC to inflamed lymph nodes in acute immunodeficiency virus infection has a pathologic consequence, bringing cells into close contact with virus, virus-infected cells and pro-apoptotic factors leading to pDC death.

5.3 INTRODUCTION

Plasmacytoid dendritic cells (pDC) are important in bridging innate and adaptive immune responses to pathogens (62, 65, 80). pDC derive from bone marrow and are recruited into lymph nodes in response to inflammation, producing type I interferons (IFN) and contributing to the generation of virus-specific T cell responses (55, 62, 63, 80). Human immunodeficiency virus-1 (HIV) infection of humans and simian immunodeficiency virus (SIV) infection of monkeys result in pDC loss from blood that is correlated with high viral load and reduced numbers of $CD4^+$ T cells (38, 41, 43, 46, 49, 54, 84, 85, 87, 91, 169). pDC-derived type I IFN limits HIV replication in $CD4^+$ T cells (76-78) and frequencies of pDC are higher in HIV-infected long-term non-progressors than healthy donors (170), suggesting that diminished pDC numbers likely contribute to the lack of immune control in this disease. However, the mechanism of pDC loss in HIV infection has not been defined.

A central hypothesis accounting for pDC depletion from blood during HIV infection is recruitment to inflamed lymphoid tissues (50, 76). Evidence for pDC recruitment comes from the finding that pDC exposed to HIV express the chemokine receptor CCR7 required for homing to lymph node paracortex (50), and recent data in rhesus macaques confirm that CCR7 is induced on circulating pDC in response to pathogenic SIV infection (171). Moreover, expression of CXCL9 is highly upregulated in lymphoid tissues in acute SIV infection (103, 104), and pDC enter lymph nodes in a CXCL9-dependent manner (63). However, there is also substantial evidence to support a role for cell death in pDC loss in HIV infection. HIV infects pDC both *in vitro* and *in vivo* and induces cytopathic effects and death following maturation (40, 95-98). In addition, pDC from HIV-infected individuals undergo death by apoptosis and necrosis following

interaction and fusion with HIV-infected cells (78). The relative contribution of recruitment to tissues and cell death to pDC loss in HIV infection remains to be determined.

To tease out the different potential mechanisms of pDC loss, we studied kinetics of the pDC response during acute infection of rhesus macaques with the pathogenic SIV strain SIVmac251. We enumerated pDC in different compartments and used in vivo labeling with the thymidine analogue 5-bromo-2'-deoxyuridine (BrdU) together with Ki-67 staining to document mobilization and recruitment of recently divided cells that would otherwise be obscured by net cell loss. We find that pDC are lost from blood and peripheral lymph nodes early in SIV infection despite massive mobilization and recruitment, associated with pDC activation, infection and death in lymph nodes. These findings demonstrate that pDC recruitment and killing work together in the context of the lymph node to bring about pDC depletion in SIV infection.

5.4 MATERIALS AND METHODS

5.4.1 Animals, virus infection and sample collection

Six adult female rhesus macaques (*Macaca mulatta)* were infected by intravenous inoculation with 1,000 $TCID_{50}$ SIVmac251 (kindly provided by Preston Marx, Tulane National Primate Research Center) and compared to a cohort of six SIV-naive controls. Blood samples were collected in either EDTA or ACD four to six times prior to infection including day 0 and on days 3, 6, 10, 11, 12, 13 and 14 post-infection. BrdU (Sigma) was prepared in Ca^{2+}/Mg^{2+}-free HBSS

at 10 mg/ml, filter-sterilized and administered by intravenous injection at 30 mg/kg at 24-hour intervals for 4 doses starting on day 10 post-infection. Parallel BrdU administration was given to two SIV-naïve monkeys. Bone marrow aspirates were obtained at least 30 days prior to and on day 12 post-SIV infection from the medullary cavity of the right femur using a Jamshidi bone marrow biopsy needle flushed with heparin. SIV-infected animals were sacrificed on day 14 post-infection and the two SIV-naive animals receiving BrdU were sacrificed 24 hours after the final drug dose. All animals underwent transcardiac saline perfusion at the time of sacrifice to ensure removal of peripheral blood from tissues. All experiments were performed using protocols approved by appropriate institutional regulatory committees.

5.4.2 Sample processing

PBMC were isolated by density gradient centrifugation over Ficoll. Alternatively, blood samples were lysed of red blood cells using ACK lysing buffer for isolation of peripheral blood leukocytes (PBL). Lymph node single-cell suspensions were generated and depleted of $CD20^+$ B cells as previously described (85). Bone marrow aspirates were passed over a 70 μm nylon cell strainer to remove spicules and diluted 1:1 with PBS prior to erythrocyte lysis and counting using trypan blue exclusion. All blood, lymph node and bone marrow preparations were frozen in medium containing 90% FBS and 10% DMSO (Sigma) using a controlled-rate freezer (CryoMed) and stored in liquid nitrogen. Viral RNA levels in plasma were determined by real-time PCR using an ABI Prism 7900H sequence detection system (Applied Biosystems) using reverse-transcribed viral RNA as templates, as described (172).

5.4.3 Flow cytometry and enumeration of cells

All antibodies were purchased from BD Biosciences unless noted otherwise. For the majority of analyses cells were stained with antibodies to Lineage markers [CD3 (clone SP34-2), CD14 (M5E2), and CD20 (2H7, eBioscience)], CD45 (D058-1283), HLA-DR (G46-6), and CD123 (7G3) with or without an amine-reactive Live/Dead cell viability dye (Invitrogen) using mutually-exclusive fluorochrome conjugates. In some experiments cells were co-stained with antibody to CD95 (DX2) or with 5.0 μg/mL 7-AAD and Annexin V (BD Biosciences). Alternatively, labeled cells were fixed and permeabilized with Cytofix/Cytoperm (BD Biosciences) and incubated with antibody to Ki-67 (B56). To detect BrdU incorporation, labeled cells were fixed with 4% formaldehyde prior to pretreatment with 10 Kunitz units DNaseI (Roche)/10^6 cells in 0.1% saponin containing 4.2 mM $MgCl_2$ and 10mM NaCl. Cells were washed with saponin and incubated with anti-BrdU-FITC (B44) prepared in the previous solution containing 10 Kunitz units DNaseI/10^6 cells for 45 min at RT. BrdU positivity was determined by staining samples from animals not delivered BrdU. Absolute numbers of $CD45^+$ mononuclear cells and $CD4^+$ T cells in blood were determined by staining 50μL of whole blood with antibodies to CD3, CD4 (L200) and CD45 using TruCOUNT tubes (BD Biosciences) as per the manufacturer's recommendations. For pDC quantification PBL were stained with antibodies to define pDC and the absolute number of pDC/μL blood calculated by multiplying the percentage of pDC within the $CD45^+$ fraction by the absolute number of $CD45^+$ cells. A similar method was used to calculate mononuclear cells and pDC in bone marrow aspirates. For analysis of intracellular cytokine expression PBMC were stimulated for 5 hours in media alone or with 10 μM of the TLR7/8 agonist 3M-007 (3M Pharmaceuticals) in the presence of 10 μg/mL brefeldin A (Sigma) for the final 3 hours. Alternatively, CD20-depleted lymph node cells

were stimulated for 12 hours with 10 μM 3M-007 agonist in the presence or absence of 10 μg/mL brefeldin A. Cells were stained with surface-labeling antibodies and fixed and permeabilized as above prior to incubation with antibodies to TNF-α (MAb11) and/or IFN- α (MMHA-2, PBL Biomedical Laboratories). Antibody to IFN- α was conjugated to Alexa 647 using Zenon labeling technology according to the manufacturer's protocol (Invitrogen). Flow cytometry data was acquired using a BD LSR II or FACS Aria flow cytometer and analyzed with BD FACS Diva software (version 5.0.2) and histogram overlays generated using FlowJo version 7.2.4 (Tree Star, Inc.).

5.4.4 Cell sorting

Previously cryopreserved lymph node cell suspensions were thawed in the presence of DNAse, strained and then stained with antibodies to Lineage markers, HLA-DR, CD123 and CD11c (S-HCL-3) along with the Live/Dead viability dye. Between 5,000 and 10,000 viable Lin^- HLA-DR^+ $CD123^+$ $CD11c^-$ pDC and Lin^- HLA-DR^+ $CD123^-$ $CD11c^+$ mDC were sorted simultaneously using a BD FACS Aria flow cytometer, making sure to exclude doublets on the basis of forward scatter and side scatter height and width parameters. For purification of $CD4^+$ T cells, lymph node suspensions were stained with antibodies to CD3, CD4 and CD8 (B9.11, Immunotech) and 50,000 viable $CD3^+CD4^+CD8^-$ cells sorted as above. Purified cells were deposited into tubes containing lysis buffer for DNA isolation or into tubes containing media followed by centrifugation onto slides (Cytospin 3, Shandon). Slides were fixed and stained using a modified Wright-Giemsa stain (Hema 3, Fisher) and images taken using an Olympus BX51 light microscope.

5.4.5 Quantification of SIV proviral DNA

Cellular DNA from sorted cells was isolated using DNAeasy blood and tissue kit (Qiagen). For quantitative PCR analysis, a plasmid was first generated by inserting sequences of SIVsmB7 LTR and SIVmac239 *gag* in the pUC19 plasmid along with macaque albumin cDNA. This plasmid was validated against serial dilutions of B7 cells containing a single integrated copy of SIVsmB7 (173) by using TaqMan real-time PCR with primers 5'-TTGAGCCCTGGGAGGTTCT-3' and 5'-CCAAGTGCTGGTGAGAGTCTAG-3', and probe 5'-CAGCACTAGCAGGTAGAGCCTGGGTGTTC-3', and used as a standard for calculating the frequency of infection in sorted cells. SIVmac251 *gag* copy number in each DNA sample was quantified by comparison with serial dilutions of the plasmid standard using TaqMan real-time PCR using primers 5'-GCCAGGATTTCAGGCACTGT-3' and 5'-GCTTGATGGTCTCCCACACAA-3', and the probe 5'-AAGGTTGCACCCCCTATGACATTAATCAGATGTTA-3' specific for sequences of *gag* that are conserved across SIV strains. In parallel, the albumin gene copy number was determined to quantify the number of cells loaded in each reaction using primers 5'-TGCATGAGAAAACGCCAGTA-3' and 5'-AGCATGGTCGCCTGTTCAC-3' and probe 5'-AAAGTCACCAAATGCTGCACGGAATCC-3'. Reactions were performed in duplicate using TaqMan Universal mix kit (Applied Biosystems), 200 nM of each primer and 125 nM probe, at 95°C for 10 min, with 40 cycles of 95°C, 15 s and 60°C, 1 min using the Prism 7900H sequences detection system (Applied Biosystems).

5.4.6 Statistical analysis

Differences between pre and post-infection time points were determined using the nonparametric Wilcoxon signed-rank test. Cross-sectional analysis of SIV-naïve and animals with acute SIV infection were performed using the nonparametric Mann-Whitney *U* test. Correlations were determined using the non-parametric Spearman rank test. Multiple comparisons between the frequencies of SIV infection in sorted populations were performed using the Kruskal-Wallis test followed by Dunn's post test. All statistical comparisons were considered significant when two-tailed $P < 0.05$.

5.5 RESULTS

5.5.1 Rapid loss of pDC from blood and lymph node during acute SIV infection

In order to document changes in pDC number in blood during HIV infection, we used the rhesus macaque model of intravenous infection with the pathogenic isolate SIVmac251. Infection resulted in detectable viremia within 3 days post infection that plateaued at day 12 and was associated with an expected decline in the number of blood $CD4^+$ T cells by day 10 post infection (Fig. 15). pDC were identified within the $CD45^+$ mononuclear cell fraction of blood as Lineage (CD3, CD14, CD20)$^-$ HLA-DR^+ $CD123^+$ cells using flow cytometry (Fig. 14*A*) (85) and enumerated by an indirect method using TruCOUNT beads as described in the Methods section. In contrast to $CD4^+$ T cells, there was a significant increase in the number of blood pDC between 3 and 6 days post infection, in some instances reaching 7 times that of pre-infection levels, indicative of peracute mobilization of pDC (Fig. 14*B*). This was followed at day 10 by a significant decrease in pDC number from baseline which remained suppressed until at least day 14 (Fig. 14*B*), when $CD4^+$ T cells had begun to recover (Fig. 15). The absolute number of pDC in blood was inversely correlated with plasma viral load and positively correlated with $CD4^+$ T cell number during the course of primary SIV infection (Fig. 14*C*). To determine whether the drop in pDC from blood at days 10-14 of infection was associated with an increase in pDC number in lymph nodes, we harvested axillary lymph nodes at 14 days post infection and determined the proportion and absolute number of pDC in cell suspensions. pDC were identified

as HLA-DR^{low} CD123^{+} cells within the Lineage^{-} HLA-DR^{+} DC fraction following exclusion of dead cells based upon staining with an amine-reactive viability dye (Fig. 14*D*) (85). Surprisingly, both the percentage of pDC within the DC fraction and the absolute number of pDC per unit weight of tissue were markedly decreased in SIV-infected lymph nodes as compared to naïve controls (Fig. 14*E*). These findings indicate that acute SIV infection results in a bimodal pDC response in blood, with rapid pDC increases followed by loss, and that this loss is paralleled by depletion of pDC from lymph nodes.

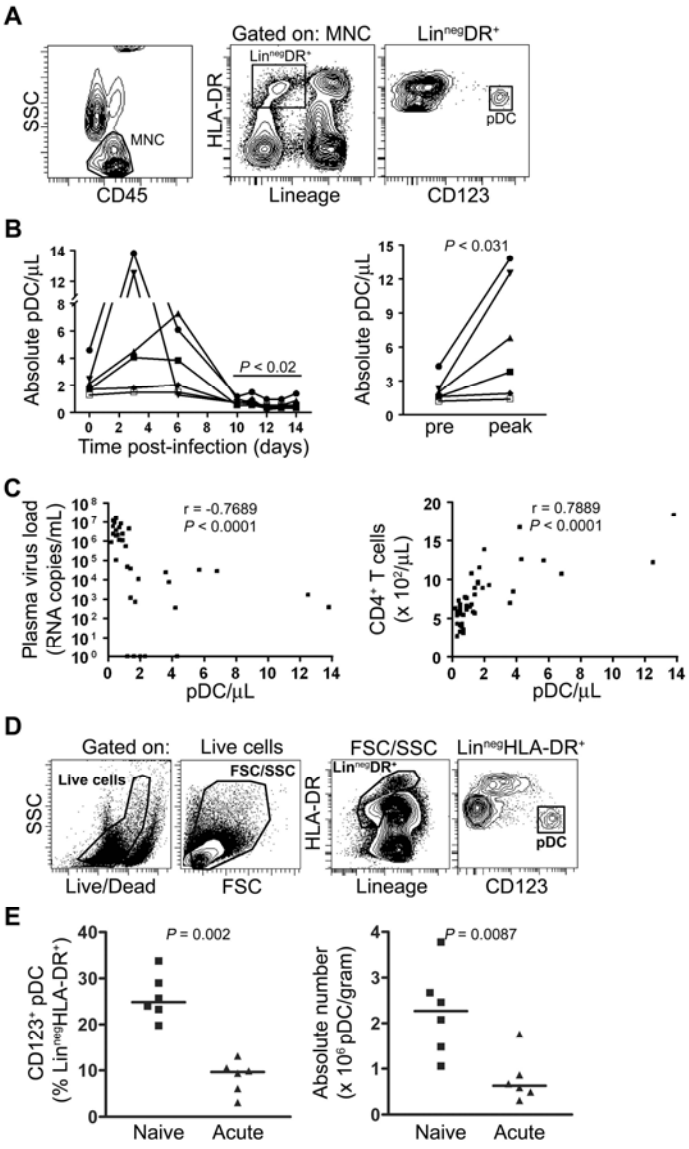

Figure 14. pDC are transiently increased and then lost from blood and lymph nodes in acute SIV infection

A, Representative contour plots demonstrating the gating strategy used to define pDC within the mononuclear cell fraction (MNC) of freshly isolated peripheral blood leukocytes. *B*, Absolute number of pDC in blood during acute SIV infection over all days (left) and comparing pre-infection to peak responses at day 3 or 6 (right). Symbols represent individual animals with the baseline number of pDC/μL blood prior to infection (day 0) representing the median of 4 independent measurements for each animal. *C*, The number of pDC in blood was inversely correlated with viral load and positively correlated with $CD4^+$ T cell counts during the 14-day period. *D*, Representative plots demonstrating the gating strategy used to delineate the $Lineage^-$ $HLA\text{-}DR^+$ fraction and $CD123^+$ pDC in axillary lymph node cell suspensions. *E*, Number of pDC in lymph nodes of naïve animals and animals at 14 days post-infection expressed as percent of pDC within the $Lineage^-$ $HLA\text{-}DR^+$ fraction (left) and as absolute number of pDC/gram of tissue (right). Symbols represent individual animals and horizontal lines represent medians.

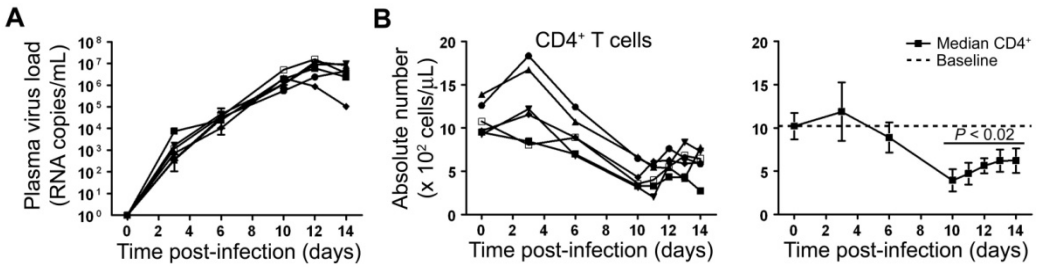

Figure 15. High dose intravenous SIVmac251 infection leads to dramatic loss of mononuclear and CD4+ T cells

*A***,** Viral RNA copy/mL of plasma was determined following 1000 $TCID_{50}$ SIVmac251 infection using real-time RT-PCR. Symbols represent individual animals and error bars the 95% confidence interval of samples run in duplicate. *B*, Changes in the absolute number of $CD4^+$ T cells/μL of blood for all animals during acute SIV-infection using BD TruCOUNT tubes. Day 0 represents the median number of cells from at least 4 independent measurements prior to infection including day 0. Symbols represent individual animals (left panel) and the group median $\pm$ 95% confidence interval (right panel). The dashed line represents the overall group median baseline cell number/μL of blood. Each timepoint starting on day 10 was significantly decreased compared to pre-infection.

5.5.2 Acute SIV infection does not alter the frequency of pDC in bone marrow

The depletion of pDC from both blood and lymph nodes during acute SIV infection could be explained by bone marrow suppression leading to a loss of pDC production. To address this possibility we analyzed the frequency of phenotypically-defined pDC in paired bone marrow samples taken prior to and 12 days following SIV infection. pDC were identified within the $Lineage^-$ $HLA\text{-}DR^+$ fraction of bone marrow mononuclear cells by expression of CD123 (Fig. 16*A*), as has previously been described (174). The frequency of total mononuclear cells was unchanged in bone marrow in response to SIV infection, and the proportion of pDC within this cell population as well as the total pDC number per volume of bone marrow aspirate were also unaffected by infection (Fig. 16*B*). We next analyzed bone marrow pDC for expression of the nuclear proliferation antigen Ki-67, which is expressed by cells in a non-G_0 phase of the cell cycle and thus provides an approximation of the recent proliferative history of a given cell

population (175). The majority of bone marrow pDC in SIV-naïve animals were Ki-67^{+} reflecting a high rate of production (55) and this was unchanged as a result of SIV infection (Fig. 16*C*). These data indicate that acute SIV infection does not alter pDC production or dynamics in bone marrow, consistent with the findings of others (174).

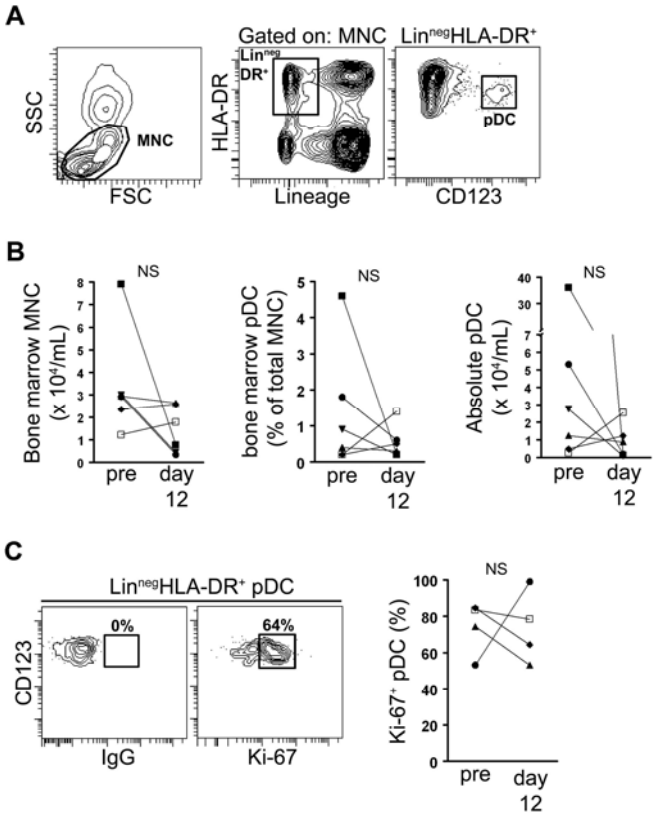

Figure 16. Normal pDC production from bone marrow in acute SIV infection

A, Representative contour plots demonstrating the gating strategy used to define pDC within the mononuclear cell (MNC) fraction of bone marrow aspirates. *B*, Paired analyses of the absolute number of MNC in bone marrow (left), the frequency of pDC within the total MNC fraction (middle) and the absolute number of pDC in bone marrow (right) before and 12 days after SIV infection. Symbols represent individual animals. *C*, pDC were gated as in (*A*) and the percentage of pDC expressing Ki-67 determined by comparing to staining with an isotype control antibody (left). Contour plots represent an analysis at day 12 post infection and numbers represent the percentage of cells within the indicated gates. Paired analysis of the percentage of Ki-67^{+} pDC before infection and at day 12 post-infection (right). NS = not significant.

5.5.3 Rapid mobilization of pDC into blood during acute SIV infection

The rapid but transient increase in the number of pDC in blood together with normal pDC frequencies in bone marrow raised the possibility that pDC were being actively mobilized from bone marrow into blood during acute SIV infection. To address this we first analyzed blood pDC for expression of Ki-67, which provides an indication of the pDC fraction that was recently mobilized from bone marrow. Prior to SIV infection, the mean percentage of Ki-67$^+$ pDC was 52% (Fig. 17, *A* and *B*), indicating that half of all pDC in the circulation were recently released from bone marrow. However, by day 14 post infection 87% of circulating pDC expressed Ki-67 indicative of mobilization (Fig. 17*B*), and this increase was inversely correlated with the absolute number of blood pDC (Fig. 17*C*). To accurately determine the rate of mobilization of pDC into blood we administered BrdU by intravenous injection at days 10, 11, 12 and 13 post infection and sampled blood 24 hours after each administration. BrdU is only incorporated into cells undergoing S-phase of the cell cycle during the time of delivery, and hence BrdU$^+$ pDC in blood will be marked as having been released from bone marrow since the time of the BrdU pulse. In SIV-naïve monkeys only 2% of blood pDC were BrdU$^+$ at 24 hours after the first pulse, reaching a maximum of 13% after the fourth pulse, indicating a relatively low rate of pDC mobilization in health (Fig. 17, *D* and *E*). In stark contrast, upwards of 20% of blood pDC from SIV-infected animals at day 11 were BrdU$^+$ after a single BrdU pulse and this approached 60% after the fourth pulse at day 14 post infection (Fig. 17, *D* and *E*). The degree of Ki-67 staining and BrdU incorporation at day 14 were strongly correlated (Fig. 17*F*). These findings indicate that acute SIV infection results in rapid mobilization of pDC into blood that is quickly obscured by declining pDC numbers.

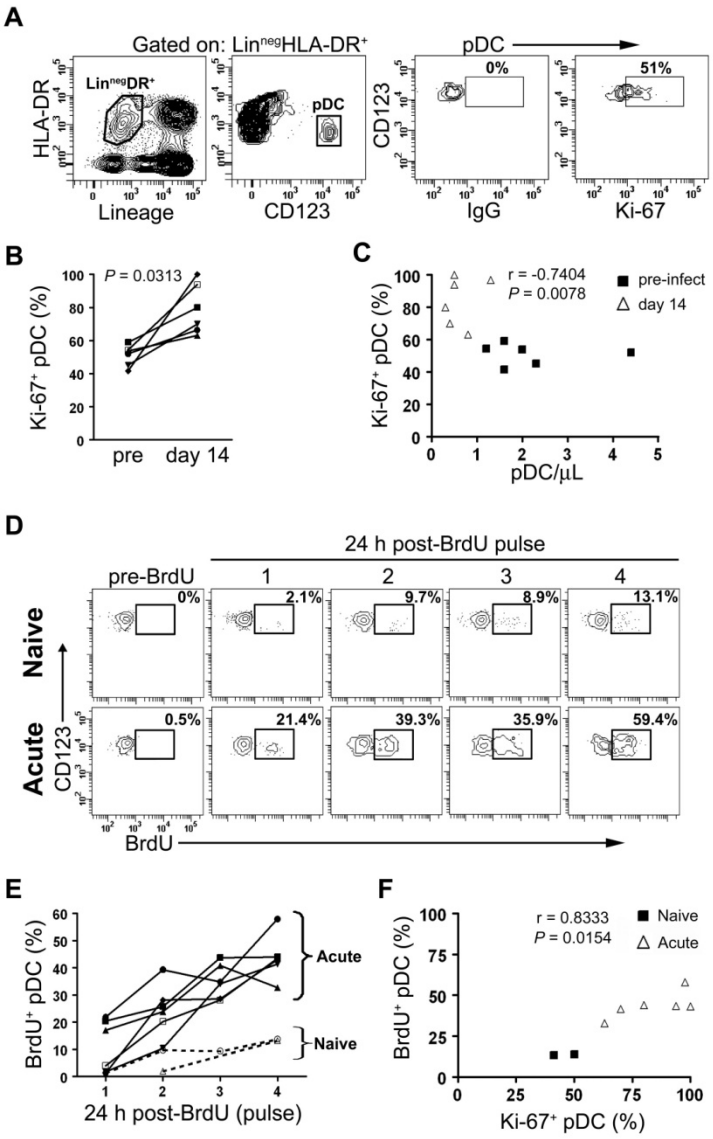

Figure 17. Rapid mobilization of pDC into blood during acute SIV infection

A, Representative contour plots from an animal prior to infection demonstrating the gating strategy used to identify Ki-67$^+$ pDC in blood. pDC were gated as in Fig. 1 and Ki-67 positivity determined based on the level of background fluorescence using the isotype-matched control antibody. Numbers represent the percentage of cells within the indicated gates. *B*, Paired analysis of percentage of Ki-67$^+$ pDC in blood prior to infection and at day 14 after infection. Symbols represent individual animals. *C*, The absolute number of pDC in blood was inversely correlated with the percentage of cells expressing Ki-67. Shown are data from individual animals prior to infection and 14 days after infection . *D*, Representative contour plots demonstrating the gating strategy used to identify BrdU$^+$ pDC prior to and 24-hour after four consecutive intravenous daily injections of BrdU in an SIV-naive and SIV-infected macaque. BrdU was delivered starting on day 10 of infection. Numbers represent the percentage of BrdU$^+$ pDC within each gate. *E*, The percent of BrdU$^+$ pDC in blood of SIV-naïve animals (dashed lines) and SIV-infected animals (solid lines) 24 hours after each BrdU pulse. *F*, The percent of BrdU$^+$ pDC was positively correlated with the percent of Ki-67$^+$ pDC 24 hours after the final BrdU administration.

5.5.4 Massive recruitment of pDC into peripheral lymph nodes during acute SIV infection

We next used BrdU incorporation and Ki-67 staining to investigate whether increased mobilization of pDC into blood was paralleled by recruitment of pDC to lymph nodes, despite the loss of pDC from these tissues. Axillary lymph nodes were harvested from SIV-infected monkeys at day 14 post infection and from SIV-naïve monkeys receiving the same course of BrdU and pDC were analyzed for BrdU incorporation (Fig. 18*A*). Only 2% of lymph node pDC were $BrdU^+$ after 4 pulses of BrdU in SIV-naïve monkeys, indicating a low level of pDC recruitment into normal lymph nodes. However, 19% of lymph node pDC from SIV-infected monkeys were $BrdU^+$, representing a ~10-fold increase in pDC recruitment over the 4-day labeling period relative to controls (Fig. 18*B*). Similarly, the mean proportion of lymph node pDC that were Ki-67^+ in SIV-naïve monkeys was only 2.5%, whereas more than 50% of lymph node pDC from monkeys at day 14 post infection stained for Ki-67. This represents a 20-fold increase in recently-divided pDC within lymph nodes as a result of SIV infection (Fig. 18, *C* and *D*). In fact, whereas the total number of lymph node pDC declined in acute SIV infection (Fig. 14*E*) the number of Ki-67^+ pDC in lymph nodes was significantly increased over SIV-naïve lymph nodes (Fig. 18*D*). Nevertheless, the proportion of pDC that expressed Ki-67 had a strong inverse correlation with the total number of pDC in lymph nodes, indicating that recruitment and loss were occurring concurrently (Fig. 18*E*). Together, these data demonstrate that pDC undergo a marked recruitment to peripheral lymph nodes during acute SIV infection but that the net result is an overall loss of pDC from these tissues.

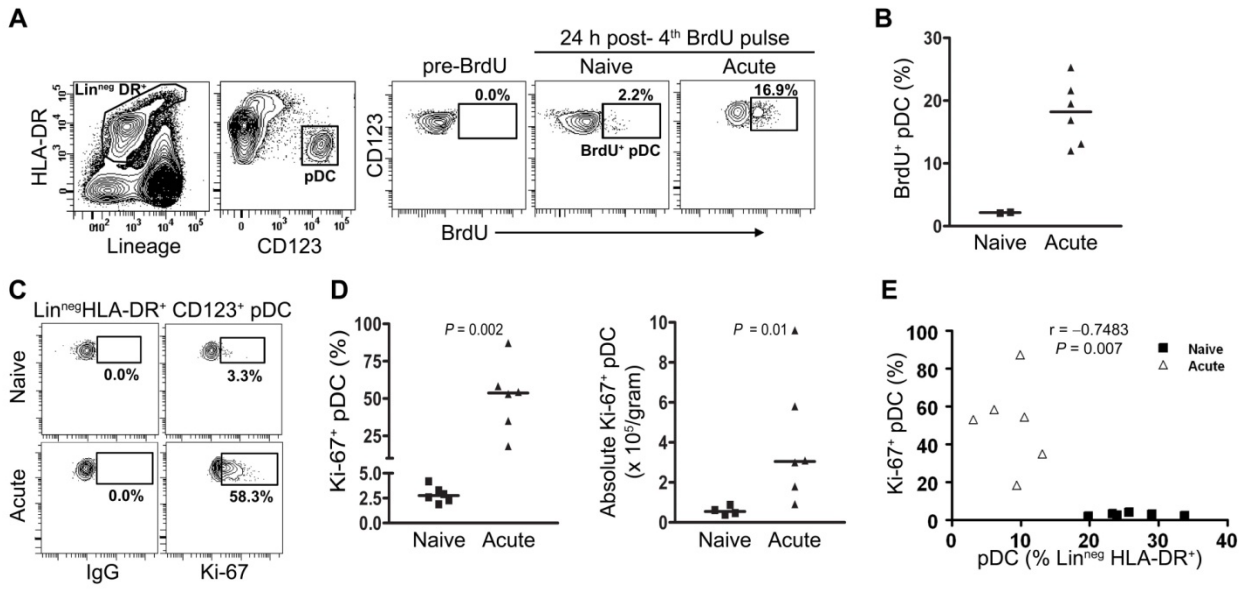

Figure 18. Massive recruitment of recently mobilized pDC to peripheral lymph nodes in acute SIV infection

A, Representative plots demonstrating the gating strategy used to identify pDC in CD20-depleted axillary lymph nodes (left). Representative plots of BrdU staining in a SIV-naïve and SIV-infected macaque (right). Numbers represent the percent of cells within the indicated gate. *B*, Percent of $BrdU^+$ pDC in lymph nodes 24 hours after the final BrdU pulse in naïve and infected animals. Symbols represent individual animals and horizontal bars represent medians. *C*, Representative plots demonstrating Ki-67 staining in pDC as gated in (*A*). *D*, Number of Ki-67^+ pDC in lymph nodes from SIV-naive animals and animals at day 14 post-infection expressed as a percent of all pDC (left) and as absolute number/gram of tissue (right). Symbols represent individual animals and horizontal bars represent medians. *E*, The frequency of pDC within the Lin^- HLA-DR^+ gate is inversely correlated with the percent of Ki-67^+ pDC in lymph nodes. Symbols represent individual SIV-naive animals and animals at 14 days post infection.

5.5.5 Activation, infection and death of pDC in lymph nodes during acute SIV infection

The overall loss of pDC from lymph nodes despite their massive recruitment strongly suggests that pDC are dying in these tissues during infection. To examine this directly, we first stained lymph node cell suspensions with antibodies to define pDC and then measured the proportion of cells that were dead based on staining with the amine-reactive viability dye. Nearly 15% of pDC from lymph nodes taken at 14 days post infection were non-viable as compared to 3% of pDC from naïve lymph nodes (Fig. 19*A*). This increase was due to an increase in late apoptosis and/or necrosis based on pDC co-labeling with Annexin V and 7-AAD (Fig. 19*B*). These data indicate that pDC resident in lymph nodes are more likely to be apoptotic or necrotic as a result of acute SIV infection. To determine whether direct virus infection could play a role in pDC death, we stained lymph node cell suspensions with antibodies and simultaneously sorted pDC as Live/Dead$^-$ Lineage$^-$ HLA-DR$^+$ CD123$^+$ CD11c$^-$ cells and myeloid DC (mDC) as Live/Dead$^-$ Lineage$^-$ HLA-DR$^+$ CD123$^-$ CD11c$^+$ to at least 95% purity (Fig. 19*C*). SIV *gag* DNA was then measured in total cellular DNA from these cells using *gag* primers and probe by quantitative PCR and the frequency of infected cells determined on the basis of *albumin* DNA quantity, as described in the Methods section (7). In separate tubes we sorted CD4$^+$ T cells as Live/Dead$^-$ CD3$^+$ CD4$^+$ cells and determined their frequency of SIV infection. These data revealed that more than 4% of lymph node pDC harbored SIV *gag* DNA at day 14, reaching up to 15% in one animal, a frequency that was slightly greater than SIV-infected CD4$^+$ T cells and well above that of the unseparated lymph node fraction (Fig. 19*C*). In contrast, mDC had almost undetectable levels of *gag* DNA (Fig. 19*C*). The negligible infection of mDC confirms that the pDC result was not due to contaminating CD4$^+$ T cells, as mDC and pDC were sorted simultaneously from the same tubes. To investigate whether indirect mechanisms of pDC death may also contribute

to the significant cell death seen in lymph nodes, we measured expression of known pro-apoptotic tumor necrosis factor (TNF) family members CD95 (Fas), TNF-related apoptosis-inducing ligand (TRAIL) and the TRAIL receptor death receptor (DR) 5 by flow cytometry. These data revealed that lymph node pDC from SIV-naïve monkeys had almost undetectable expression of CD95, whereas CD95 was uniformly expressed by pDC from SIV-infected lymph nodes, indicative of activation (176) (Fig. 19*D*). However, we were not able to detect differences in apoptosis of lymph node pDC from uninfected or infected monkeys after incubation with CD178 (Fas ligand; data not shown), consistent with earlier reports (78). No expression of TRAIL or DR5 was detected on lymph node pDC regardless of SIV infection status (data not shown). These data show that pDC in lymph nodes of monkeys with acute SIV infection are activated and have increased death through apoptosis and necrosis, and that a significant fraction of pDC are infected with virus.

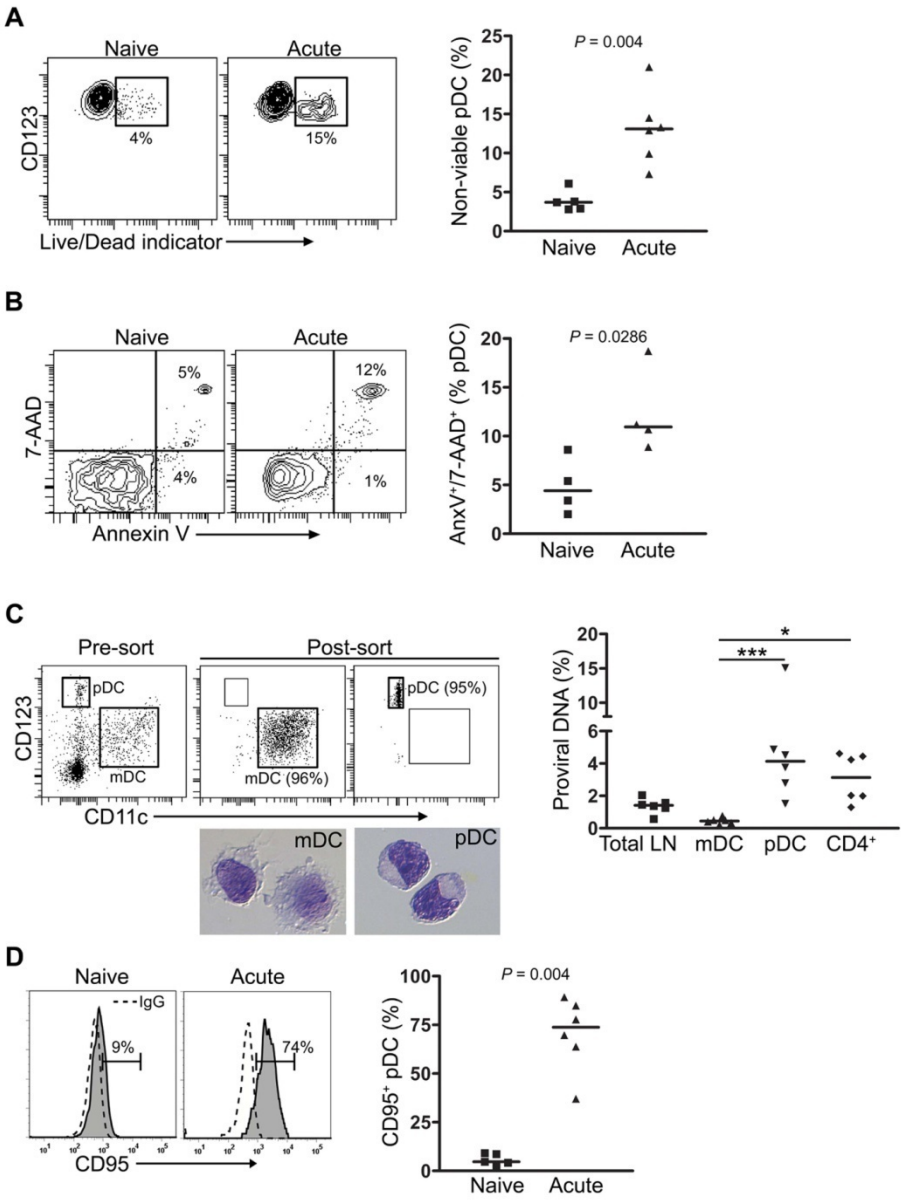

Figure 19. Activation, infection and death of pDC in SIV-infected lymph nodes

A, Representative contour plots demonstrating staining of pDC from CD20-depleted axillary lymph nodes from SIV-naïve and SIV-infected animals with the amine-reactive Live/Dead viability dye (left). pDC were gated as in Fig. 4. Numbers represent the percentage of non-viable pDC. Percent of non-viable pDC in lymph nodes of SIV-naive animals and animals at 14 days post-infection (right). Symbols represent individual animals and horizontal lines represent medians. *B*, Representative contour plots demonstrating the quadrant gates used to define early apoptotic (Annexin V^+/7-AAD^-) and late apoptotic/necrotic (Annexin V^+/7-AAD^+) pDC from lymph nodes from SIV-naive and SIV-infected animals (left). Numbers represent the percent of cells in respective quadrants. Percent of late apoptotic/necrotic pDC in lymph nodes from SIV-naive animals and animals at 14 days after infection (right). Symbols represent individual animals and horizontal lines represent medians. *C*, Representative dot plots demonstrating pDC and mDC in the $Lineage^-$ HLA-DR^+ gate prior to and after sorting from the axillary lymph node of a monkey 14 days after infection (left). Numbers in parentheses indicate the purity of mDC and pDC. Sorted cells were spun onto slides and stained with Wright Giemsa stain. Frequency of total lymph node (LN) cells or sorted mDC, pDC and $CD4^+$ T cells containing proviral DNA as determined by quantitative PCR (right). $*P < 0.05$,

***$P < 0.001$. Symbols represent individual animals and horizontal lines represent medians. *D*, Lymph node pDC were analyzed for surface CD95 expression. Representative histograms demonstrating CD95 expression (solid histogram) compared to isotype control (dotted line) in naïve and SIV-infected lymph nodes (left). Numbers represent percent of $CD95^+$ cells. Percent of CD95-expressing pDC in lymph nodes of SIV-naive macaques and animals with acute SIV infection. Symbols represent individual animals and horizontal lines represent medians.

5.5.6 Blood and lymph node pDC have largely normal function in acute SIV infection

We next examined the function of pDC in blood and lymph nodes during acute SIV infection. Given that SIV and HIV stimulate pDC in large part through Toll-like receptor 7 (TLR7)(79, 171), we analyzed pDC function by stimulating cells through TLR7 engagement using the TLR7/8 agonist 3M-007. We did a short-term stimulation of unseparated PBMC taken before infection or at day 14 post infection with 3M-007 and determined expression of TNF-α by flow cytometry, gating on $CD123^+$ pDC (Fig. 20*A*). Between 20% and 40% of pDC in blood produced TNF-α in response to TLR7 stimulation regardless of infection status (Fig. 20*A*). We next stimulated CD20-depleted lymph node cells taken from SIV-naïve monkeys or monkeys at 14 days post infection and stimulated them in the same manner, this time analyzing cells for expression of IFN-α and TNF-α. Approximately half of all lymph node pDC produced both TNF-α and IFN-α in response to this stimulation regardless of whether lymph nodes were taken from SIV-naïve or SIV-infected monkeys, whereas endogenous cytokine production in the absence of stimulation was negligible (Fig. 20*B* and data not shown). Interestingly, the small proportion of pDC producing IFN-α alone was undiminished by SIV infection, although lymph node pDC from SIV-infected monkeys had a reduced capacity to produce TNF-α alone (Fig. 20*B*). These findings indicate that despite a net loss of pDC the remaining cells in blood and lymph node retained largely normal functional responses to TLR7 stimulation during primary SIV infection.

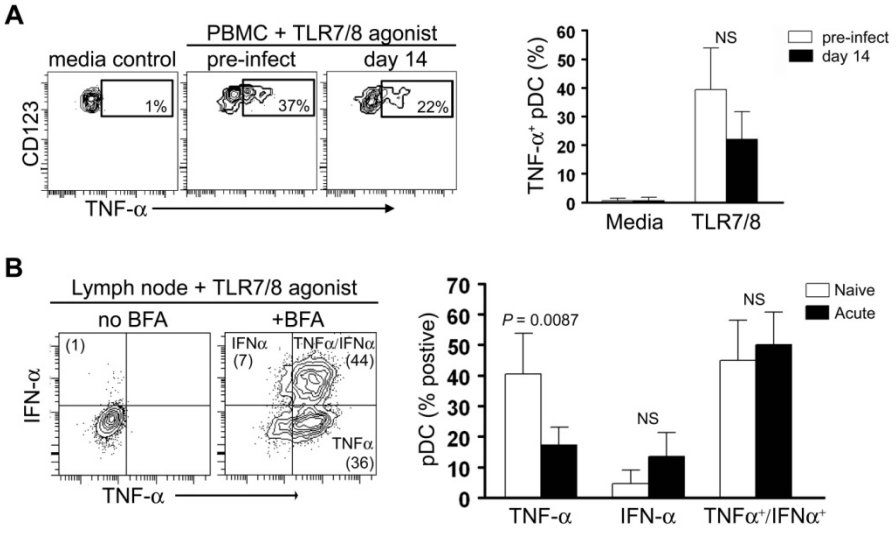

Figure 20. pDC retain largely normal function in response to TLR7 stimulation during acute SIV infection

A, Contour plots demonstrating the gating strategy used to identify TNF-α^+ pDC in PBMC from SIV-naïve and SIV-infected monkeys following stimulation with 3M-007 (left). Numbers represent the percentage of TNF-α^+ pDC within the indicated gates. Percent of TNF-α^+ pDC in PBMC from SIV-naïve and SIV-infected monkeys in response to media or 3M-007 (right). Bars represent the median and error bars the 95% confidence interval.
B, Representative contour plots demonstrating the gating strategy used to identify TNF-α^+, IFN-α^+, or TNF-α^+/ IFN-α^+ pDC in lymph nodes following 3M-007 stimulation in the absence or presence of Brefeldin A (BFA) (left). Numbers in parentheses represent the percentage of cells expressing the respective cytokines. Percent of lymph node pDC from SIV-naïve and SIV-infected monkeys expressing TNF-α, IFN-α, or both in response to TLR7/8 agonist (right). Bars represent the median and error bars the 95% confidence interval.

5.6 DISCUSSION

In this study we used rhesus macaques infected with the pathogenic SIVmac251 strain to model kinetics of the acute pDC response to HIV infection of humans. We combined enumeration of cells in blood and lymphoid tissues with BrdU incorporation and Ki-67 staining to document pDC production. Since pDC are generated in bone marrow and enter the blood as end stage cells without further replication in tissues (55) we were to able to use these complementary approaches to effectively track pDC from bone marrow to blood and then to lymph nodes and to relate this migration to changes in cell number over time.

Our findings reveal a rapid and highly dynamic pDC response to SIV infection with mobilization of cells into blood occurring as soon as 3 days after intravenous virus challenge. By 11 days after infection around 20% of blood pDC had mobilized from bone marrow in the previous 24-hour period following a single BrdU administration, and this reached 60% by day 14 after four administrations of BrdU. In fact this is likely to be an underestimate of the extent of pDC mobilization given that BrdU has a half-life of only 2 hours in the circulation (177). This mobilization is likely the result of increased systemic TNF-α (178) which has been shown to control pDC mobilization in murine models (63). By days 10 to 14 of infection the number of pDC in blood had dramatically declined despite normal production from bone marrow, coincident with massive recruitment of pDC to lymph nodes. At day 14 of infection the proportion of lymph node pDC that had recently been released from bone marrow as determined by Ki-67 staining or BrdU incorporation was 20-fold greater than that of naïve monkeys, reaching 50% of all cells. Rapid pDC recruitment is consistent with the TNF-α-driven expression of CXCL9 and upregulation of CCL19 in lymph nodes (63, 103, 104, 179) and

induction of CCR7 on activated pDC in the circulation (50, 171). These data show that the inflammatory response in acute SIV infection is highly effective at inducing the coordinated mobilization and recruitment of large numbers of pDC into blood and lymph nodes.

Paradoxically, pDC recruitment was occurring as pDC numbers in lymph nodes were dramatically declining, indicating that cells were dying at a rate faster than they could be replenished. Rapid influx of pDC to lymph nodes at a time when virus is highly concentrated in these tissues (180) would increase the potential for pDC to virus-infected $CD4^+$ T cell contact, potentially leading to death by apoptosis and necrosis (78). Consistent with this possibility, we found around 15% of pDC undergoing late apoptosis and/or necrosis in acutely infected lymph nodes. In addition, high virus levels in lymph nodes would promote direct infection of pDC, and we show that a fraction of pDC harbored proviral DNA. Therefore, viral infection of pDC had occurred and proceeded at least to the point of reverse transcription. While the frequency of infected pDC was relatively modest at 4% it was similar to that of $CD4^+$ T cells, the principle cells infected in lymph nodes at this time (181), suggesting that pDC are a significant target of virus infection. Previous reports have described Gag-expressing pDC in lymphoid tissues and pDC harboring proviral DNA in blood of HIV-infected individuals (40, 96), but up to now the efficiency of pDC infection *in vivo* was not known. By contrast, the frequency of infected mDC was almost below detection, indicating that these cells may not be a significant source of virus in lymph nodes (182). While limited cell numbers did not allow us to directly determine whether infection resulted in cell death, *in vitro* data indicate that pDC infection concurrent with activation through CD40L results in giant cell formation and death (97). *In vivo*, activated $CD4^+$ T cells that engage infected pDC in the lymph node paracortex would provide CD40L.

Furthermore, Gag-expressing $CD123^+$ multinucleated giant cells have been identified in HIV-infected lymphoid tissues (96), consistent with the notion of virus-induced pDC death. It is possible that the inflammatory environment in the lymph node also impacts pDC survival via factors that remain to be defined. pDC from SIV-infected lymph nodes uniformly expressed CD95, and in mice exposed to inflammatory and microbial stimuli CD95 expression induced on activated pDC is linked to apoptotic cell death (176). However, while CD95/CD178 interactions play a role in $CD4^+$ T cell loss in HIV and SIV infection (115, 183) the role for this pathway in pDC death is yet to be established (78).

Our data strongly support the hypothesis that the physiologic response of pDC to enter inflamed lymph nodes is actually deleterious in immunodeficiency virus infection as it brings pDC into an environment rich with virus, virus-infected cells and pro-apoptotic factors that lead to cell death. Depletion of pDC from lymphoid tissues subsequent to recruitment is likely to have a significant impact on virus control at a number of levels. Activated pDC directly suppress HIV replication in $CD4^+$ T cells (78) and can stimulate antigen-specific $CD4^+$ T cell responses (50). Virus-exposed pDC induce maturation of mDC *in vitro*, and pDC cooperate with mDC in the induction of virus-specific cytotoxic T cell responses *in vivo* (50, 80). Type I IFN production by pDC inhibits HIV replication (77) but also may have a harmful effect by promoting TRAIL expression and subsequent apoptosis of $CD4^+$ T cells (184).

Nonpathogenic SIV infection of sooty mangabeys is characterized by lower levels of chronic immune activation than SIV infection of rhesus macaques (185), and a recent study has suggested that this lack of pathogenicity is due in part to muted pDC homing to lymph nodes

together with an inability of pDC to respond appropriately to SIV stimulation in this species (171). However, these findings conflict with studies using a similar nonpathogenic model of SIV infection in African green monkeys that revealed a significant increase in the number of pDC in lymph nodes concurrent with increased IFN-α production during acute infection (89). Hence the potential for pDC recruitment and activation in these nonpathogenic models remains unclear. In addition, data from other pathogenic SIV models, including SIVsm infection of rhesus macaques and SIVmac251 infection of cynomolgus macaques, suggest that acute infection may be associated with increased numbers of pDC in lymph nodes (84, 171). While it is difficult to directly compare data generated using different virus strains and species of monkey, it is apparent from our studies that enumeration of cells by itself provides limited information about pDC kinetics. It is likely that massive pDC recruitment to inflamed lymph nodes during acute infection in some pathogenic SIV models compensates for and masks an underlying pDC death within tissues for a period of time. However, our data would indicate that newly-arrived cells would have a short life span within the hostile environment of the lymph node and may therefore have limited opportunity to function. Ultimately, pDC death exceeds replenishment as infection progresses, leading to the substantial pDC depletion from lymph nodes consistently observed in chronic HIV and SIV infection (54, 85, 186).

Reduction in circulating type I IFN in HIV infected individuals is correlated with pDC loss and is generally thought to be due to impaired pDC function (46, 87, 91, 92, 169, 187), although this is rarely studied directly. In our study, pDC from blood and lymph nodes in monkeys with acute SIVmac251 infection were largely normal in their response to TLR7 stimulation, with lymph node pDC producing TNF-α and IFN-α together at high levels that were indistinguishable from

controls. It is possible that pDC function early in infection remains intact, and studies of HIV-infected patients indicate that impaired production of IFN-α by pDC is most apparent in individuals with advanced disease (91). Whether IFN-α production by the limited number of surviving pDC in acute infection is sufficient to induce chronic $CD4^+$ T cell activation in lymph nodes, as has recently been proposed (171, 188), remains to be determined.

6.0 OVERALL DISCUSSION

The rhesus macaque/SIV model is useful for elucidating the pathogenesis of HIV and subsequent development of efficacious vaccines derived from analyses of SIV infected nonhuman primates. Depletion of mDC and pDC has been well documented in HIV-infected patients although the underlying mechanism of loss has not been defined. Primate models of HIV infection provide a means to study the dynamics of DC following viral infection in multiple tissue compartments not readily available for study in humans. Moreover, phenotypic and functional counterparts of human DC have been identified in rhesus macaques.

The aims of the current proposal were to: 1) determine whether rhesus macaque DC could be further defined into phenotypically distinct subsets similar to humans, 2) determine whether DC were recruited to lymphoid tissues during simian AIDS and 3) determine the dynamic pDC response during acute SIV infection taking into account pDC production, mobilization, recruitment, infection and death.

6.1 PHENOTYPIC DEFINITION OF RHESUS MACAQUE mDC

Human blood contains four distinct non-overlapping subsets of pDC (one) and mDC (three) (25). Similar to humans, rhesus macaque pDC were phenotypically homogeneous and defined as CD3, CD14, CD20 – negative (Lin^-) HLA-DR^+ $CD123^+$ cells lacking expression of CD11b, CD56, CD8, and CD16, representing approximately 3% of the DC fraction in blood. The three phenotypically distinct human mDC subsets are defined as within the DC fraction of blood as CD1b/c^+, $CD16^+$ and BDCA-3^+ with all three containing a fraction of $CD56^+$ cells (25). In contrast to human mDC subsets, nearly 100% of macaque mDC expressed CD16 (FcγRIII), traditionally believed to only be expressed by rhesus NK cells (132) and a minor fraction of monocytes, similar to humans (139, 189, 190). However, rhesus $CD16^+$ mDC expressed moderate levels of CD11b and CD56, characteristic markers of monocytes and a minor subset of NK cells (132, 133). In contrast to human mDC, rhesus mDC did not express CD1c. However a subset of rhesus B cells were found to express CD1c, consistent with human B cells (138). Therefore, rhesus macaque mDC are phenotypically similar to human mDC expressing CD56 and CD16 but are largely defined as a single phenotypic subset.

The finding that rhesus macaque mDC express CD16 raises a few points for consideration. Treatment of macaques with CD16-depleting mAbs would not only remove the majority of $CD16^+$ NK cells but also $CD16^+$ mDC making it difficult to discern the role of NK cells alone in the pathogenesis of SIV infection (141, 191). In addition, phenotypic identification of NK cells as $CD3^-CD16^+$ cells would also include mDC, leading to discrepancies in alterations of absolute NK cell numbers (140). Importantly, inclusion of CD16 as a lineage marker would exclude both

NK cells and mDC as lineage-positive cells resulting in dramatic reductions in absolute mDC numbers (114), inconsistent with findings from other studies (17, 85).

6.2 LOSS OF mDC IN BLOOD DURING SIMIAN AIDS

Consistent with findings in HIV-infected individuals, circulating mDC were depleted in rhesus macaques with simian AIDS. This loss has been hypothesized to be due to the redistribution of mDC to peripheral lymphoid tissues based on the bystander maturation of mDC leading to upregulation of functional CCR7 (50). However, we found no evidence of mDC recruitment to peripheral lymphoid tissues such as axillary and mesenteric lymph nodes or spleen in rhesus macaques with simian AIDS. The majority of mDC in lymph nodes expressed the Langerhans cell marker CD1a, indicating they were derived from DC in peripheral tissues not blood. However, following mammary tumor virus infection, mDC migrate directly from blood into lymph nodes by a L-selectin-dependent mechanism (192), leaving open the possibility that mDC migrate directly to lymph nodes through high endothelial venules (HEV). Nevertheless, the increased death of mDC during simian AIDS may occur faster than recruitment, resulting in the net loss of cells observed. *In vitro* studies have shown that mDC are weakly activated by exposure to HIV (98) and undergo bystander maturation induced by pDC-derived IFN-α (50). In chronic HIV, IFN-α production by pDC is impaired supporting the lack of mDC activation and recruitment to lymph nodes *in vivo.* Circulating mDC in animals with AIDS showed no evidence of increased maturation or costimulatory molecule expression and splenic DC from HIV^+ patients displayed a normal phenotype, showing no signs of *in vivo* activation but impaired

maturation following culture (145). However, in HIV-1 viremic patients, increased costimulatory molecule expression has been observed (39, 41), leaving the effect of HIV or SIV on mDC activation unclear.

6.3 LOSS OF MIGRATORY DC DURING SIMIAN AIDS

Previously, we have shown that a significant factor in the loss of mature DC in lymph nodes may be impaired trafficking of DC from epithelial surfaces (52). Consistent with this finding, the predominant mDC population lost from lymph nodes of monkeys with AIDS was the mature, $CD1a^+$ skin derived DC. The mechanism underlying suppressed migration remains unknown, although it is unlikely due to direct viral infection of DC (52). HIV and SIV are able to infect Langerhans cells (166, 167) however evidence for significant infection of Langerhans cells during advanced disease is lacking. In addition, Langerhans cell migration is unaltered during acute SIV infection when virus load is at its peak (52) and less than 1% of lymph node mDC, the majority being migratory DC, contained evidence direct SIV infection. In SIV-infected macaques with AIDS, expression of the CCR7 ligand, CCL21/6Ckine is reduced in lymph nodes (179) likely contributing to the loss of migratory $CD1a^+$ DC. Preliminary experiments using autologous delivery of *in vitro* matured monocyte-derived DC have demonstrated normal trafficking of injected cells to draining lymph nodes. This indicates that the chemokine network required for DC migration is relatively intact in monkeys with AIDS (data not shown). Thus, it is likely that the cytokine milieu of the skin and possibly other epithelial surfaces are involved in the failure of DC migration and loss in lymph nodes as discussed elsewhere (52). Increasing evidence suggests mDC are important in the induction of HIV-specific $CD4^+$ T cell responses

(50). Therefore, loss of mDC in advanced HIV infection would clearly reduce the capacity to respond to HIV or opportunistic infections, contributing to the onset of immunodeficiency.

6.4 INCREASED FREQUENCY OF 'IMMUNOSUPPRESSIVE' DC DURING AIDS

In contrast to the reduction of DC in lymph nodes of monkeys with AIDS, we observed an increase in a population of Lin^- HLA-$DR^{mod}CD11c^-CD123^-$ cells within the DC fraction of lymph nodes that morphologically resembled monocytoid cells. Overnight culture of rhesus macaque blood DC lacking CD11c or CD123 in GM-CSF and IL-4 resulted in the majority of these cells acquiring an mDC phenotype (17). Interestingly, similar culture conditions failed to induce further differentiation of Lin^- HLA-DR^{mod} cells or increase cell survival, indicating GM-CSF and IL-4 are not survival factors. Although the origin of these cells remains undefined, an increased frequency of circulating blood DC lacking CD11c and CD123 expression eliciting poor T cell proliferation and IFN-γ secretion has been identified in cancer patients (128). In addition, a similar population of cells has been identified in lymph nodes from patients with chronic HIV which induced allogenic T cells to develop a regulatory phenotype (168). The low CD86 and lack of CD80 expression of the Lin^- HLA-$DR^{mod}CD11c^-CD123^-$ cells in lymph nodes or animals with AIDS is consistent with regulatory rather than immunostimulatory DC.

6.5 pDC LOSS DURING ACUTE SIV INFECTION

To further elucidate the possible mechanisms of DC loss, we focused our final studies on pDC dynamics during the first two weeks of highly pathogenic SIV infection. Our findings demonstrate that rapid pDC increases were followed by depletion during primary SIV infection despite active mobilization from bone marrow and migration to lymph nodes. Repeated sampling over short time intervals revealed a rapid bimodal pDC response with depletion below steady state levels within 10 days of SIV infection. Importantly, the well-defined sustained reduction of blood pDC numbers in both HIV and SIV infection after peak viremia indicates the early events of infection may influence pDC frequency in the chronic phase (45, 54, 85, 169), similar to the massive depletion of memory T cells (7). Comparatively, nonpathogenic infection of African green monkeys leads to reduced frequencies of pDC in blood but increases in lymph node and IFN-α production followed by complete pDC recovery, highlighting that pDC loss likely plays a critical role in disease pathogenesis (89).

Consistent with the observed phenotypic and functional activation of HIV-1 exposed pDC (50, 68) and increased levels of inflammatory chemokines (103, 179), pDC were actively recruited to lymph nodes following pathogenic SIV infection. Considering the balance of pDC in blood and lymph nodes, we cannot exclude the possibility that sustained loss of circulating pDC in blood is partially due to both lymph node recruitment as well as death. Bone marrow from animals infected with SIV contained pDC frequencies similar to pre-infection indicating pDC depletion was not due to a primary defect in hematopoiesis supporting the effective mobilization of pDC from bone marrow in SIV-infected macaques(114). Our results point to the sustained reductions

in blood pDC reflect the inability of pDC production and mobilization to keep pace with lymph node recruitment and death.

Investigation of pDC dynamics using BrdU and Ki-67 provides initial evidence that pDC depletion is coupled with profound increases in mobilization from bone marrow as well as lymph node recruitment during acute SIV infection. The strong correlation between *in vivo* BrdU labeling and Ki-67 expression by pDC indicates future studies may incorporate Ki-67 as a relative indicator of changes in pDC mobilization and lymph node recruitment during viral infection.

6.6 ROLE OF DIRECT VIRAL INFECTION IN DC LOSS

Circulating mDC express the viral receptor and coreceptor, CD4 and CCR5, suggesting direct viral infection may lead to mDC loss. mDC are susceptible to both CCR5 and CXCR4-tropic HIV *in vitro* (98, 99) and mDC from untreated HIV-infected individuals show evidence of infection *in vivo* (40). Although the frequency of infection of blood mDC is not known, splenic DC are known to harbor 10 to 100 times less HIV DNA than infected $CD4^+$ T cells (163). Furthermore, DC from patients on virally suppressed HAART did not contain proviral DNA (100) suggesting partial recovery of mDC following anti-retroviral therapy may be due in part to decreased infection. However, until the frequency of directly infected mDC in blood is determined, the pathogenic relevance of infection in DC loss remains speculative.

Similar to mDC, circulating pDC also express the HIV receptor CD4 and coreceptors CCR5 and CXCR4, and are susceptible to HIV infection *in vitro* (95-99) and infected *in vivo* in both humans (40) and macaques (54). We identified approximately 4% of pDC were infected with SIV at the peak of plasma viremia in lymph nodes, implicating direct infection plays a minor role in pDC loss early after infection. Preliminary evidence indicates that less than 1% of lymph node pDC are infected with SIV in animals with AIDS (data not shown) and macaque pDC are infected during the acute rather than the chronic phase of infection, when pDC numbers remain depleted (54). Therefore, the continued role of direct infection in pDC loss as infection progresses remains to be determined.

6.7 APOPTOSIS AND NECROSIS OF DC

We showed that increased apoptosis or necrosis plays a role in the loss of both mDC and pDC in lymphoid tissues during acute SIV infection and animals with simian AIDS. In peripheral lymph nodes and spleen, DC were more prone to spontaneous cell death in animals with AIDS. It is possible that apoptosis of DC in HIV and SIV infection is mediated by the binding of TNF family ligands to death receptors involving Fas/FasL binding or TRAIL/DR5 interactions, known to play a role in the apoptosis of T cells in HIV/SIV infection (115, 122-124, 164). Indeed, both Fas- and TRAIL-mediated pathways have been implicated in mDC apoptosis during measles virus infection (127, 165). However, an alternative mechanism may be responsible for pDC death.

During acute SIV infection, increased frequencies of late apoptotic/necrotic pDC were found associated with direct viral infection and increased expression of CD95 (Fas). Although the direct effects of virus exposure on pDC death and survival are conflicting(50, 78, 97), pDC loss is likely due to both direct viral infection and indirect or 'bystander' killing mechanisms. pDC exposure to, or endocytosis of HIV leads to increased pDC survival and activation(50, 79) not death, whereas exposure to virus-infected cells induces pDC death in a fusion-dependant manner(78). The increased frequency of Fas-expressing pDC during acute SIV infection suggests pDC may be undergoing Fas-mediated death. However, while Fas/FasL interactions play a role in $CD4^+$ T cell loss in HIV and SIV infection(115, 183), evidence is lacking for this pathway in pDC death in HIV infection(78). Ultimately, future studies will need to focus on elucidating the exact mechanisms leading to pDC death during pathogenic HIV/SIV infection.

6.8 FUNCTIONAL TLR7 SIGNALING OF pDC DURING ACUTE SIV INFECTION

Reduction in circulating type I IFN in HIV infected individuals is correlated with pDC loss and is generally thought to be due to impaired pDC function (46, 87, 91, 92, 169, 187), although this is rarely studied directly. Despite early and sustained pDC depletion, the frequency of pDC in lymph nodes simultaneously producing TNF-α and IFN-α following TLR7 stimulation was similar to uninfected macaques. Consistent with this finding, endocytosis of HIV-1 activates pDC via TLR7 (79) and pDC exposed to HIV-1 *in vitro* were functionally normal following TLR7 stimulation and stimulation-induced DC maturation did not increase HIV-1 replication (98). It is possible that pDC function early in infection remains intact, and studies of HIV-infected patients indicate that impaired production of IFN-α by pDC is most apparent in

individuals with advanced disease and stimulated via TLR9 (91, 93, 169). Supportingly, direct interaction of HIV-1 gp120 interferes with TLR9 but not TLR7 activation of pDC (193), suggesting selective impairment of TLR9 signaling. Whether IFN-α production by the limited number of surviving pDC in acute infection is sufficient to induce chronic $CD4^+$ T cell activation in lymph nodes, as has recently been proposed (171, 188), remains to be determined.

7.0 PUBLIC HEALTH SIGNIFICANCE

There are an estimated 37 million people living with HIV-1/AIDS worldwide and in 2007, there were 2.7 million new HIV infections and 2 million HIV-related deaths (1). Moreover, HIV-1/AIDS reduces the quality of life and impacts traditional family structures in areas with high prevalence of HIV, evidenced by the increasing number of AIDS orphans in Africa (1). mDC and pDC play a critical role in bridging innate and adaptive immune responses and collaborate to induce potent anti-viral immunity. Thus DC depletion during HIV infection likely contributes to the lack of adequate immune control. Despite the benefits of anti-retroviral therapy in extending the survival of infected individuals, DC numbers and function remain below normal levels controls (38, 42-44, 46-49, 54, 84-87) . The sustained DC alterations highlight the need to determine the mechanisms leading to DC loss and dysfunction during HIV-1 infection. In this study, we found that DC loss during primary SIV infection was mainly driven by increased recruitment to lymph nodes and death, the latter being a common feature in systemic DC loss at the onset of AIDS. Collectively, these findings suggest new therapeutic strategies aimed at reducing the dysregulation of DC trafficking and dysfunction is necessary for improved control of HIV-infection.

8.0 FUTURE DIRECTIONS

8.1 FUNCTIONAL ROLE OF CD16 EXPRESSION BY mDC

Evaluating the phenotypic complexity of rhesus macaque DC raises many questions regarding differences in DC biology between humans and rhesus macaques. Firstly, CD16 is an Fc receptor that binds the Fc region of Abs, and cross-linking of Ab Fc receptors by Ab-opsonized Ag complexes initiates cellular immune responses, including phagocytosis, Ab-dependent cell-mediated cytotoxicity (ADCC), respiratory burst, and release of cytokines and inflammatory mediators (194). In rhesus macaques, sustained ADCC correlates with delayed onset of AIDS pathogenesis (195) and CD16 is critical for NK cell-targeted destruction of HIV-infected cells through ADCC (196). However, CD16 expression also plays a role in viral persistence and transmission by follicular DC (197). Therefore, the functional consequence of CD16 expression by mDC in both humans and rhesus macaques and its role in the immunopathogenesis of HIV/SIV infection requires further exploration.

The disparate expression of CD1c by species of macaques will need to be resolved as it may lead to alterations in the early dynamics of lentiviral infection. Both cynomolgus macaque and human mDC express CD1c (25, 49) and in humans, HIV has been found to productively infect a subset of $CD1c^+$ mDC *in vitro* (198). However, during chronic SIV infection of cynomolgus

macaques, the absolute number of $CD1c^+$ mDC were similar to pre-infection levels, leaving the effects of infection on $CD1c^+$ mDC in humans unclear.

8.2 mDC DEPLETION IN BLOOD

Both HIV and SIV infection lead to a significant reduction in the frequency of circulating mDC in blood. However, the exact mechanism for this loss remains undefined. A major unresolved factor in mDC loss is the frequency of direct infection in blood. mDC are infected *in vivo* (40) but until the frequency of infection is known, the role of direct infection in mDC loss will remain speculative. The major hypothesis proposed to account for DC loss has been recruitment to lymphoid tissues although support for this hypothesis is conflicting (52, 53). mDC are mainly derived from bone marrow progenitor cells implicating a primary defect in hematopoiesis may lead to reduced mDC numbers. Alternatively, monocytes may differentiate into DC under inflammatory conditions (20, 199), implicating a defect in mDC differentiation from monocytes during HIV/SIV infection may lead to mDC loss. Therefore, future studies will need to determine whether mDC frequencies are reduced due to failures in hematopoiesis or monocyte differentiation.

8.3 INFLAMMATION-DRIVEN LOSS OF DC

A characteristic of pathogenic SIV infection in nonhuman primates is a pronounced inflammatory response in lymphoid tissues (180, 200-202), including increased expression of CXCR3 ligands required for pDC recruitment (103, 104). In addition, the CCR7 ligand CCL19 is upregulated in lymphoid tissues during acute SIV infection, which may promote increased recruitment of activated DC to lymphoid tissues (179). Treatment with anti-retroviral drugs decreases viral load in HIV/SIV infection associated with recovery of DC numbers in humans (38, 42, 44, 46-48). In addition, anti-retroviral therapy is known to reduce immune activation in blood and lymph nodes in HIV infection (203-206) with recent evidence indicating restoration of pro-apoptotic factors such as Fas, TRAIL and caspase-3 to levels comparable to uninfected controls (207). Moreover, non-pathogenic SIV infection of sooty mangabeys or African green monkeys, results in preservation of at least pDC numbers (89) as well as lack of inflammation and limited immune activation in lymphoid tissues (185, 208), which may be associated with differences in DC recruitment and death. Therefore, exploring whether early anti-retroviral treatment reduces the inflammation driven recruitment of DC and death during SIV infection needs further exploration.

8.4 MECHANISM OF INCREASED DC APOPTOSIS

It is clear from our findings that both mDC and pDC undergo increased levels of apoptosis or necrosis during SIV infection. Apoptosis as a consequence of chronic immune activation is a well-described mechanism of T cell loss in HIV and SIV infection. In nonpathogenic models of SIV infection, reduced inflammation leads to less T cell apoptosis. It is clear from our findings that both mDC and pDC undergo increased levels of apoptosis or necrosis during SIV infection, indicating future experiments will need to address the exact mechanism leading to DC death. While the mechanism is likely to be complex, initial studies should focus on the effects of pDC exposure to virus-infected cells (78) and the role of TRAIL/DR5 or Fas/FasL signaling pathways in mDC death (209).

8.5 IMMUNOTHERAPEUTIC USE OF TLR7/8 AGONISTS

TLR agonists are gaining increased interest as vaccine adjuvants (210). In nonhuman primates, primary immunization with HIV Gag protein + a TLR7/8 agonist resulted in high frequencies of Th1 responses and increases in HIV Gag-specific $CD8^+$ T cell responses after an adenoviral vector boost (211). mDC infected in vitro with HIV respond to TLR7/8 ligation with full maturation and TNF-α production, similar to uninfected cells without increasing HIV-1 replication (98). In addition, direct interaction of HIV-1 gp120 interferes with TLR9 but not TLR7 activation of pDC (193) and TLR7 engagement of pDC leads to increased expression of a network of anti-apoptotic and pro-survival genes (212). Thus, early therapeutic interventions targeting TLR7 and 8 may improve immunologic control of HIV by increasing survival of both mDC and pDC.

BIBLIOGRAPHY

1. UNAIDS. 2008. 2008 report on the global AIDS epidemic. www.unaids.gov.

2. CDC. 2008. HIV/AIDS among African Americans. In *CDC HIV/AIDS fact sheet*.

3. Veazey, R. S., M. DeMaria, L. V. Chalifoux, D. E. Shvetz, D. R. Pauley, H. L. Knight, M. Rosenzweig, R. P. Johnson, R. C. Desrosiers, and A. A. Lackner. 1998. Gastrointestinal tract as a major site of CD4+ T cell depletion and viral replication in SIV infection. *Science* 280:427-431.

4. Veazey, R. S., P. A. Marx, and A. A. Lackner. 2003. Vaginal CD4+ T cells express high levels of CCR5 and are rapidly depleted in simian immunodeficiency virus infection. *J Infect Dis* 187:769-776.

5. Brenchley, J. M., T. W. Schacker, L. E. Ruff, D. A. Price, J. H. Taylor, G. J. Beilman, P. L. Nguyen, A. Khoruts, M. Larson, A. T. Haase, and D. C. Douek. 2004. CD4+ T cell depletion during all stages of HIV disease occurs predominantly in the gastrointestinal tract. *J Exp Med* 200:749-759.

6. Mehandru, S., M. A. Poles, K. Tenner-Racz, A. Horowitz, A. Hurley, C. Hogan, D. Boden, P. Racz, and M. Markowitz. 2004. Primary HIV-1 infection is associated with preferential depletion of CD4+ T lymphocytes from effector sites in the gastrointestinal tract. *J Exp Med* 200:761-770.

7. Mattapallil, J. J., D. C. Douek, B. Hill, Y. Nishimura, M. Martin, and M. Roederer. 2005. Massive infection and loss of memory CD4+ T cells in multiple tissues during acute SIV infection. *Nature* 434:1093-1097.

8. Li, Q., L. Duan, J. D. Estes, Z. M. Ma, T. Rourke, Y. Wang, C. Reilly, J. Carlis, C. J. Miller, and A. T. Haase. 2005. Peak SIV replication in resting memory CD4+ T cells depletes gut lamina propria CD4+ T cells. *Nature* 434:1148-1152.

9. Miller, C. J., Q. Li, K. Abel, E. Y. Kim, Z. M. Ma, S. Wietgrefe, L. La Franco-Scheuch, L. Compton, L. Duan, M. D. Shore, M. Zupancic, M. Busch, J. Carlis, S. Wolinsky, and A. T. Haase. 2005. Propagation and dissemination of infection after vaginal transmission of simian immunodeficiency virus. *J Virol* 79:9217-9227.

10. Koup, R. A., J. T. Safrit, Y. Cao, C. A. Andrews, G. McLeod, W. Borkowsky, C. Farthing, and D. D. Ho. 1994. Temporal association of cellular immune responses with the initial control of viremia in primary human immunodeficiency virus type 1 syndrome. *J Virol* 68:4650-4655.

11. Kuroda, M. J., J. E. Schmitz, W. A. Charini, C. E. Nickerson, M. A. Lifton, C. I. Lord, M. A. Forman, and N. L. Letvin. 1999. Emergence of CTL coincides with clearance of virus during primary simian immunodeficiency virus infection in rhesus monkeys. *J Immunol* 162:5127-5133.

12. Schmitz, J. E., M. J. Kuroda, S. Santra, V. G. Sasseville, M. A. Simon, M. A. Lifton, P. Racz, K. Tenner-Racz, M. Dalesandro, B. J. Scallon, J. Ghrayeb, M. A. Forman, D. C. Montefiori, E. P. Rieber, N. L. Letvin, and K. A. Reimann. 1999. Control of viremia in simian immunodeficiency virus infection by CD8+ lymphocytes. *Science* 283:857-860.

13. Borrow, P., H. Lewicki, B. H. Hahn, G. M. Shaw, and M. B. Oldstone. 1994. Virus-specific CD8+ cytotoxic T-lymphocyte activity associated with control of viremia in primary human immunodeficiency virus type 1 infection. *J Virol* 68:6103-6110.

14. Letvin, N. L., and N. W. King. 1990. Immunologic and pathologic manifestations of the infection of rhesus monkeys with simian immunodeficiency virus of macaques. *J Acquir Immune Defic Syndr* 3:1023-1040.

15. Joag, S. V. 2000. Primate models of AIDS. *Microbes Infect* 2:223-229.

16. Banchereau, J., F. Briere, C. Caux, J. Davoust, S. Lebecque, Y. J. Liu, B. Pulendran, and K. Palucka. 2000. Immunobiology of dendritic cells. *Annu Rev Immunol* 18:767-811.

17. Coates, P. T., S. M. Barratt-Boyes, L. Zhang, V. S. Donnenberg, P. J. O'Connell, A. J. Logar, F. J. Duncan, M. Murphey-Corb, A. D. Donnenberg, A. E. Morelli, C. R. Maliszewski, and A. W. Thomson. 2003. Dendritic cell subsets in blood and lymphoid tissue of rhesus monkeys and their mobilization with Flt3 ligand. *Blood* 102:2513-2521.

18. Pulendran, B., J. Banchereau, S. Burkeholder, E. Kraus, E. Guinet, C. Chalouni, D. Caron, C. Maliszewski, J. Davoust, J. Fay, and K. Palucka. 2000. Flt3-ligand and granulocyte colony-stimulating factor mobilize distinct human dendritic cell subsets in vivo. *J Immunol* 165:566-572.

19. Teleshova, N., J. Jones, J. Kenney, J. Purcell, R. Bohm, A. Gettie, and M. Pope. 2004. Short-term Flt3L treatment effectively mobilizes functional macaque dendritic cells. *J Leukoc Biol* 75:1102-1110.

20. Randolph, G. J., K. Inaba, D. F. Robbiani, R. M. Steinman, and W. A. Muller. 1999. Differentiation of phagocytic monocytes into lymph node dendritic cells in vivo. *Immunity* 11:753-761.

21. Geissmann, F., S. Jung, and D. R. Littman. 2003. Blood monocytes consist of two principal subsets with distinct migratory properties. *Immunity* 19:71-82.

22. Ginhoux, F., F. Tacke, V. Angeli, M. Bogunovic, M. Loubeau, X. M. Dai, E. R. Stanley, G. J. Randolph, and M. Merad. 2006. Langerhans cells arise from monocytes in vivo. *Nat Immunol* 7:265-273.

23. Naik, S. H., D. Metcalf, A. van Nieuwenhuijze, I. Wicks, L. Wu, M. O'Keeffe, and K. Shortman. 2006. Intrasplenic steady-state dendritic cell precursors that are distinct from monocytes. *Nat Immunol* 7:663-671.

24. Shortman, K., and Y. J. Liu. 2002. Mouse and human dendritic cell subtypes. *Nat Rev Immunol* 2:151-161.

25. MacDonald, K. P., D. J. Munster, G. J. Clark, A. Dzionek, J. Schmitz, and D. N. Hart. 2002. Characterization of human blood dendritic cell subsets. *Blood* 100:4512-4520.

26. Dieu, M. C., B. Vanbervliet, A. Vicari, J. M. Bridon, E. Oldham, S. Ait-Yahia, F. Briere, A. Zlotnik, S. Lebecque, and C. Caux. 1998. Selective recruitment of immature and mature dendritic cells by distinct chemokines expressed in different anatomic sites. *J Exp Med* 188:373-386.

27. Sallusto, F., P. Schaerli, P. Loetscher, C. Schaniel, D. Lenig, C. R. Mackay, S. Qin, and A. Lanzavecchia. 1998. Rapid and coordinated switch in chemokine receptor expression during dendritic cell maturation. *Eur J Immunol* 28:2760-2769.

28. Saeki, H., A. M. Moore, M. J. Brown, and S. T. Hwang. 1999. Cutting edge: secondary lymphoid-tissue chemokine (SLC) and CC chemokine receptor 7 (CCR7) participate in the emigration pathway of mature dendritic cells from the skin to regional lymph nodes. *J Immunol* 162:2472-2475.

29. Chan, V. W., S. Kothakota, M. C. Rohan, L. Panganiban-Lustan, J. P. Gardner, M. S. Wachowicz, J. A. Winter, and L. T. Williams. 1999. Secondary lymphoid-tissue chemokine (SLC) is chemotactic for mature dendritic cells. *Blood* 93:3610-3616.

30. Wilson, N. S., D. El-Sukkari, G. T. Belz, C. M. Smith, R. J. Steptoe, W. R. Heath, K. Shortman, and J. A. Villadangos. 2003. Most lymphoid organ dendritic cell types are phenotypically and functionally immature. *Blood* 102:2187-2194.

31. Summers, K. L., B. D. Hock, J. L. McKenzie, and D. N. Hart. 2001. Phenotypic characterization of five dendritic cell subsets in human tonsils. *Am J Pathol* 159:285-295.

32. Cox, K., M. North, M. Burke, H. Singhal, S. Renton, N. Aqel, S. Islam, and S. C. Knight. 2005. Plasmacytoid dendritic cells (PDC) are the major DC subset innately producing cytokines in human lymph nodes. *J Leukoc Biol* 78:1142-1152.

33. Santegoets, S. J., S. Gibbs, K. Kroeze, R. van de Ven, R. J. Scheper, C. A. Borrebaeck, T. D. de Gruijl, and M. Lindstedt. 2008. Transcriptional profiling of human skin-resident Langerhans cells and CD1a+ dermal dendritic cells: differential activation states suggest distinct functions. *J Leukoc Biol* 84:143-151.

34. Valladeau, J., O. Ravel, C. Dezutter-Dambuyant, K. Moore, M. Kleijmeer, Y. Liu, V. Duvert-Frances, C. Vincent, D. Schmitt, J. Davoust, C. Caux, S. Lebecque, and S. Saeland. 2000. Langerin, a novel C-type lectin specific to Langerhans cells, is an endocytic receptor that induces the formation of Birbeck granules. *Immunity* 12:71-81.

35. Ratzinger, G., J. Baggers, M. A. de Cos, J. Yuan, T. Dao, J. L. Reagan, C. Munz, G. Heller, and J. W. Young. 2004. Mature human Langerhans cells derived from CD34+ hematopoietic progenitors stimulate greater cytolytic T lymphocyte activity in the absence of bioactive IL-12p70, by either single peptide presentation or cross-priming, than do dermal-interstitial or monocyte-derived dendritic cells. *J Immunol* 173:2780-2791.

36. Morelli, A. E., J. P. Rubin, G. Erdos, O. A. Tkacheva, A. R. Mathers, A. F. Zahorchak, A. W. Thomson, L. D. Falo, Jr., and A. T. Larregina. 2005. CD4+ T cell responses elicited by different subsets of human skin migratory dendritic cells. *J Immunol* 175:7905-7915.

37. Peiser, M., R. Wanner, and G. Kolde. 2004. Human epidermal Langerhans cells differ from monocyte-derived Langerhans cells in CD80 expression and in secretion of IL-12 after CD40 cross-linking. *J Leukoc Biol* 76:616-622.

38. Pacanowski, J., S. Kahi, M. Baillet, P. Lebon, C. Deveau, C. Goujard, L. Meyer, E. Oksenhendler, M. Sinet, and A. Hosmalin. 2001. Reduced blood CD123+ (lymphoid) and CD11c+ (myeloid) dendritic cell numbers in primary HIV-1 infection. *Blood* 98:3016-3021.

39. Grassi, F., A. Hosmalin, D. McIlroy, V. Calvez, P. Debre, and B. Autran. 1999. Depletion in blood CD11c-positive dendritic cells from HIV-infected patients. *Aids* 13:759-766.

40. Donaghy, H., B. Gazzard, F. Gotch, and S. Patterson. 2003. Dysfunction and infection of freshly isolated blood myeloid and plasmacytoid dendritic cells in patients infected with HIV-1. *Blood* 101:4505-4511.

41. Barron, M. A., N. Blyveis, B. E. Palmer, S. MaWhinney, and C. C. Wilson. 2003. Influence of plasma viremia on defects in number and immunophenotype of blood dendritic cell subsets in human immunodeficiency virus 1-infected individuals. *J Infect Dis* 187:26-37.

42. Finke, J. S., M. Shodell, K. Shah, F. P. Siegal, and R. M. Steinman. 2004. Dendritic cell numbers in the blood of HIV-1 infected patients before and after changes in antiretroviral therapy. *J Clin Immunol* 24:647-652.

43. Donaghy, H., A. Pozniak, B. Gazzard, N. Qazi, J. Gilmour, F. Gotch, and S. Patterson. 2001. Loss of blood CD11c(+) myeloid and CD11c(-) plasmacytoid dendritic cells in patients with HIV-1 infection correlates with HIV-1 RNA virus load. *Blood* 98:2574-2576.

44. Schmidt, B., S. H. Fujimura, J. N. Martin, and J. A. Levy. 2006. Variations in plasmacytoid dendritic cell (PDC) and myeloid dendritic cell (MDC) levels in HIV-infected subjects on and off antiretroviral therapy. *J Clin Immunol* 26:55-64.

45. Killian, M. S., S. H. Fujimura, F. M. Hecht, and J. A. Levy. 2006. Similar changes in plasmacytoid dendritic cell and CD4 T-cell counts during primary HIV-1 infection and treatment. *AIDS* 20:1247-1252.

46. Chehimi, J., D. E. Campbell, L. Azzoni, D. Bacheller, E. Papasavvas, G. Jerandi, K. Mounzer, J. Kostman, G. Trinchieri, and L. J. Montaner. 2002. Persistent decreases in blood plasmacytoid dendritic cell number and function despite effective highly active antiretroviral therapy and increased blood myeloid dendritic cells in HIV-infected individuals. *J Immunol* 168:4796-4801.

47. Zhang, Z., J. Fu, Q. Zhao, Y. He, L. Jin, H. Zhang, J. Yao, L. Zhang, and F. S. Wang. 2006. Differential restoration of myeloid and plasmacytoid dendritic cells in HIV-1-infected children after treatment with highly active antiretroviral therapy. *J Immunol* 176:5644-5651.

48. Lichtner, M., R. Rossi, M. C. Rizza, F. Mengoni, I. Sauzullo, A. P. Massetti, G. Luzi, A. Hosmalin, C. M. Mastroianni, and V. Vullo. 2008. Plasmacytoid dendritic cells count in antiretroviral-treated patients is predictive of HIV load control independent of CD4+ T-cell count. *Curr HIV Res* 6:19-27.

49. Malleret, B., I. Karlsson, B. Maneglier, P. Brochard, B. Delache, T. Andrieu, M. Muller-Trutwin, T. Beaumont, J. M. McCune, J. Banchereau, R. Le Grand, and B. Vaslin. 2008. Effect of SIVmac infection on plasmacytoid and CD1c+ myeloid dendritic cells in cynomolgus macaques. *Immunology* 124:223-233.

50. Fonteneau, J. F., M. Larsson, A. S. Beignon, K. McKenna, I. Dasilva, A. Amara, Y. J. Liu, J. D. Lifson, D. R. Littman, and N. Bhardwaj. 2004. Human immunodeficiency virus type 1 activates plasmacytoid dendritic cells and concomitantly induces the bystander maturation of myeloid dendritic cells. *J Virol* 78:5223-5232.

51. Lore, K., A. Sonnerborg, C. Brostrom, L. E. Goh, L. Perrin, H. McDade, H. J. Stellbrink, B. Gazzard, R. Weber, L. A. Napolitano, Y. van Kooyk, and J. Andersson. 2002. Accumulation of DC-SIGN+CD40+ dendritic cells with reduced CD80 and CD86 expression in lymphoid tissue during acute HIV-1 infection. *Aids* 16:683-692.

52. Zimmer, M. I., A. T. Larregina, C. M. Castillo, S. Capuano, 3rd, L. D. Falo, Jr., M. Murphey-Corb, T. A. Reinhart, and S. M. Barratt-Boyes. 2002. Disrupted homeostasis of Langerhans cells and interdigitating dendritic cells in monkeys with AIDS. *Blood* 99:2859-2868.

53. Dillon, S. M., K. B. Robertson, S. C. Pan, S. Mawhinney, A. L. Meditz, J. M. Folkvord, E. Connick, M. D. McCarter, and C. C. Wilson. 2008. Plasmacytoid and myeloid dendritic cells with a partial activation phenotype accumulate in lymphoid tissue during asymptomatic chronic HIV-1 infection. *J Acquir Immune Defic Syndr* 48:1-12.

54. Reeves, R. K., and P. N. Fultz. 2007. Disparate effects of acute and chronic infection with SIVmac239 or SHIV-89.6P on macaque plasmacytoid dendritic cells. *Virology* 365:356-368.

55. Liu, K., C. Waskow, X. Liu, K. Yao, J. Hoh, and M. Nussenzweig. 2007. Origin of dendritic cells in peripheral lymphoid organs of mice. *Nat Immunol* 8:578-583.

56. Maraskovsky, E., E. Daro, E. Roux, M. Teepe, C. R. Maliszewski, J. Hoek, D. Caron, M. E. Lebsack, and H. J. McKenna. 2000. In vivo generation of human dendritic cell subsets by Flt3 ligand. *Blood* 96:878-884.

57. Farkas, L., K. Beiske, F. Lund-Johansen, P. Brandtzaeg, and F. L. Jahnsen. 2001. Plasmacytoid dendritic cells (natural interferon- alpha/beta-producing cells) accumulate in cutaneous lupus erythematosus lesions. *Am J Pathol* 159:237-243.

58. Jahnsen, F. L., F. Lund-Johansen, J. F. Dunne, L. Farkas, R. Haye, and P. Brandtzaeg. 2000. Experimentally induced recruitment of plasmacytoid (CD123high) dendritic cells in human nasal allergy. *J Immunol* 165:4062-4068.

59. Wollenberg, A., M. Wagner, S. Gunther, A. Towarowski, E. Tuma, M. Moderer, S. Rothenfusser, S. Wetzel, S. Endres, and G. Hartmann. 2002. Plasmacytoid dendritic cells: a new cutaneous dendritic cell subset with distinct role in inflammatory skin diseases. *J Invest Dermatol* 119:1096-1102.

60. Penna, G., S. Sozzani, and L. Adorini. 2001. Cutting edge: selective usage of chemokine receptors by plasmacytoid dendritic cells. *J Immunol* 167:1862-1866.

61. Zou, W., V. Machelon, A. Coulomb-L'Hermin, J. Borvak, F. Nome, T. Isaeva, S. Wei, R. Krzysiek, I. Durand-Gasselin, A. Gordon, T. Pustilnik, D. T. Curiel, P. Galanaud, F. Capron, D. Emilie, and T. J. Curiel. 2001. Stromal-derived factor-1 in human tumors recruits and alters the function of plasmacytoid precursor dendritic cells. *Nat Med* 7:1339-1346.

62. Cella, M., D. Jarrossay, F. Facchetti, O. Alebardi, H. Nakajima, A. Lanzavecchia, and M. Colonna. 1999. Plasmacytoid monocytes migrate to inflamed lymph nodes and produce large amounts of type I interferon. *Nat Med* 5:919-923.

63. Yoneyama, H., K. Matsuno, Y. Zhang, T. Nishiwaki, M. Kitabatake, S. Ueha, S. Narumi, S. Morikawa, T. Ezaki, B. Lu, C. Gerard, S. Ishikawa, and K. Matsushima. 2004. Evidence for recruitment of plasmacytoid dendritic cell precursors to inflamed lymph nodes through high endothelial venules. *Int Immunol* 16:915-928.

64. Colonna, M., G. Trinchieri, and Y. J. Liu. 2004. Plasmacytoid dendritic cells in immunity. *Nat Immunol* 5:1219-1226.

65. Siegal, F. P., N. Kadowaki, M. Shodell, P. A. Fitzgerald-Bocarsly, K. Shah, S. Ho, S. Antonenko, and Y. J. Liu. 1999. The nature of the principal type 1 interferon-producing cells in human blood. *Science* 284:1835-1837.

66. Heil, F., H. Hemmi, H. Hochrein, F. Ampenberger, C. Kirschning, S. Akira, G. Lipford, H. Wagner, and S. Bauer. 2004. Species-specific recognition of single-stranded RNA via toll-like receptor 7 and 8. *Science* 303:1526-1529.

67. Diebold, S. S., T. Kaisho, H. Hemmi, S. Akira, and C. Reis e Sousa. 2004. Innate antiviral responses by means of TLR7-mediated recognition of single-stranded RNA. *Science* 303:1529-1531.

68. Yonezawa, A., R. Morita, A. Takaori-Kondo, N. Kadowaki, T. Kitawaki, T. Hori, and T. Uchiyama. 2003. Natural alpha interferon-producing cells respond to human immunodeficiency virus type 1 with alpha interferon production and maturation into dendritic cells. *J Virol* 77:3777-3784.

69. Mandl, J. N., A. P. Barry, T. H. Vanderford, N. Kozyr, R. Chavan, S. Klucking, F. J. Barrat, R. L. Coffman, S. I. Staprans, and M. B. Feinberg. 2008. Divergent TLR7 and TLR9 signaling and type I interferon production distinguish pathogenic and nonpathogenic AIDS virus infections. *Nat Med* 14:1077-1087.

70. Pichyangkul, S., K. Yongvanitchit, U. Kum-arb, H. Hemmi, S. Akira, A. M. Krieg, D. G. Heppner, V. A. Stewart, H. Hasegawa, S. Looareesuwan, G. D. Shanks, and R. S. Miller. 2004. Malaria blood stage parasites activate human plasmacytoid dendritic cells and murine dendritic cells through a Toll-like receptor 9-dependent pathway. *J Immunol* 172:4926-4933.

71. Iwasaki, A., and R. Medzhitov. 2004. Toll-like receptor control of the adaptive immune responses. *Nat Immunol* 5:987-995.

72. Takeda, K., T. Kaisho, and S. Akira. 2003. Toll-like receptors. *Annu Rev Immunol* 21:335-376.

73. Decalf, J., S. Fernandes, R. Longman, M. Ahloulay, F. Audat, F. Lefrerre, C. M. Rice, S. Pol, and M. L. Albert. 2007. Plasmacytoid dendritic cells initiate a complex chemokine and cytokine network and are a viable drug target in chronic HCV patients. *J Exp Med* 204:2423-2437.

74. Cervantes-Barragan, L., R. Zust, F. Weber, M. Spiegel, K. S. Lang, S. Akira, V. Thiel, and B. Ludewig. 2007. Control of coronavirus infection through plasmacytoid dendritic-cell-derived type I interferon. *Blood* 109:1131-1137.

75. Lund, J. M., M. M. Linehan, N. Iijima, and A. Iwasaki. 2006. Cutting Edge: Plasmacytoid dendritic cells provide innate immune protection against mucosal viral infection in situ. *J Immunol* 177:7510-7514.

76. Muller-Trutwin, M., and A. Hosmalin. 2005. Role for plasmacytoid dendritic cells in anti-HIV innate immunity. *Immunol Cell Biol* 83:578-583.

77. Gurney, K. B., A. D. Colantonio, B. Blom, H. Spits, and C. H. Uittenbogaart. 2004. Endogenous IFN-alpha production by plasmacytoid dendritic cells exerts an antiviral effect on thymic HIV-1 infection. *J Immunol* 173:7269-7276.

78. Meyers, J. H., J. S. Justement, C. W. Hallahan, E. T. Blair, Y. A. Sun, M. A. O'Shea, G. Roby, S. Kottilil, S. Moir, C. M. Kovacs, T. W. Chun, and A. S. Fauci. 2007. Impact of HIV on cell survival and antiviral activity of plasmacytoid dendritic cells. *PLoS ONE* 2:e458.

79. Beignon, A. S., K. McKenna, M. Skoberne, O. Manches, I. DaSilva, D. G. Kavanagh, M. Larsson, R. J. Gorelick, J. D. Lifson, and N. Bhardwaj. 2005. Endocytosis of HIV-1 activates plasmacytoid dendritic cells via Toll-like receptor-viral RNA interactions. *J Clin Invest* 115:3265-3275.

80. Yoneyama, H., K. Matsuno, E. Toda, T. Nishiwaki, N. Matsuo, A. Nakano, S. Narumi, B. Lu, C. Gerard, S. Ishikawa, and K. Matsushima. 2005. Plasmacytoid DCs help lymph node DCs to induce anti-HSV CTLs. *J Exp Med* 202:425-435.

81. Krug, A., A. R. French, W. Barchet, J. A. Fischer, A. Dzionek, J. T. Pingel, M. M. Orihuela, S. Akira, W. M. Yokoyama, and M. Colonna. 2004. TLR9-dependent recognition of MCMV by IPC and DC generates coordinated cytokine responses that activate antiviral NK cell function. *Immunity* 21:107-119.

82. Biron, C. A. 2001. Interferons alpha and beta as immune regulators--a new look. *Immunity* 14:661-664.

83. Kolumam, G. A., S. Thomas, L. J. Thompson, J. Sprent, and K. Murali-Krishna. 2005. Type I interferons act directly on CD8 T cells to allow clonal expansion and memory formation in response to viral infection. *J Exp Med* 202:637-650.

84. Malleret, B., B. Maneglier, I. Karlsson, P. Lebon, M. Nascimbeni, L. Perie, P. Brochard, B. Delache, J. Calvo, T. Andrieu, O. Spreux-Varoquaux, A. Hosmalin, R. Le Grand, and B. Vaslin. 2008. Primary infection with simian immunodeficiency virus: plasmacytoid dendritic cell homing to lymph nodes, type I IFN, and immune suppression. *Blood*.

85. Brown, K. N., A. Trichel, and S. M. Barratt-Boyes. 2007. Parallel loss of myeloid and plasmacytoid dendritic cells from blood and lymphoid tissue in simian AIDS. *J Immunol* 178:6958-6967.

86. Pacanowski, J., L. Develioglu, I. Kamga, M. Sinet, M. Desvarieux, P. M. Girard, and A. Hosmalin. 2004. Early plasmacytoid dendritic cell changes predict plasma HIV load rebound during primary infection. *J Infect Dis* 190:1889-1892.

87. Soumelis, V., I. Scott, F. Gheyas, D. Bouhour, G. Cozon, L. Cotte, L. Huang, J. A. Levy, and Y. J. Liu. 2001. Depletion of circulating natural type 1 interferon-producing cells in HIV-infected AIDS patients. *Blood* 98:906-912.

88. Azzoni, L., R. M. Rutstein, J. Chehimi, M. A. Farabaugh, A. Nowmos, and L. J. Montaner. 2005. Dendritic and natural killer cell subsets associated with stable or declining CD4+ cell counts in treated HIV-1-infected children. *J Infect Dis* 191:1451-1459.

89. Diop, O. M., M. J. Ploquin, L. Mortara, A. Faye, B. Jacquelin, D. Kunkel, P. Lebon, C. Butor, A. Hosmalin, F. Barre-Sinoussi, and M. C. Muller-Trutwin. 2008. Plasmacytoid dendritic cell dynamics and alpha interferon production during Simian immunodeficiency virus infection with a nonpathogenic outcome. *J Virol* 82:5145-5152.

90. Pichyangkul, S., T. P. Endy, S. Kalayanarooj, A. Nisalak, K. Yongvanitchit, S. Green, A. L. Rothman, F. A. Ennis, and D. H. Libraty. 2003. A blunted blood plasmacytoid dendritic cell response to an acute systemic viral infection is associated with increased disease severity. *J Immunol* 171:5571-5578.

91. Feldman, S., D. Stein, S. Amrute, T. Denny, Z. Garcia, P. Kloser, Y. Sun, N. Megjugorac, and P. Fitzgerald-Bocarsly. 2001. Decreased interferon-alpha production in HIV-infected patients correlates with numerical and functional deficiencies in circulating type 2 dendritic cell precursors. *Clin Immunol* 101:201-210.

92. Martinson, J. A., A. Roman-Gonzalez, A. R. Tenorio, C. J. Montoya, C. N. Gichinga, M. T. Rugeles, M. Tomai, A. M. Krieg, S. Ghanekar, L. L. Baum, and A. L. Landay. 2007. Dendritic cells from HIV-1 infected individuals are less responsive to toll-like receptor (TLR) ligands. *Cell Immunol* 250:75-84.

93. Tilton, J. C., M. M. Manion, M. R. Luskin, A. J. Johnson, A. A. Patamawenu, C. W. Hallahan, N. A. Cogliano-Shutta, J. M. Mican, R. T. Davey, Jr., S. Kottilil, J. D. Lifson, J. A. Metcalf, R. A. Lempicki, and M. Connors. 2008. Human immunodeficiency virus viremia induces plasmacytoid dendritic cell activation in vivo and diminished alpha interferon production in vitro. *J Virol* 82:3997-4006.

94. Howell, D. M., S. B. Feldman, P. Kloser, and P. Fitzgerald-Bocarsly. 1994. Decreased frequency of functional natural interferon-producing cells in peripheral blood of patients with the acquired immune deficiency syndrome. *Clin Immunol Immunopathol* 71:223-230.

95. Patterson, S., A. Rae, N. Hockey, J. Gilmour, and F. Gotch. 2001. Plasmacytoid dendritic cells are highly susceptible to human immunodeficiency virus type 1 infection and release infectious virus. *J Virol* 75:6710-6713.

96. Fong, L., M. Mengozzi, N. W. Abbey, B. G. Herndier, and E. G. Engleman. 2002. Productive infection of plasmacytoid dendritic cells with human immunodeficiency virus type 1 is triggered by CD40 ligation. *J Virol* 76:11033-11041.

97. Schmidt, B., I. Scott, R. G. Whitmore, H. Foster, S. Fujimura, J. Schmitz, and J. A. Levy. 2004. Low-level HIV infection of plasmacytoid dendritic cells: onset of cytopathic effects and cell death after PDC maturation. *Virology* 329:280-288.

98. Smed-Sorensen, A., K. Lore, J. Vasudevan, M. K. Louder, J. Andersson, J. R. Mascola, A. L. Spetz, and R. A. Koup. 2005. Differential susceptibility to human immunodeficiency virus type 1 infection of myeloid and plasmacytoid dendritic cells. *J Virol* 79:8861-8869.

99. Lore, K., A. Smed-Sorensen, J. Vasudevan, J. R. Mascola, and R. A. Koup. 2005. Myeloid and plasmacytoid dendritic cells transfer HIV-1 preferentially to antigen-specific CD4+ T cells. *J Exp Med* 201:2023-2033.

100. Otero, M., G. Nunnari, D. Leto, J. Sullivan, F. X. Wang, I. Frank, Y. Xu, C. Patel, G. Dornadula, J. Kulkosky, and R. J. Pomerantz. 2003. Peripheral blood Dendritic cells are not a major reservoir for HIV type 1 in infected individuals on virally suppressive HAART. *AIDS Res Hum Retroviruses* 19:1097-1103.

101. Schmidt, B., B. M. Ashlock, H. Foster, S. H. Fujimura, and J. A. Levy. 2005. HIV-infected cells are major inducers of plasmacytoid dendritic cell interferon production, maturation, and migration. *Virology* 343:256-266.

102. Del Corno, M., M. C. Gauzzi, G. Penna, F. Belardelli, L. Adorini, and S. Gessani. 2005. Human immunodeficiency virus type 1 gp120 and other activation stimuli are highly effective in triggering alpha interferon and CC chemokine production in circulating plasmacytoid but not myeloid dendritic cells. *J Virol* 79:12597-12601.

103. Reinhart, T. A., B. A. Fallert, M. E. Pfeifer, S. Sanghavi, S. Capuano, 3rd, P. Rajakumar, M. Murphey-Corb, R. Day, C. L. Fuller, and T. M. Schaefer. 2002. Increased expression of the inflammatory chemokine CXC chemokine ligand 9/monokine induced by interferon-gamma in lymphoid tissues of rhesus macaques during simian immunodeficiency virus infection and acquired immunodeficiency syndrome. *Blood* 99:3119-3128.

104. Sarkar, S., V. Kalia, M. Murphey-Corb, R. C. Montelaro, and T. A. Reinhart. 2003. Expression of IFN-gamma induced CXCR3 agonist chemokines and compartmentalization of CXCR3+ cells in the periphery and lymph nodes of rhesus macaques during simian immunodeficiency virus infection and acquired immunodeficiency syndrome. *J Med Primatol* 32:247-264.

105. Geissler, R. G., O. G. Ottmann, K. Kleiner, U. Mentzel, A. Bickelhaupt, D. Hoelzer, and A. Ganser. 1993. Decreased haematopoietic colony growth in long-term bone marrow cultures of HIV-positive patients. *Res Virol* 144:69-73.

106. Marandin, A., A. Katz, E. Oksenhendler, M. Tulliez, F. Picard, W. Vainchenker, and F. Louache. 1996. Loss of primitive hematopoietic progenitors in patients with human immunodeficiency virus infection. *Blood* 88:4568-4578.

107. Steinberg, H. N., C. S. Crumpacker, and P. A. Chatis. 1991. In vitro suppression of normal human bone marrow progenitor cells by human immunodeficiency virus. *J Virol* 65:1765-1769.

108. Beltz, L., O. Narayan, R. J. Adams, S. J. Noga, and A. D. Donnenberg. 1991. Recovery of the simian immunodeficiency virus (SIV) and depression of colony formation in in vitro infected progenitor cell-enriched rhesus bone marrow (BM). *J Med Primatol* 20:144-151.

109. Hillyer, C. D., D. A. Lackey, 3rd, F. Villinger, E. F. Winton, H. M. McClure, and A. A. Ansari. 1993. CD34+ and CFU-GM progenitors are significantly decreased in SIVsmm9 infected rhesus macaques with minimal evidence of direct viral infection by polymerase chain reaction. *Am J Hematol* 43:274-278.

110. Thiebot, H., B. Vaslin, S. Derdouch, J. M. Bertho, F. Mouthon, S. Prost, G. Gras, P. Ducouret, D. Dormont, and R. Le Grand. 2005. Impact of bone marrow hematopoiesis failure on T-cell generation during pathogenic simian immunodeficiency virus infection in macaques. *Blood* 105:2403-2409.

111. Moses, A., J. Nelson, and G. C. Bagby, Jr. 1998. The influence of human immunodeficiency virus-1 on hematopoiesis. *Blood* 91:1479-1495.

112. Shen, H., T. Cheng, F. I. Preffer, D. Dombkowski, M. H. Tomasson, D. E. Golan, O. Yang, W. Hofmann, J. G. Sodroski, A. D. Luster, and D. T. Scadden. 1999. Intrinsic human immunodeficiency virus type 1 resistance of hematopoietic stem cells despite coreceptor expression. *J Virol* 73:728-737.

113. Lee, C. I., M. J. Cowan, D. B. Kohn, and A. F. Tarantal. 2004. Simian immunodeficiency virus infection of hematopoietic stem cells and bone marrow stromal cells. *J Acquir Immune Defic Syndr* 36:553-561.

114. Koopman, G., H. Niphuis, A. G. Haaksma, A. M. Farese, D. B. Casey, L. E. Kahn, D. Mann, T. J. MacVittie, S. L. Woulfe, and J. L. Heeney. 2004. Increase in plasmacytoid and myeloid dendritic cells by progenipoietin-1, a chimeric Flt-3 and G-CSF receptor agonist, in SIV-Infected rhesus macaques. *Hum Immunol* 65:303-316.

115. Hurtrel, B., F. Petit, D. Arnoult, M. Muller-Trutwin, G. Silvestri, and J. Estaquier. 2005. Apoptosis in SIV infection. *Cell Death Differ* 12 Suppl 1:979-990.

116. Finkel, T. H., G. Tudor-Williams, N. K. Banda, M. F. Cotton, T. Curiel, C. Monks, T. W. Baba, R. M. Ruprecht, and A. Kupfer. 1995. Apoptosis occurs predominantly in bystander cells and not in productively infected cells of HIV- and SIV-infected lymph nodes. *Nat Med* 1:129-134.

117. Bell, D. J., and D. H. Dockrell. 2003. Apoptosis in HIV-1 infection. *J Eur Acad Dermatol Venereol* 17:178-183.

118. Ahr, B., V. Robert-Hebmann, C. Devaux, and M. Biard-Piechaczyk. 2004. Apoptosis of uninfected cells induced by HIV envelope glycoproteins. *Retrovirology* 1:12.

119. Holm, G. H., C. Zhang, P. R. Gorry, K. Peden, D. Schols, E. De Clercq, and D. Gabuzda. 2004. Apoptosis of bystander T cells induced by human immunodeficiency virus type 1 with increased envelope/receptor affinity and coreceptor binding site exposure. *J Virol* 78:4541-4551.

120. Kameoka, M., S. Suzuki, T. Kimura, K. Fujinaga, W. Auwanit, R. B. Luftig, and K. Ikuta. 1997. Exposure of resting peripheral blood T cells to HIV-1 particles generates CD25+ killer cells in a small subset, leading to induction of apoptosis in bystander cells. *Int Immunol* 9:1453-1462.

121. Zhang, M., X. Li, X. Pang, L. Ding, O. Wood, K. Clouse, I. Hewlett, and A. I. Dayton. 2001. Identification of a potential HIV-induced source of bystander-mediated apoptosis in T cells: upregulation of trail in primary human macrophages by HIV-1 tat. *J Biomed Sci* 8:290-296.

122. Lelievre, J. D., F. Petit, D. Arnoult, J. C. Ameisen, and J. Estaquier. 2005. Interleukin 7 increases human immunodeficiency virus type 1 LAI-mediated Fas-induced T-cell death. *J Virol* 79:3195-3199.

123. Oyaizu, N., Y. Adachi, F. Hashimoto, T. W. McCloskey, N. Hosaka, N. Kayagaki, H. Yagita, and S. Pahwa. 1997. Monocytes express Fas ligand upon CD4 cross-linking and induce CD4+ T cells apoptosis: a possible mechanism of bystander cell death in HIV infection. *J Immunol* 158:2456-2463.

124. Petit, F., J. Corbeil, J. D. Lelievre, L. Moutouh-de Parseval, G. Pinon, D. R. Green, J. C. Ameisen, and J. Estaquier. 2001. Role of CD95-activated caspase-1 processing of IL-1beta in TCR-mediated proliferation of HIV-infected CD4(+) T cells. *Eur J Immunol* 31:3513-3524.

125. Salvato, M. S., C. C. Yin, H. Yagita, T. Maeda, K. Okumura, I. Tikhonov, and C. D. Pauza. 2007. Attenuated disease in SIV-infected macaques treated with a monoclonal antibody against FasL. *Clin Dev Immunol* 2007:93462.

126. Rescigno, M., V. Piguet, B. Valzasina, S. Lens, R. Zubler, L. French, V. Kindler, J. Tschopp, and P. Ricciardi-Castagnoli. 2000. Fas engagement induces the maturation of dendritic cells (DCs), the release of interleukin (IL)-1beta, and the production of interferon gamma in the absence of IL-12 during DC-T cell cognate interaction: a new role for Fas ligand in inflammatory responses. *J Exp Med* 192:1661-1668.

127. Fugier-Vivier, I., C. Servet-Delprat, P. Rivailler, M. C. Rissoan, Y. J. Liu, and C. Rabourdin-Combe. 1997. Measles virus suppresses cell-mediated immunity by interfering with the survival and functions of dendritic and T cells. *J Exp Med* 186:813-823.

128. Pinzon-Charry, A., C. S. Ho, R. Laherty, T. Maxwell, D. Walker, R. A. Gardiner, L. O'Connor, C. Pyke, C. Schmidt, C. Furnival, and J. A. Lopez. 2005. A population of HLA-DR+ immature cells accumulates in the blood dendritic cell compartment of patients with different types of cancer. *Neoplasia* 7:1112-1122.

129. Pinzon-Charry, A., T. Maxwell, M. A. McGuckin, C. Schmidt, C. Furnival, and J. A. Lopez. 2006. Spontaneous apoptosis of blood dendritic cells in patients with breast cancer. *Breast Cancer Res* 8:R5.

130. Koopman, G., D. Mortier, H. Niphuis, A. M. Farese, L. E. Kahn, D. Mann, R. Wagner, T. J. MacVittie, S. L. Woulfe, and J. L. Heeney. 2005. Systemic mobilization of antigen presenting cells, with a chimeric Flt-3 and G-CSF receptor agonist, during immunization of Macaca mulatta with HIV-1 antigens is insufficient to modulate immune responses or vaccine efficacy. *Vaccine* 23:4195-4202.

131. Mehlhop, E., L. A. Villamide, I. Frank, A. Gettie, C. Santisteban, D. Messmer, R. Ignatius, J. D. Lifson, and M. Pope. 2002. Enhanced in vitro stimulation of rhesus macaque dendritic cells for activation of SIV-specific T cell responses. *J Immunol Methods* 260:219-234.

132. Webster, R. L., and R. P. Johnson. 2005. Delineation of multiple subpopulations of natural killer cells in rhesus macaques. *Immunology* 115:206-214.

133. Carter, D. L., T. M. Shieh, R. L. Blosser, K. R. Chadwick, J. B. Margolick, J. E. Hildreth, J. E. Clements, and M. C. Zink. 1999. CD56 identifies monocytes and not natural killer cells in rhesus macaques. *Cytometry* 37:41-50.

134. Mandy, F. F., J. K. Nicholson, and J. S. McDougal. 2003. Guidelines for performing single-platform absolute CD4+ T-cell determinations with CD45 gating for persons infected with human immunodeficiency virus. Centers for Disease Control and Prevention. *MMWR Recomm Rep* 52:1-13.

135. Lichtner, M., R. Rossi, F. Mengoni, S. Vignoli, B. Colacchia, A. P. Massetti, I. Kamga, A. Hosmalin, V. Vullo, and C. M. Mastroianni. 2006. Circulating dendritic cells and interferon-alpha production in patients with tuberculosis: correlation with clinical outcome and treatment response. *Clin Exp Immunol* 143:329-337.

136. Vuckovic, S., D. Gardiner, K. Field, G. V. Chapman, D. Khalil, D. Gill, P. Marlton, K. Taylor, S. Wright, A. Pinzon-Charry, C. M. Pyke, R. Rodwell, R. L. Hockey, M. Gleeson, S. Tepes, D. True, A. Cotterill, and D. N. Hart. 2004. Monitoring dendritic cells in clinical practice using a new whole blood single-platform TruCOUNT assay. *J Immunol Methods* 284:73-87.

137. Herzenberg, L. A., J. Tung, W. A. Moore, L. A. Herzenberg, and D. R. Parks. 2006. Interpreting flow cytometry data: a guide for the perplexed. *Nat Immunol* 7:681-685.

138. Dzionek, A., A. Fuchs, P. Schmidt, S. Cremer, M. Zysk, S. Miltenyi, D. W. Buck, and J. Schmitz. 2000. BDCA-2, BDCA-3, and BDCA-4: three markers for distinct subsets of dendritic cells in human peripheral blood. *J Immunol* 165:6037-6046.

139. Munn, D. H., A. G. Bree, A. C. Beall, M. D. Kaviani, H. Sabio, R. G. Schaub, R. K. Alpaugh, L. M. Weiner, and S. J. Goldman. 1996. Recombinant human macrophage colony-stimulating factor in nonhuman primates: selective expansion of a CD16+ monocyte subset with phenotypic similarity to primate natural killer cells. *Blood* 88:1215-1224.

140. Lore, K., R. Seggewiss, F. J. Guenaga, S. Pittaluga, R. E. Donahue, A. Krouse, M. E. Metzger, R. A. Koup, C. Reilly, D. C. Douek, and C. E. Dunbar. 2006. In vitro culture during retroviral transduction improves thymic repopulation and output after total body irradiation and autologous peripheral blood progenitor cell transplantation in rhesus macaques. *Stem Cells* 24:1539-1548.

141. Choi, E. I., R. Wang, L. Peterson, N. L. Letvin, and K. A. Reimann. 2008. Use of an anti-CD16 antibody for in vivo depletion of natural killer cells in rhesus macaques. *Immunology* 124:215-222.

142. Randolph, G. J., V. Angeli, and M. A. Swartz. 2005. Dendritic-cell trafficking to lymph nodes through lymphatic vessels. *Nat Rev Immunol* 5:617-628.

143. Wilson, N. S., D. El-Sukkari, G. T. Belz, C. M. Smith, R. J. Steptoe, W. R. Heath, K. Shortman, and J. A. Villadangos. 2003. Most lymphoid organ dendritic cell types are phenotypically and functionally immature. *Blood.* 102:2187-2194.

144. Schlecht, G., S. Garcia, N. Escriou, A. A. Freitas, C. Leclerc, and G. Dadaglio. 2004. Murine plasmacytoid dendritic cells induce effector/memory CD8+ T-cell responses in vivo after viral stimulation. *Blood* 104:1808-1815.

145. McIlroy, D., B. Autran, J. P. Clauvel, E. Oksenhendler, P. Debre, and A. Hosmalin. 1998. Low CD83, but normal MHC class II and costimulatory molecule expression, on spleen dendritic cells from HIV+ patients. *AIDS Res Hum Retroviruses* 14:505-513.

146. Teleshova, N., J. Kenney, J. Jones, J. Marshall, G. Van Nest, J. Dufour, R. Bohm, J. D. Lifson, A. Gettie, and M. Pope. 2004. CpG-C immunostimulatory oligodeoxyribonucleotide activation of plasmacytoid dendritic cells in rhesus macaques to augment the activation of IFN-gamma-secreting simian immunodeficiency virus-specific T cells. *J Immunol.* 173:1647-1657.

147. Coates, P. T., S. M. Barratt-Boyes, L. Zhang, V. S. Donnenberg, P. J. O'Connell, A. J. Logar, F. J. Duncan, M. Murphey-Corb, A. D. Donnenberg, A. E. Morelli, C. R. Maliszewski, and A. W. Thomson. 2003. Dendritic cell subsets in blood and lymphoid tissue of rhesus monkeys and their mobilization with Flt3 ligand. *Blood.* 102:2513-2521.

148. Soderlund, J., C. Nilsson, K. Lore, E. Castanos-Velez, M. Ekman, T. Heiden, G. Biberfeld, J. Andersson, and P. Biberfeld. 2004. Dichotomy between CD1a+ and CD83+ dendritic cells in lymph nodes during SIV infection of macaques. *J Med Primatol* 33:16-24.

149. Amedee, A. M., N. Lacour, J. L. Gierman, L. N. Martin, J. E. Clements, R. Bohm, Jr., R. M. Harrison, and M. Murphey-Corb. 1995. Genotypic selection of simian immunodeficiency virus in macaque infants infected transplacentally. *J Virol* 69:7982-7990.

150. Seman, A. L., W. F. Pewen, L. F. Fresh, L. N. Martin, and M. Murphey-Corb. 2000. The replicative capacity of rhesus macaque peripheral blood mononuclear cells for simian immunodeficiency virus in vitro is predictive of the rate of progression to AIDS in vivo. *J Gen Virol* 81:2441-2449.

151. Barratt-Boyes, S. M., M. I. Zimmer, L. A. Harshyne, E. M. Meyer, S. C. Watkins, S. Capuano, 3rd, M. Murphey-Corb, L. D. Falo, Jr., and A. D. Donnenberg. 2000. Maturation and trafficking of monocyte-derived dendritic cells in monkeys: implications for dendritic cell-based vaccines. *J Immunol* 164:2487-2495.

152. Barratt-Boyes, S. M., S. C. Watkins, and O. J. Finn. 1997. In vivo migration of dendritic cells differentiated in vitro: a chimpanzee model. *J Immunol* 158:4543-4547.

153. Mavilio, D., J. Benjamin, D. Kim, G. Lombardo, M. Daucher, A. Kinter, E. Nies-Kraske, E. Marcenaro, A. Moretta, and A. S. Fauci. 2005. Identification of NKG2A and NKp80 as specific natural killer cell markers in rhesus and pigtailed monkeys. *Blood* 106:1718-1725.

154. Nestle, F. O., X. G. Zheng, C. B. Thompson, L. A. Turka, and B. J. Nickoloff. 1993. Characterization of dermal dendritic cells obtained from normal human skin reveals phenotypic and functionally distinctive subsets. *J Immunol* 151:6535-6545.

155. Huang, A., J. W. Gilmour, N. Imami, P. Amjadi, D. C. Henderson, and T. G. Allen-Mersh. 2003. Increased serum transforming growth factor-beta1 in human colorectal cancer correlates with reduced circulating dendritic cells and increased colonic Langerhans cell infiltration. *Clin Exp Immunol* 134:270-278.

156. Ruedl, C., P. Koebel, M. Bachmann, M. Hess, and K. Karjalainen. 2000. Anatomical origin of dendritic cells determines their life span in peripheral lymph nodes. *J Immunol* 165:4910-4916.

157. McKenna, K., A. S. Beignon, and N. Bhardwaj. 2005. Plasmacytoid dendritic cells: linking innate and adaptive immunity. *J Virol* 79:17-27.

158. Barratt-Boyes, S. M., M. I. Zimmer, and L. Harshyne. 2002. Changes in dendritic cell migration and activation during SIV infection suggest a role in initial viral spread and eventual immunosuppression. *J Med Primatol* 31:186-193.

159. Servet, C., L. Zitvogel, and A. Hosmalin. 2002. Dendritic cells in innate immune responses against HIV. *Curr Mol Med* 2:739-756.

160. Knight, S. C., and S. Patterson. 1997. Bone marrow-derived dendritic cells, infection with human immunodeficiency virus, and immunopathology. *Annu Rev Immunol* 15:593-615.

161. Perfetto, S. P., P. K. Chattopadhyay, L. Lamoreaux, R. Nguyen, D. Ambrozak, R. A. Koup, and M. Roederer. 2006. Amine reactive dyes: an effective tool to discriminate live and dead cells in polychromatic flow cytometry. *J Immunol Methods* 313:199-208.

162. Hu, J., C. J. Miller, U. O'Doherty, P. A. Marx, and M. Pope. 1999. The dendritic cell-T cell milieu of the lymphoid tissue of the tonsil provides a locale in which SIV can reside and propagate at chronic stages of infection. *AIDS Res Hum Retroviruses* 15:1305-1314.

163. McIlroy, D., B. Autran, R. Cheynier, S. Wain-Hobson, J. P. Clauvel, E. Oksenhendler, P. Debre, and A. Hosmalin. 1995. Infection frequency of dendritic cells and CD4+ T lymphocytes in spleens of human immunodeficiency virus-positive patients. *J Virol* 69:4737-4745.

164. Herbeuval, J. P., J. C. Grivel, A. Boasso, A. W. Hardy, C. Chougnet, M. J. Dolan, H. Yagita, J. D. Lifson, and G. M. Shearer. 2005. CD4+ T-cell death induced by infectious and noninfectious HIV-1: role of type 1 interferon-dependent, TRAIL/DR5-mediated apoptosis. *Blood* 106:3524-3531.

165. Vidalain, P. O., O. Azocar, B. Lamouille, A. Astier, C. Rabourdin-Combe, and C. Servet-Delprat. 2000. Measles virus induces functional TRAIL production by human dendritic cells. *J Virol* 74:556-559.

166. Kawamura, T., F. O. Gulden, M. Sugaya, D. T. McNamara, D. L. Borris, M. M. Lederman, J. M. Orenstein, P. A. Zimmerman, and A. Blauvelt. 2003. R5 HIV productively infects Langerhans cells, and infection levels are regulated by compound CCR5 polymorphisms. *Proc Natl Acad Sci U S A* 100:8401-8406.

167. Hu, J., M. B. Gardner, and C. J. Miller. 2000. Simian immunodeficiency virus rapidly penetrates the cervicovaginal mucosa after intravaginal inoculation and infects intraepithelial dendritic cells. *J Virol* 74:6087-6095.

168. Krathwohl, M. D., T. W. Schacker, and J. L. Anderson. 2006. Abnormal presence of semimature dendritic cells that induce regulatory T cells in HIV-infected subjects. *J Infect Dis* 193:494-504.

169. Kamga, I., S. Kahi, L. Develioglu, M. Lichtner, C. Maranon, C. Deveau, L. Meyer, C. Goujard, P. Lebon, M. Sinet, and A. Hosmalin. 2005. Type I interferon production is profoundly and transiently impaired in primary HIV-1 infection. *J Infect Dis* 192:303-310.

170. Levy, J. A., I. Scott, and C. Mackewicz. 2003. Protection from HIV/AIDS: the importance of innate immunity. *Clin Immunol* 108:167-174.

171. Mandl, J. N., A. P. Barry, T. H. Vanderford, N. Kozyr, R. Chavan, S. Klucking, F. J. Barrat, R. L. Coffman, S. I. Staprans, and M. B. Feinberg. 2008. Divergent TLR7 and TLR9 signaling and type I interferon production distinguish pathogenic and nonpathogenic AIDS virus infections. *Nature medicine*.

172. Barratt-Boyes, S. M., A. C. Soloff, W. Gao, E. Nwanegbo, X. Liu, P. A. Rajakumar, K. N. Brown, P. D. Robbins, M. Murphey-Corb, R. D. Day, and A. Gambotto. 2006. Broad cellular immunity with robust memory responses to simian immunodeficiency virus following serial vaccination with adenovirus 5- and 35-based vectors. *J Gen Virol* 87:139-149.

173. Martinez, I., L. Giavedoni, and E. Kraiselburd. 2002. Clone B7 cells have a single copy of SIVsmB7 integrated in chromosome 20. *Arch Virol* 147:217-223.

174. Reeves, R. K., and P. N. Fultz. 2008. Characterization of plasmacytoid dendritic cells in bone marrow of pig-tailed macaques. *Clin Vaccine Immunol* 15:35-41.

175. Scholzen, T., and J. Gerdes. 2000. The Ki-67 protein: from the known and the unknown. *J Cell Physiol* 182:311-322.

176. Stranges, P. B., J. Watson, C. J. Cooper, C. M. Choisy-Rossi, A. C. Stonebraker, R. A. Beighton, H. Hartig, J. P. Sundberg, S. Servick, G. Kaufmann, P. J. Fink, and A. V. Chervonsky. 2007. Elimination of antigen-presenting cells and autoreactive T cells by Fas contributes to prevention of autoimmunity. *Immunity* 26:629-641.

177. Penit, C. 1986. In vivo thymocyte maturation. BUdR labeling of cycling thymocytes and phenotypic analysis of their progeny support the single lineage model. *J Immunol* 137:2115-2121.

178. Graziosi, C., K. R. Gantt, M. Vaccarezza, J. F. Demarest, M. Daucher, M. S. Saag, G. M. Shaw, T. C. Quinn, O. J. Cohen, C. C. Welbon, G. Pantaleo, and A. S. Fauci. 1996. Kinetics of cytokine expression during primary human immunodeficiency virus type 1 infection. *Proceedings of the National Academy of Sciences of the United States of America* 93:4386-4391.

179. Choi, Y. K., B. A. Fallert, M. A. Murphey-Corb, and T. A. Reinhart. 2003. Simian immunodeficiency virus dramatically alters expression of homeostatic chemokines and dendritic cell markers during infection in vivo. *Blood* 101:1684-1691.

180. Abel, K., D. M. Rocke, B. Chohan, L. Fritts, and C. J. Miller. 2005. Temporal and anatomic relationship between virus replication and cytokine gene expression after vaginal simian immunodeficiency virus infection. *J Virol* 79:12164-12172.

181. Zhang, Z., T. Schuler, M. Zupancic, S. Wietgrefe, K. A. Staskus, K. A. Reimann, T. A. Reinhart, M. Rogan, W. Cavert, C. J. Miller, R. S. Veazey, D. Notermans, S. Little, S. A. Danner, D. D. Richman, D. Havlir, J. Wong, H. L. Jordan, T. W. Schacker, P. Racz, K. Tenner-Racz, N. L. Letvin, S. Wolinsky, and A. T. Haase. 1999. Sexual transmission and propagation of SIV and HIV in resting and activated CD4+ T cells. *Science (New York, N.Y* 286:1353-1357.

182. Piguet, V., and R. M. Steinman. 2007. The interaction of HIV with dendritic cells: outcomes and pathways. *Trends in immunology* 28:503-510.

183. Katsikis, P. D., E. S. Wunderlich, C. A. Smith, and L. A. Herzenberg. 1995. Fas antigen stimulation induces marked apoptosis of T lymphocytes in human immunodeficiency virus-infected individuals. *J Exp Med* 181:2029-2036.

184. Herbeuval, J. P., and G. M. Shearer. 2007. HIV-1 immunopathogenesis: how good interferon turns bad. *Clinical immunology (Orlando, Fla* 123:121-128.

185. Silvestri, G., D. L. Sodora, R. A. Koup, M. Paiardini, S. P. O'Neil, H. M. McClure, S. I. Staprans, and M. B. Feinberg. 2003. Nonpathogenic SIV infection of sooty mangabeys is characterized by limited bystander immunopathology despite chronic high-level viremia. *Immunity* 18:441-452.

186. Biancotto, A., J. C. Grivel, S. J. Iglehart, C. Vanpouille, A. Lisco, S. F. Sieg, R. Debernardo, K. Garate, B. Rodriguez, L. B. Margolis, and M. M. Lederman. 2007. Abnormal activation and cytokine spectra in lymph nodes of people chronically infected with HIV-1. *Blood* 109:4272-4279.

187. Hosmalin, A., and P. Lebon. 2006. Type I interferon production in HIV-infected patients. *Journal of leukocyte biology* 80:984-993.

188. Sedaghat, A. R., J. German, T. M. Teslovich, J. Cofrancesco, Jr., C. C. Jie, C. C. Talbot, Jr., and R. F. Siliciano. 2008. Chronic CD4+ T-cell activation and depletion in human immunodeficiency virus type 1 infection: type I interferon-mediated disruption of T-cell dynamics. *Journal of virology* 82:1870-1883.

189. Ziegler-Heitbrock, H. W. 1996. Heterogeneity of human blood monocytes: the CD14+ CD16+ subpopulation. *Immunol Today* 17:424-428.

190. Ziegler-Heitbrock, H. W., G. Fingerle, M. Strobel, W. Schraut, F. Stelter, C. Schutt, B. Passlick, and A. Pforte. 1993. The novel subset of CD14+/CD16+ blood monocytes exhibits features of tissue macrophages. *Eur J Immunol* 23:2053-2058.

191. Choi, E. I., K. A. Reimann, and N. L. Letvin. 2008. In vivo natural killer cell depletion during primary simian immunodeficiency virus infection in rhesus monkeys. *J Virol* 82:6758-6761.

192. Martin, P., S. R. Ruiz, G. M. del Hoyo, F. Anjuere, H. H. Vargas, M. Lopez-Bravo, and C. Ardavin. 2002. Dramatic increase in lymph node dendritic cell number during infection by the mouse mammary tumor virus occurs by a CD62L-dependent blood-borne DC recruitment. *Blood* 99:1282-1288.

193. Martinelli, E., C. Cicala, D. Van Ryk, D. J. Goode, K. Macleod, J. Arthos, and A. S. Fauci. 2007. HIV-1 gp120 inhibits TLR9-mediated activation and IFN-{alpha} secretion in plasmacytoid dendritic cells. *Proc Natl Acad Sci U S A* 104:3396-3401.

194. Ravetch, J. V., and S. Bolland. 2001. IgG Fc receptors. *Annu Rev Immunol* 19:275-290.

195. Banks, N. D., N. Kinsey, J. Clements, and J. E. Hildreth. 2002. Sustained antibody-dependent cell-mediated cytotoxicity (ADCC) in SIV-infected macaques correlates with delayed progression to AIDS. *AIDS Res Hum Retroviruses* 18:1197-1205.

196. Ahmad, A., and J. Menezes. 1996. Antibody-dependent cellular cytotoxicity in HIV infections. *FASEB J* 10:258-266.

197. Smith-Franklin, B. A., B. F. Keele, J. G. Tew, S. Gartner, A. K. Szakal, J. D. Estes, T. C. Thacker, and G. F. Burton. 2002. Follicular dendritic cells and the persistence of HIV infectivity: the role of antibodies and Fcgamma receptors. *J Immunol* 168:2408-2414.

198. Granelli-Piperno, A., I. Shimeliovich, M. Pack, C. Trumpfheller, and R. M. Steinman. 2006. HIV-1 selectively infects a subset of nonmaturing BDCA1-positive dendritic cells in human blood. *J Immunol* 176:991-998.

199. Randolph, G. J., S. Beaulieu, S. Lebecque, R. M. Steinman, and W. A. Muller. 1998. Differentiation of monocytes into dendritic cells in a model of transendothelial trafficking. *Science* 282:480-483.

200. Abel, K., M. J. Alegria-Hartman, K. Rothaeusler, M. Marthas, and C. J. Miller. 2002. The relationship between simian immunodeficiency virus RNA levels and the mRNA levels of alpha/beta interferons (IFN-alpha/beta) and IFN-alpha/beta-inducible Mx in lymphoid tissues of rhesus macaques during acute and chronic infection. *J Virol* 76:8433-8445.

201. Abel, K., L. La Franco-Scheuch, T. Rourke, Z. M. Ma, V. De Silva, B. Fallert, L. Beckett, T. A. Reinhart, and C. J. Miller. 2004. Gamma interferon-mediated inflammation is associated with lack of protection from intravaginal simian immunodeficiency virus SIVmac239 challenge in simian-human immunodeficiency virus 89.6-immunized rhesus macaques. *J Virol* 78:841-854.

202. LaFranco-Scheuch, L., K. Abel, N. Makori, K. Rothaeusler, and C. J. Miller. 2004. High beta-chemokine expression levels in lymphoid tissues of simian/human immunodeficiency virus 89.6-vaccinated rhesus macaques are associated with uncontrolled replication of simian immunodeficiency virus challenge inoculum. *J Virol* 78:6399-6408.

203. Behbahani, H., A. Landay, B. K. Patterson, P. Jones, J. Pottage, M. Agnoli, J. Andersson, and A. L. Spetz. 2000. Normalization of immune activation in lymphoid tissue following highly active antiretroviral therapy. *J Acquir Immune Defic Syndr* 25:150-156.

204. Brazille, P., N. Dereuddre-Bosquet, C. Leport, P. Clayette, O. Boyer, J. L. Vilde, D. Dormont, and O. Benveniste. 2003. Decreases in plasma TNF-alpha level and IFN-gamma mRNA level in peripheral blood mononuclear cells (PBMC) and an increase in IL-2 mRNA level in PBMC are associated with effective highly active antiretroviral therapy in HIV-infected patients. *Clin Exp Immunol* 131:304-311.

205. Imami, N., C. Antonopoulos, G. A. Hardy, B. Gazzard, and F. M. Gotch. 1999. Assessment of type 1 and type 2 cytokines in HIV type 1-infected individuals: impact of highly active antiretroviral therapy. *AIDS Res Hum Retroviruses* 15:1499-1508.

206. Li, Q., T. Schacker, J. Carlis, G. Beilman, P. Nguyen, and A. T. Haase. 2004. Functional genomic analysis of the response of HIV-1-infected lymphatic tissue to antiretroviral therapy. *J Infect Dis* 189:572-582.

207. Ehrhard, S., M. Wernli, G. Kaufmann, G. Pantaleo, G. P. Rizzardi, F. Gudat, P. Erb, and M. Battegay. 2008. Effect of antiretroviral therapy on apoptosis markers and morphology in peripheral lymph nodes of HIV-infected individuals. *Infection* 36:120-129.

208. Kornfeld, C., M. J. Ploquin, I. Pandrea, A. Faye, R. Onanga, C. Apetrei, V. Poaty-Mavoungou, P. Rouquet, J. Estaquier, L. Mortara, J. F. Desoutter, C. Butor, R. Le Grand, P. Roques, F. Simon, F. Barre-Sinoussi, O. M. Diop, and M. C. Muller-Trutwin. 2005. Antiinflammatory profiles during primary SIV infection in African green monkeys are associated with protection against AIDS. *J Clin Invest* 115:1082-1091.

209. Muller, D. B., M. J. Raftery, A. Kather, T. Giese, and G. Schonrich. 2004. Frontline: Induction of apoptosis and modulation of c-FLIPL and p53 in immature dendritic cells infected with herpes simplex virus. *Eur J Immunol* 34:941-951.

210. Jiang, Z. H., and R. R. Koganty. 2003. Synthetic vaccines: the role of adjuvants in immune targeting. *Curr Med Chem* 10:1423-1439.

211. Wille-Reece, U., B. J. Flynn, K. Lore, R. A. Koup, A. P. Miles, A. Saul, R. M. Kedl, J. J. Mattapallil, W. R. Weiss, M. Roederer, and R. A. Seder. 2006. Toll-like receptor agonists influence the magnitude and quality of memory T cell responses after prime-boost immunization in nonhuman primates. *J Exp Med* 203:1249-1258.

212. Birmachu, W., R. M. Gleason, B. J. Bulbulian, C. L. Riter, J. P. Vasilakos, K. E. Lipson, and Y. Nikolsky. 2007. Transcriptional networks in plasmacytoid dendritic cells stimulated with synthetic TLR 7 agonists. *BMC Immunol* 8:26.